SECTION B

THE EFFECT OF NON-THERMAL 900 MHz GSM MOBILE PHONE RADIATION ON HUMAN SPERMATOZOA

Chapter 3

Capacitation & Zona Pellucida Binding

Chapter 4

Apoptosis

Chapter 5

Heat Shock Protein & Stress Fibre Activation

CHAPTER 3

CAPACITATION AND ZONA PELLUCIDA BINDING OF HUMAN SPERMATOZOA

3.1 INTRODUCTION - MOLECULAR BASIS FOR CAPACITATION IN HUMAN SPERMATOZOA

Human spermatozoa are unable to fertilize oocytes immediately after ejaculation even when they are brought into close contact with the oocyte surface. Only after transit through the female genital tract do they undergo a physiological change called *capacitation* that renders them competent for fertilization (Visconti *et al*., 2002; Breitbart, 2003). Sperm capacitation involves multiple metabolic, biochemical, membrane and ionic changes (de Lamirande *et al*., 1997; Yanagimachi, 1994). Intracellular changes known to occur in the capacitated spermatozoon include increases in membrane fluidity, cholesterol efflux, changes in intracellular calcium (Ca^{2+}) and 3', 5'-cyclic adenosine monophosphate (cAMP) concentrations, protein tyrosine phosphorylation and changes in the swimming pattern and chemotatic motility (Breitbart, 2002; Visconti *et al*., 2002). Capacitation is marked by two distinct processes namely hyperactivated motility and the acrosome reaction (AR).

Hyperactivated motility is described as a deviation from the relatively linear and progressive swimming pattern associated with spermatozoa in seminal plasma (De Jonge and Barratt, 2006). It is characterised by an almost frantic, whiplash movement of the flagellum (Yanagimachi, 1994) and is designed to assist spermatozoa in penetrating highly viscous and dense oviductal fluids (Ho and Suárez, 2001). The AR on the other hand is an exocytotic event that occurs immediately prior to fertilisation (Jeyendran, 2000). In this reaction the outer acrosomal membrane fuses with the surrounding plasma membrane, cumulating in the release and dispersal of the acrosomal content (Yanagimachi, 1994).

3.1.1 Hyperactivated motility

Intracellular Ca^{2+} plays a significant role in the regulation of sperm hyperactivation and is responsible for the increased asymmetrical flagellar movement (Darszon *et al.*, 1999, 2001; Ho and Suarez, 2001). It acts on the axoneme thereby increasing the principal flagellar bend curvature. However, the source of the Ca^{2+} required for hyperactivation is still uncertain, some report it arises from an extracellular influx (Ho and Suarez, 2001) or release from intracellular stores (Harper *et al.*, 2004). Ionic changes represent only a small part in the complex process of sperm hyperactivation. The anion, bicarbonate also regulates hyperactivation (Burkman, 1991).

Bicarbonate increases intracellular pH, thereby promoting the alkaline environment required for hyperactivation (Burkman, 1991). Furthermore, this anion activates adenylyl cyclase (Okamura *et al.*, 1985) resulting in cAMP production, but in insufficient amounts for the hyperactivation of whole spermatozoa (Mujica *et al.*, 1994). It is proposed that the influx of Ca^{2+} activates cyclic nucleotide-gated channels, which could indicate a possible role by which cAMP is involved in hyperactivation (Ho and Suarez, 2001). In addition, sperm are known to produce low and controlled amounts of extracellular ROS, which promotes hyperactivation (de Lamirande and Gagnon, 1993a,b; de Lamirande *et al.*, 1997; Herrero and Gagnon, 2001).

The sperm enzyme responsible for the ROS generation has as yet not been identified (de Lamirande and Gagnon, 1995; Ford, 2004), but it is presumed that the sulfhydryl/disulfide pair on sperm proteins could be the targets for ROS (de Lamirande *et al.*, 1998; de Lamirande and Gagnon, 2003). Sperm capacitation is also associated with an increase in tyrosine phosphorylation, however, it is unclear what role, if any this plays in hyperactivation (de Lamirande *et al.*, 1997; Leclerc *et al.*, 1996, 1997). Several substances found in seminal plasma can either promote or inhibit hyperactivation. Semenogelin (a main protein of the semen coagulum) (de Lamirande *et al.*, 2001), as well as other constituents of seminal plasma, including cholesterol (Purdy and Graham, 2004), zinc (Andrews *et al.*, 1994; de Lamirande *et al.*, 1997), and ROS scavengers (de Lamirande and Gagnon, 1993a), all play a preventative role in premature hyperactivation of spermatozoa. Other factors also

found in seminal plasma can induce sperm hyperactivation (de Lamirande *et al.*, 1993b). On the whole, a fine balance of inhibitory and stimulatory factors that prevent premature hyperactivation regulates this process in spermatozoa.

3.1.2 The human acrosome reaction

The acrosome is a secretory vesicle derived from the Golgi apparatus and is located in the anterior region of the sperm head (Brucker and Lipford, 1995). Austin and Bishop (1958) first reported on the AR in mammals and described it as (a) the multiple fusions between the outer acrosome membrane of the spermatozoa and the overlaying plasma membrane; and (b) exposure and release of the acrosomal contents.

During fertilisation, the acrosome intact sperm penetrates the cumulus oophorus and corona radiata of the oocyte and binds to the surface of the zona pellucida (ZP) by the plasma membrane overlying the acrosome (Baker *et al.*, 2000). The AR is triggered by this binding process with the ZP and continues until the sperm reaches the inner third of the ZP. The sperm then traverses the perivitelline space and binds the oocyte oolemma. Initially, the contact is between the microvillous processes of the oocyte oolemma and the plasma membrane overlying the equatorial segment of the sperm. When fusion is completed, the sperm is consequently engulfed by the oocyte which then triggers the cortical granule reaction. This causes changes in the inner third of the ZP and the oolemma thereby inhibiting further sperm penetration and preventing polyspermia (Yanagimachi, 1994). These events are illustrated in Figure 3.1.

3.1.2.1 Signal transduction between the zona pellucida and the spermatozoon

When capacitated spermatozoa come into contact with the ZP of the oocyte, ion channels on the sperm plasma membrane are mobilized and facilitate the rapid diffusion of extracellular Ca^{2+} (Darszon *et al.*, 1999; Tosti and Boni, 2004). Darszon *et al.* (2001) further reported that Ca^{2+} influx is involved in the dehiscence of the acrosomal vesicle and in membrane fusion. This is probably accomplished due to the massive influx of Ca^{2+} inactivating Na^{+}-K^{+} ATPase (pumping Na^{+} out of and K^{+} into the cell), resulting in a rapid increase in intracellular Na^{+}.

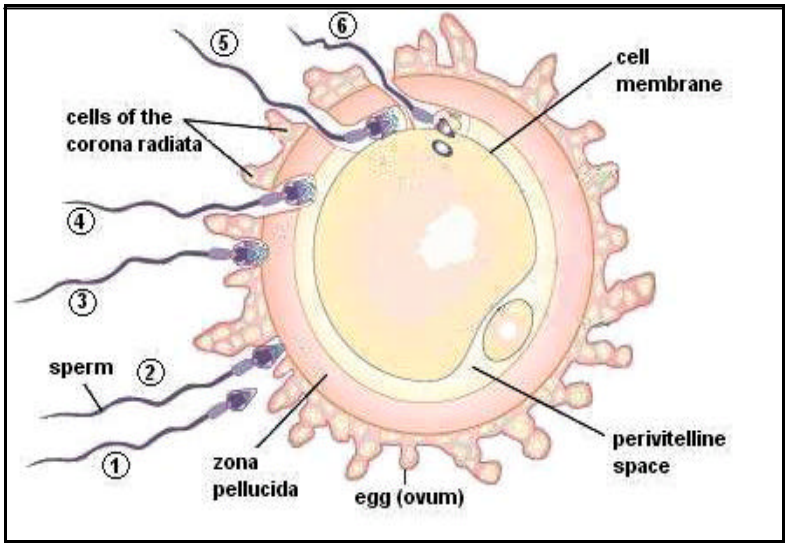

Figure 3.1 The human fertilisation process (Adapted from "fertilization." Encyclopædia Britannica Online, 2007): **(1)** Chemoattraction, **(2)** specific recognition – loose association, **(3)** acrosomal exocytosis, **(4)** penetration – sperm-egg binding, **(5)** membrane fusion, **(6)** sperm invagination.

In turn this causes an efflux of H^+ (through the Na^+/ H^+ antiport), which eventuates in the increase of intracellular pH (Lièvano *et al*., 1985; González-Martínez and Darszon, 1987; Yanagimachi *et al*., 1990; González-Martínez *et al*., 1992). A change in trans-membrane resting potential (RP) occurs due to the K^+ channel induced Na^+/H^+ exchange and pH rise causing a fast and transient hyperpolarisation followed by a Ca^{2+} mediated depolarisation (Florman *et al*., 1998; Arnoult *et al*., 1999; Patrat *et al*., 2000 and Darszon *et al*., 2001). In addition, the intracellular rise in Ca^{2+} results in the dispersion of F-actin, facilitating the close contact between the outer acrosomal and plasma membranes which eventuates in membrane fusion and completion of the AR (Breitbart, 2003).

Ion channels on the head of the sperm cell responsible for the Ca^{2+} entry and cytosolic increase include: low and high voltage-activated channels, receptor operated Ca^{2+} channels, and store-operated Ca^{2+} channels (Benoff, 1998). T-Type voltage gated Ca^{2+} channels play an important part in mediating the acrosome reaction (Florman *et al*., 1998; Darszon *et al*., 2001). Gating of these channels have

been demonstrated by AR inducers such as progesterone (Garcia and Meizel, 1999). A mechanism for gating plasma membrane Ca^{2+} channels in human sperm was proposed by Rossato *et al.* (2001). They demonstrated the existence of intracellular Ca^{2+} stores whose depletion could bring forth gating of Ca^{2+} activated K^+, with K^+ efflux causing a hyperpolarisation and the capacitative gating of voltage gated Ca^{2+} channels resulting in depolarisation of the plasma membrane.

Anion Cl^- channels have also been indicated to play a possible role in the AR (Morales *et al.*, 1993). However, the mechanism by which these channels are gated by the ZP or other agents during fertilization, have not yet been elucidated (Tosti and Boni, 2004). Electrophysiological studies found different types of Cl^- channels with dissimilar conductance on the sperm head (Bai and Shi, 2001). Since sperm have been shown to contain a high intracellular Cl^- concentration, it is plausible that a Cl^- efflux could cause the depolarisation of the RP (Sato *et al.*, 2000). Furthermore, progesterone, while inducing the AR, also seems to induce a Cl^- efflux (Meizel, 1997).

It is important to note that hyperactivated movement, although associated with capacitation, is not a prerequisite for sperm-egg fusion; a live acrosome-reacted spermatozoon has the potential to fertilize. The actual mechanism that triggers AR and ZP binding is also not well understood. Franken (1998) elucidated on the possible role of G-proteins, molecular modifications of the sperm plasma membrane that result in areas with “high- fluidity”. They may present the sites for sperm binding to the ZP and AR as well as the involvement of a selectin-like ligand structure on the ZP that recognise selectin-like receptors on the sperm membrane surface (Oehninger *et al.*, 1998). It has since been established that sperm binding is mediated by means of O-linked carbohydrate side chains of the glycoproteins ZP1/ZPB, ZP2/ZPA, ZP3/ZPA comprising the zona of various species (Florman and Wassarman, 1985; Harris *et al.*, 1994; Wassarman and Litscher, 1995). In particular, the ZP protein-3 (ZP3) serves as a primary receptor for spermatozoa (Miller *et al.*, 1992).

Furthermore, although the identity and unambiguous function of the components serving as putative sperm receptors have not been identified (Töpfer-Petersen, 1999),

Oehninger (2001) provided evidence of the presence of specific carbohydrate moieties on human spermatozoa that recognise selectin ligands on the ZP. In addition, multiple concerted and collaborative interactions between ZP3 and various surface components of sperm, possibly involving receptor aggregation and phosphorylation, may be required to achieve AR (Darzon *et al*., 1995).

It has previously been reported that the ability of spermatozoa to undergo induced AR following exposure to different effectors including chemical components, such as calcium ionophore (Aitken *et al*., 1993) and pentoxifylline (Tesarik and Mendoza, 1993), as well as physiological inducers, such as oocyte-cumulus complexes (Stock *et al*., 1989), follicular fluid (Siegel *et al*., 1990), progesterone-binding protein corticoid-binding globulin (Baldi *et al*., 1998), and ZP (Cross *et al*., 1988; Coddington, 1990; Hoshi *et al*., 1993) are of clinical value in predicting the fertilizing capacity of men (Cummins *et al*., 1991; Henkel *et al*., 1993). In addition, capacitated sperm that have acrosome reacted prior to reaching the ZP show poor penetration and reduced viability (Corselli and Talbot, 1986; Cummins and Yanagimachi, 1986; Lui and Baker, 1990). If an external source, like RF-EMF, could influence sperm specific functions, such as the acrosome reaction prior to the sperm reaching the ZP, it could have a far-reaching effect on male fertilizing potential.

The objective of the first part of the study was therefore to investigate the effect of RF-EMF exposure on sperm capacitation. Sperm motility parameters, including hyperactivation, were evaluated by computer aided sperm analysis (CASA) while the AR was assessed by flow cytometry. If RF-EMF irradiation of human sperm could in any way affect the AR, then investigating the physiological action of sperm-zona binding could confirm this. The second part of the study therefore focused on the consequence of RF-EMF on the spermatozoa's binding ability to the human ZP.

3.2 RF-EMF EXPOSURE SYSTEM AND EXPERIMENTAL PROTOCOL

3.2.1 Experimental set-up

The exposure system previously described by Leszczynski *et al*. (2002) was installed at the Reproductive Biology Laboratory (University of Pretoria, South Africa) and calibrated by technicians from STUK (Finland). Mobile phone microwave radiation (900 MHz pulse modulated RF) was simulated in a specially constructed exposure system (described in Annexure A), based on the use of a high Q waveguide resonator operating in TE_{10} mode. The irradiation chamber (Figure 3.2) was placed vertically inside a Forma CO_2 incubator (Class 100, Labothech, SA). Two 55 mm-diameter glass petri dishes (Schott dishes, Merck Chemicals (Pty) Ltd, South Africa) were placed inside the irradiation chamber, with the plane of the culture medium aligned parallel to the E-field vector. Temperature controlled water was circulated through a thin (9 mm) rectangular glass-fibre-moulded waterbed underneath the petri dishes. The RF-EMF signal was generated with an EDSG-1240 signal generator and modulated with pulse duration of 0.577 ms and repetition rate of 4.615 ms to match the GSM signal modulation scheme. The signal was amplified with an RF-EMF Power Labs R720F amplifier and fed to the exposure waveguide via a monopole type feed post.

Cells were exposed for 1 hr to a 900 MHz GSM-like signal at an average SAR of either 2.0 or 5.7 W/kg. The SAR distribution in the cell culture was determined using SEMCAD 1.8 software (SPEAG, Switzerland) with a graded simulation grid. More than 70% of the cells were within ± 3 dB of the average SAR. A total of 440 000 voxels were used to simulate the medium with the largest grid size in the culture medium being 0.1 x 0.1 x 0.1 mm^3. Simulation results were verified with temperature rise based SAR measurements using a calibrated Vitek- type temperature probe (BSD-Medical, Salt Lake City, UT, USA). Temperature measurements were also performed to assure that the cells remained at a constant temperature level during the exposures. Results indicated that at the higher SAR level (5.7 W/kg) the temperature of cells ranged between 36.7ºC and 37.3ºC, while at the lower SAR level (2 W/kg) temperature ranged from 36.8 ºC to 37.2 ºC.

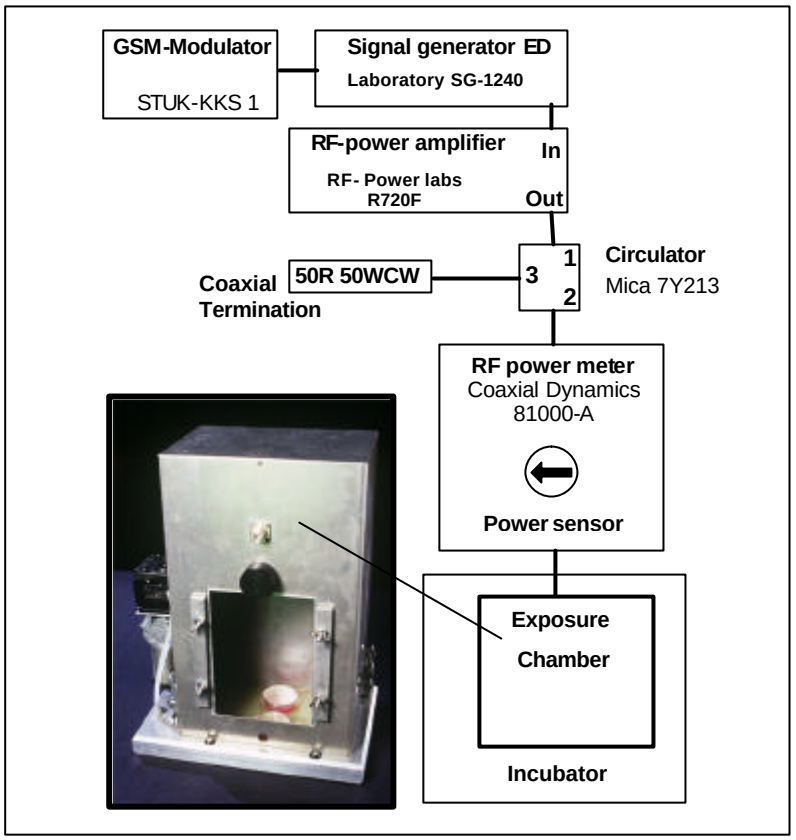

Figure 3.2 Front view and set-up of RF-EMF exposure chamber. Two glass petri dishes are placed inside the chamber on top of a temperature regulated waterbed. The RF-EMF signal is fed into the chamber placed inside a CO_2 incubator via a monopole type feed post.

3.2.2 Collection of semen

Semen samples were collected from healthy, non-smoking donors (n = 12) by masturbation after 2 to 3 days of sexual abstinence (mean age 23 ± 5 years). The study was conducted according to the Declaration of Helsinki for medical research and institutional approval was also granted (Faculty of Health Sciences Research Ethics Committee, University of Pretoria, no. 163/2003). The semen samples were allowed to liquefy at 37°C, after which standard semen parameters were evaluated according to the World Health Organisation (WHO, 1999) criteria (outlined in Annexure B). All semen samples conformed to the WHO criteria and sperm morphology assessments were performed according to Tygerberg criteria (Kruger *et al.* 1986) (mean sperm parameters, motility >50%, morphology 7.85 ± 4.2 % - results

are summarised in Annexure C). From the time of specimen collection and throughout all procedures and tests, spermatozoa were maintained under capacitating conditions (37°C in a humidified 6% CO_2 incubator, pH of media 7.3). Samples used had less than 1 x 10^6 leukocytes/ml (CD45 staining) and were antibody-free (mixed antiglobulin reaction - MAR negative).

3.2.3 Density gradient purification and preparation of spermatozoa

Sperm washing is routinely performed before IVF and intrauterine insemination (Zini *et al.*, 2000). The purpose of using a sperm processing technique is to recover a highly functional sperm population. To purify spermatozoa, a three-step discontinuous Percoll gradient (95-70-50%) diluted in Ham's F-10 medium, supplemented with penicillin G and calcium and further supplemented with 0.5% BSA was used (all reagents were from Sigma Chemical Co., St Louis, MO, USA). After the processing step, the purified population of highly motile spermatozoa (from the 95% layer) was washed in 3 ml of the same media by centrifugation (300 g for 10 min), recovered and re-suspended in 1 ml 0.5% BSA supplemented Ham's F-10 medium before preparation for RF-EMF exposure. The motile sperm concentration of the total sample (total ejaculate), after Percoll density centrifugation, was ≥ 40 x 10^6/ml, which provided sufficient number of cells for experimentation.

Processed spermatozoa were counted (improved Neubauer Haemocytometer) and concentrations adjusted to 20 x 10^6 sperm/ml. Of this sperm suspension, 1 ml was seeded into sterile glass petri dishes containing 2 ml of 0.5% BSA supplemented Ham's F-10 medium. Control and RF-EMF exposed dishes (2 each) were simultaneously prepared and exposed for one hour inside the RF-EMF chamber (RF-EMF exposed samples) and next to the chamber (control exposed samples) inside a humidified CO_2 incubator maintained at 37°C. Exposure to the different SAR levels, were performed for each of the donors at two separate occasions.

Directly after the control/RF-EMF exposure, sperm were gently recovered from the petri dishes, transferred to separate conical test tubes (Lasec, SA) and concentrations adjusted to 20 x 10^6 /ml by centrifugation (300 g for 5 min). Spermatozoa were then

incubated under capacitating conditions and assessed at different time points, directly (T_1), 2 (T_2) and 24 (T_3) hours post-exposure. All tests were run in duplicate.

3.3 CAPACITATION: ASSESSMENT OF THE HUMAN MOTILITY AND THE ACROSOME REACTION

A graphic presentation of the exposure protocol is given in Figure 3.3. The AR was evaluated using flow cytometry (FCM) (methods outlined in paragraph 3.3.1) while the motion characteristics were determined using CASA (method outlined in paragraph 3.3.2). Acrosomal status and sperm motility were all assessed on the same day at three different time points over a period of 4 weeks for all twelve donors. In addition, during experimentation, slides were prepared for morphology assessment pre- and post- RF exposure using the same computer assisted sperm analysis software as for motility assessment. The hemi-zona assay designed to determine the binding ability of spermatozoa was assessed for all twelve donors at a later date.

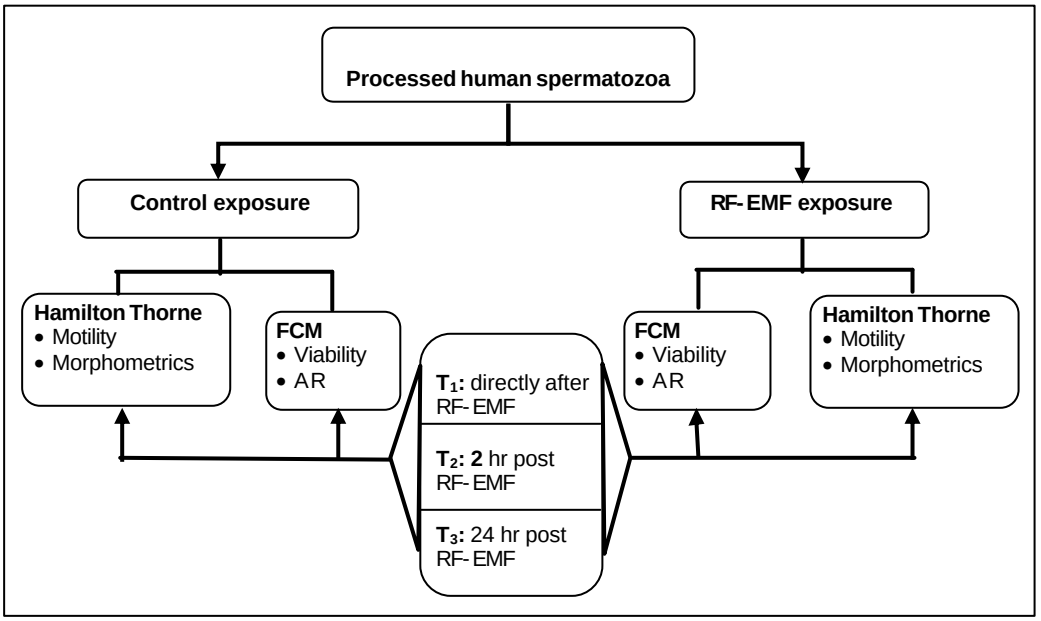

Figure 3.3 RF-EMF exposure protocol: Assessment of the acrosome reaction and motility characteristics post RF-EMF and control exposure.

3.3.1 Capacitation: assessment of motility

To determine the effect of RF-EMF (2.0 and 5.7 W/kg) radiation on sperm motility, computer aided sperm analysis was performed. At each time point, post RF-EMF exposure, 5 µl of the sperm suspension from the RF-EMF, and control exposed sperm were loaded into two 20 µml Microcell chambers (2X-CEL, Hamilton Thorne Research, Danvers, MA). The chambers were then placed on a heated microscope plate (Nikon, Optiphot, Japan), which was maintained at 37°C. Video recordings were made of at least 10 random fields per chamber. Each field was recorded for 30 seconds. At a later time, the pre-recorded video was analysed using the Hamilton Thorne Integrated Visual Optical System (IVOS) (Hamilton Thorne Research, Danvers, MA). The Hamilton Thorne computer calibrations were set at 30 frames, at a frame rate of 30 images/second. Data from each individual cell track were recorded and analysed. At least 200 sperm were analysed, per field, of the 10 fields recorded for each aliquot sampled.

The sperm kinetic parameters evaluated included: motile (MOT) and progressively (PRG) motile sperm, curvilinear velocity (VCL - a measure of the total distance travelled by a given sperm during the acquisition divided by the time elapsed), average path velocity (VAP - the spatially averaged path that eliminates the wobble of the sperm head), straight line velocity (VSL - the straight-line distance from beginning to end of track divided by time taken), beat-cross frequency (BCF - frequency at which the sperm's curvilinear path crosses the average path), amplitude of lateral head displacement (ALH - the mean width of sperm head oscillation), and the derivatives; straightness (STR = VSL / VAP x 100) and linearity (LIN = VSL / VCL x 100, departure of sperm track from a straight line) as well as hyperactivated motility (HYPA, to be classified as hyperactivated, a trajectory had to meet all of the 60 Hz SORT criteria, *i.e.*, VCL = 150 µm/s, LIN = 50% and ALH = 7 µm (Mortimer *et al.*, 1998)). Data from each individual cell track were recorded and analysed.

3.3.1.1 Morphometric assessment

Slides from each donor (n = 12) were prepared in duplicate prior to exposure and at two time points after exposure (T_1-directly after and T_2 - 2h after RF-exposure) and left to air-dry until staining at a later time. A rapid staining procedure for sperm

morphology assessment (Hemacolor, Merck Chemicals, Darmstadt, Germany) was used to stain cells (Cooper *et al*., 1992).

Morphology was evaluated with the Hamilton Thorne IVOS using Metrix Software (Hamilton Thorne Research). The following parameters were evaluated: major and minor axis (µm), elongation (%), area (μm^2), perimeter (µm) and the acrosomal region (%). All samples were divided into 3 morphological categories (Annexure C). A typical Metrix evaluation of morphometric parameters is depicted in Figure 3.4 A and B.

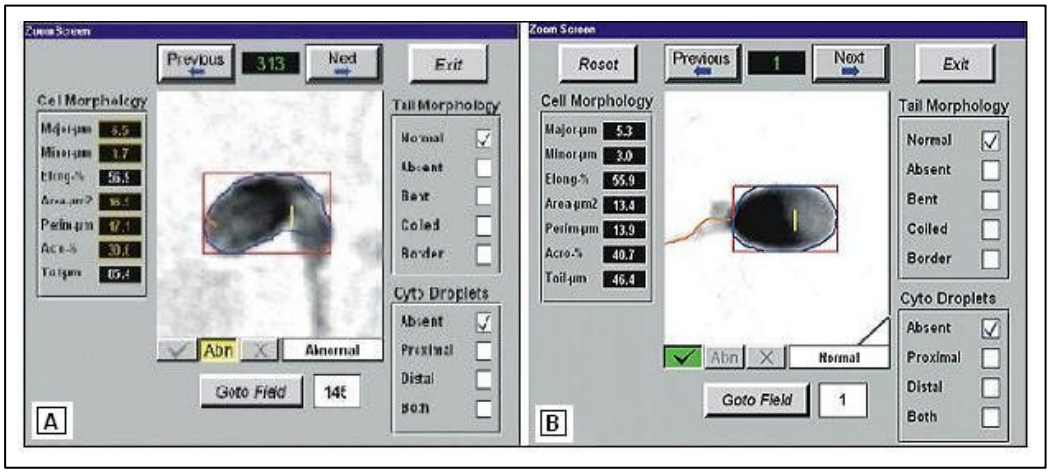

Figure 3.4 Metrix calculation of sperm morphometric parameters: (A) an abnormal spermatozoon, (B) a normal spermatozoon.

3.3.2 Capacitation: Assessment of the acrosomal status

The AR is associated with the release of proteolitic enzymes from the acrosomal vesicle. These enzymes, specifically acrosin, are targeted by the fluorescent-labelled lectin *Pisum sativum* agglutinin conjugated with fluoro-isothiocyanate (PSA-FITC) (Cross *et al*., 1986). The proportion of spermatozoa undergoing the AR can then be evaluated by the decrease in the fluorescence intensity of PSA-FITC (Nikolaeva *et al*., 1998). Acrosome intact sperm will have intensely fluorescent acrosomes while acrosome reacted spermatozoa will bind significantly less PSA. In order to determine acrosomal status, the acrosomal membrane has to be permeabilised to facilitate lectin

binding of the acrosomal contents. However, since the AR is only evaluated in viable sperm, dead cell discrimination is very important to accurately quantify acrosomal status. Therefore, the staining ability of two fluorescent viability probes compatible with flow cytometry were compared.

The first part of this study focussed on the evaluation of viability probes used in conjunction with PSA-FITC to determine acrosomal status in live spermatozoa. Secondly the AR was assessed by flow cytometry after RF-EMF and ionophore challenge.

3.3.2.1 Viability probes used in the acrosome reaction

It is important to be able to differentiate between live acrosome reacted and dead reacted sperm to accurately assess the effect of an acrosome promoter. Therefore a viability probe is used for dead cell exclusion. Traditional viability probes used include non-fluorescent trypan blue (triple stain, Talbot and Chancon, 1981) and fluorescent probes including bisbenzimide (Hoechst 33258) (Cross *et al.*, 1986), ethidium bromide (Carver-Ward *et al.*, 1996), and propidium iodide (Miyazaki *et al.*, 1990). However, as the fluorescence emission of some of these probes overlap with those used for combined surface and intracellular staining, it is difficult to accurately assess acrosomal status and viability at the same time. Propidium iodide (PI) is normally used as the viability probe of choice in flow cytometry.

Propidium iodide's spectral emission extensively overlaps with FITC and phyco-erythrin (PE) (Schmid *et al.*, 1992). In addition, it has also been shown to "leach" from permeabilised sperm over time due to weak or reversible binding (Trestappen *et al.*, 1988; Riedy *et al.*, 1991). Furthermore, for single argon laser instruments, the UV excitable Hoechst 33258 stain cannot be used. Evaluation of the AR entails the fixation and permeabilisation of sperm, therefore another viability probe, 7-amino-actinomycin D (7-AAD) was compared to PI's staining post fixation at different time points (for 1 hr) to optimise the detection of dead sperm. This study was performed to confirm the suitability of using 7-AAD for dead cell exclusion with the flow cytometry AR protocol.

(i) 7-Amino-Actinomycin D

The viability stain 7-AAD (λ_{ex} = 499 nm and λ_{emm} = 655 nm) is a fluorescent DNA-binding agent that intercalates between cytosine and guanine bases (Philpott *et al.*, 1996) and has a high DNA binding constant and a slow post fixation and permeabilisation dissociation rate (O'Brien and Bolton, 1995; Philpott *et al.*, 1996). The emission spectra of 7-AAD, allows it to be used in conjunction with other flourocromes (PE and FITC) with minimal fluorescence emission overlap (O'Brien and Bolton, 1995; Nunez *et al.*, 2004). In addition, 7-AAD has previously been used to discriminate between dead and live sperm (Bronson *et al.*, 1999; Nunez *et al.*, 2004).

The exact mechanism of 7-AAD is not known, but it has been proposed that the chromophore intercalates between G-C bases and the large peptide moiety upon binding to DNA interacts with the minor groove of the double helix (Evenson *et al.*, 1986).

(ii) Propidium Iodide

Propidium Iodide (λ_{ex}= 488 nm and λ_{emm} = 655 nm) is a supravital stain that rapidly penetrates non-viable sperm through disrupted plasma membranes (Riedy *et al.*, 1991) and strongly intercalates DNA depending on the degree of unwinding (Darzynkiewicz *et al.*, 1997).

(iii) Comparison between 7-AAD and PI as viability probes used in the acrosome reaction

Spermatozoa recovered from the 95% motile sperm suspension after the density gradient technique (described previously), were re-suspended at a cell density of 1 x 10^6/ml in Ham's F-10 (supplemented with 0.5% BSA). Two sets of triplicate tubes were respectively labelled with 10 µl 7-AAD (50 µg/ml, BD PharMingen, BD Bioscience, NJ, USA) and 10 µl of PI (50 µg/ml, BD Biosciences, USA). The sperm were then gently vortexed and 7-AAD and PI labelled sperm were left to incubate for 20 min at room temperature (25°C) in the dark.

Cytofix/Cytoperm^{TM} (BD Biosciences, USA) solution, containing neutral pH-buffered saline, saponin and 4% (w/v) paraformaldehyde, was used for the

simultaneous fixation and permeabilisation of sperm. After addition of 250 µl Cytofix/Cytoperm^{TM} solution, sperm were incubated for 20 min on ice, pelleted (300 g for 5 min) and the supernatant discarded after which sperm were washed twice (300 g for 5 min) with 2 ml PBS (Sigma Chemical Co.). Directly following, and at specific time points post fixation and permeabilisation, viability staining was assessed on a Beckman Coulter Epics ALTRA flow cytometer. Fluorescence emission from 7-AAD was detected in the far-red range of the spectrum (650 nm long-pass filter) and uptake of 7-AAD was measured in PMT 5. PI fluorescence was detected in the orange range of the spectrum (562-588 nm band pass filter) (Schmid *et al*., 1992; O'Brien and Bolton, 1995) and PI-labelled sperm were measured in PMT 4. A flow chart presenting the protocol used in assessing viable spermatozoa is given in Figure 3.5.

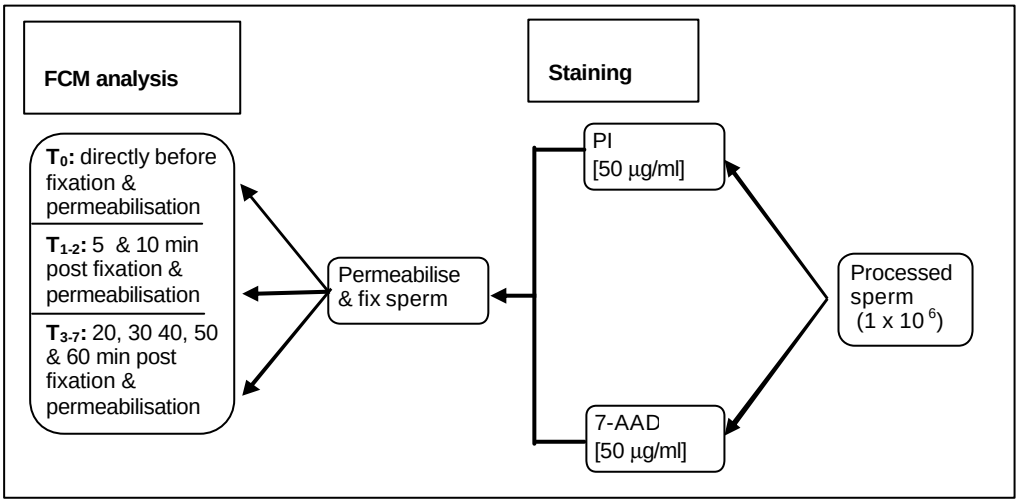

Figure 3.5 Flow cytometric assessment of 7-AAD and PI as viability probes after fixation and permeabilisation of human spermatozoa.

3.3.2.2 Evaluation of the acrosome reaction by flow cytometry

The techniques described by Uhler *et al*. (1993) and Henley *et al*. (1994) were adapted. Spermatozoa recovered from the 95% motile sperm suspension after density gradient purification was re-suspended (20 x 10^6 /ml in Ham's F-10, 5% BSA) in glass petri dishes (two dishes each for RF-EMF and control exposure). The sperm were then exposed for 1 hour to 900 MHz RF-EMF (2.0 W/kg).

After irradiation, spermatozoa were incubated under capacitating conditions (5% CO_2 at 37° C) and assessed directly (T_1), 2 (T_2) and 24 (T_3) hours post exposure. At the same time, points aliquots were taken to assess motility using the Hamilton Thorne Integrated Visual Optical System (Hamilton Thorne Research, Danvers, MA, USA).

For assessment of acrosomal status, duplicate tubes taken from the RF-EMF exposed and control sperm (1 x 10^6 /ml) were stained with the viability probe 7-AAD (50 µg/ml) and incubated for 20 min at room temperature in the dark. Remaining sperm were kept in a humidified CO_2 incubator at 37°C for assessment at later time points. Sperm were then pelleted at 300 g for 5 min. The supernatant was discarded and the sperm washed twice (300 g for 5 min.) with 2 ml PBS. Sperm were re-suspended in 250 µl Cytofix/Cytoperm™ solution and incubated for 20 min on ice.

After the fixation and permeabilisation procedure, sperm were again washed twice by centrifugation (300 g for 5 min) with 2 ml PBS before the human acrosome was assessed with fluorescein-labelled *Pisum sativum* agglutinin (PSA-FITC, Sigma Chemical Co.). PBS dissolved PSA-FITC was added at a final concentration of 1 mg/ml and samples were incubated at room temperature in the dark for 15 min. After PSA-FITC staining, spermatozoa were finally washed by centrifugation with 2 ml PBS before re-suspending the pellet in 1 ml PBS. Specimens were gated by light scatter properties (size and granularity) of spermatozoa and analysed for dual colour fluorescence. Dead sperm (7-AAD-stained) were excluded and PSA-FITC staining was assessed only among live sperm and detected on PMT 2. Flow cytometric analysis was performed with a Coulter Epics® XL.MCL flow cytometer (Beckman Coulter, Miami, Florida, USA) using System II software. Results are expressed as the mean cell number with a total of 10 000 events acquired for each endpoint.

(i) Visual assessment of the acrosome reaction

Loading of the stains was visually inspected (Zeiss confocal microscope, LSM 510 META, Carl Zeiss (Pty) Ltd, Germany) by preparing smears from small aliquots taken of the sperm suspension after addition of PSA-FITC. Slides were left to air-dry after which they were mounted and evaluated under oil immersion and 100x

magnification. Acrosome intact sperm have intensely green fluorescent acrosomal regions while acrosome reacted sperm could be differentiated by patchy fluorescence (undergoing AR) a fluorescent equatorial segment (almost completed AR) or no fluorescence (acrosome reacted).

(ii) Induction of the acrosome reaction by calcium ionophore

For a positive control, sperm following 3 hr capacitation were re-seeded in sterile 10 ml conical test tubes at a final concentration of 1 x 10^6 sperm/ml. A frozen stock solution (5 mM) of calcium ionophore (A23187, Sigma Chemical Co.) in dimethyl sulphoxide (DMSO, Sigma Chemical Co.) was diluted in Ham's F-10 medium (0.5% BSA) and 10 µl was added to 1 ml of the capacitated sperm suspension making a final concentration of 10 µM A23187. The samples were incubated for 30 min at 37 °C in a 5% CO_2, 95% humidity incubator. A duplicate aliquot was treated with 10 µl of 1:10 diluted DMSO. Detection of the acrosome after calcium ionophore (A23187) challenge was assessed with PSA-FITC staining, using FCM analysis as described previously.

3.4 HEMI-ZONA ASSAY

3.4.1 Zona pellucida binding - mechanism:

Tight binding of human spermatozoa to the outer surface of the human ZP is an essential event in gamete interaction leading to fertilization (Burkman *et al.*, 1988; Mortimer and Mortimer, 1999; WHO, 1999). Spermatozoa penetrate through the cumulus oophorus to bind tightly to the zona protein ZP3; this in turn triggers the spermatozoa AR. Only acrosome reacted spermatozoa will bind to the zona protein (ZP3) thereby facilitating penetration of the zona matrix and progression into the perivitelline space (Franken, 1998; Mortimer and Mortimer, 1999).

The hemi-zona assay was originally designed as a diagnostic test for male factor infertility (Burkman *et al.*, 1990; Franken *et al.*, 1990; Oehninger *et al.*, 1991; Franken and Oehninger, 2006) and has since been utilized to investigate the effect of various substances on human sperm-ZP binding. The assay (illustrated in Figure 3.6) utilizes non-viable, non-fertilizable human oocytes (obtained from *in vitro*

fertilization programmes). The bisected oocyte provides two matched halves (hemi-zonae) with functionally equal zona surfaces, yielding a controlled comparison of sperm binding (Franken *et al.*, 1990). By calculating the ratio of spermatozoa bound to the two halves, an indication of the binding capacity of the control sperm sample versus the stressor (RF-EMF) exposed sample can be obtained.

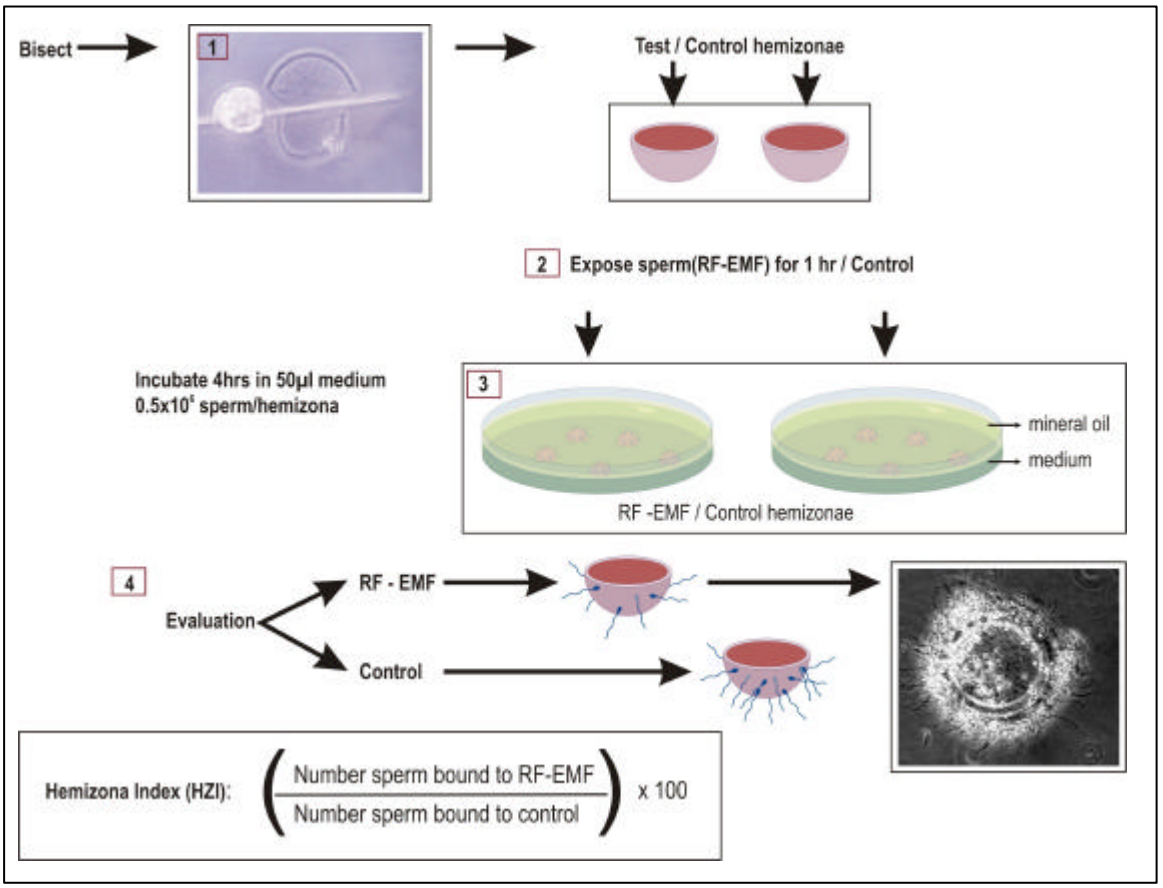

Figure 3.6 The hemi-zona assay: (1) Oocytes from IVF were bisected and kept at room temperature while **(2)** spermatozoa were exposed for 1 hour to RF-EMF (SAR 2.0 and 5.7 W/kg). **(3)** After exposure hemi-zonae were added to 50 µl spermatozoa droplets (0.5 x 10^6 cells/ml). **(4)** Spermatozoa and hemi-zonae were co-incubated for an additional 4 h before visual assessment of binding.

3.4.2 Source and preparation of human zonae pellucidae

Institutional Ethics approval was obtained for the use of non-fertilized oocytes from patients with access oocytes undergoing IVF treatment (Faculty of Health Sciences

Research Ethics Committee, University of Pretoria, no. 5/2006). A total of 5 oocytes (metaphase II) were used per donor (unless otherwise indicated). Non-fertilized oocytes were prepared for cryostorage using the technique described by Hammitt *et al.* (1993). Oocytes were incubated for 3 min in a solution of 2.5 M Sucrose, 3% BSA, 3.5 M DMSO in Ham's F-10 medium (all reagents were from Sigma Chemical Co.), transferred to 0.25 ml cryo- straws and kept in liquid nitrogen until further use.

On the day of use, the straw's content was emptied by pushing a steel plunger gently through the straw, thus expelling the oocytes into a petri dish. The oocytes were transferred to a droplet containing thawing medium (2.5 M Sucrose, 3% BSA in Ham's F-10 medium). Oocytes were then washed three times before commencing with bisection. Cutting was performed under an inverted phase contrast microscope (Axiovert 200, Carl Zeiss (Pty) Ltd, Germany) with a micromanipulation system (Narishige, MM-89, Japan). Once bisected, mouth micro pipetting dislodged the ooplasm. The hemi-zonae were kept at room temperature until addition of spermatozoa.

3.4.3 Sperm-oocyte interaction

The procedure is schematically illustrated in Figure 3.6. Spermatozoa (from 10 donors) were collected from the 95% layer after a 3-step Percoll density gradient separation (as described previously), concentrations were adjusted to 20 x 10^6 cells/ml and cells seeded into glass petri dishes (one dish per donor) already containing 2 ml Ham's F-10 medium supplemented with 3% BSA. Control samples were prepared simultaneously. Spermatozoa were then exposed for an hour to RF-EMF (2.0 and 5.7 W/kg), while control dishes were kept at 37ºC in the same incubator.

After exposure, 50 µl droplets containing 0.5 x 10^6 cells/ml of RF-EMF exposed and control spermatozoa were placed into separate petri dishes. The hemi-zonae were then transferred to the droplets, the droplets were covered with mineral oil and incubated for a further 4 hours until assessment. By calculating the ratio of spermatozoa bound to the two halves, an indication of the binding capacity of the control sperm sample versus the sample exposed to RF-EMF was obtained.

3.5 STATISTICAL ANALYSIS

A sample of 12 donors were chosen to have a 95% power to detect a clinical relevant difference of 5% in mean increase over 24 h between RF and control exposed samples using a paired t-test at the 0.05 level of significance. A standard deviation of 4.95% was assumed.

To analyse the effect of RF-EMF on motility and acrosomal status results from a within subject design considering two treatments, control vs. RF-EMF (SAR 2.0 and 5.7 W/kg), at three time points (T_1- directly after exposure, T_2- 2 hours after exposure and T_3- 24 hours after exposure) were analysed as a mixed linear model (time series regression) with Stata Statistical Software Release 8.0 (Stata Corp. 2003, USA). Similarly morphometry, was assessed at two time points (T_1- directly after exposure and T_2- 2 hours after exposure). Throughout the analysis no interaction between time and dose was present therefore the p-values associated with dose only was reported. Data is presented as mean values ± SD (standard deviation). Correlations between routine semen parameters (morphology), motility, and the results obtained from flow cytometry analysis were computed using the Spearman rank correlation coefficient.

Comparison between PI and 7-AAD staining, post fixation/permeabilisation over time was accomplished using linear regression analysis. Slopes were considered significantly different if $p < 0.05$. For comparison of two groups (RF-EMF and control exposed sperm), a two-tailed Mann-Whitney U-test was performed.

To determine the effect of RF-EMF on the hemi-zona binding assay, data were analysed using a Wilcoxon signed ranks test (Stata Statistical Software) while the correlation between morphology and number of cells bound to the hemi-zona were calculated using a Spearman's rank correlation coefficient (GraphPadPrism® version 3.00 software, GraphPadSoftware, San Diego, CA, USA). All statistical tests were two-sided and statistical significance was considered when $p < 0.05$. Repeatability of duplicate tests was confirmed with the intraclass correlation coefficient for assays = 0.92.

3.6 RESULTS

3.6.1 Motility and morphology: CASA

Computer aided sperm analysis was used in the assessment of sperm motility and morphology after RF-EMF exposure. The progressive motility (type "a + b" motility, rapid + slow motility) of RF-EMF exposed compared to control spermatozoa for SAR levels 2.0 and 5.7 W/kg respectively were determined directly after (T_1), 2 hours (T_2) and 24 hours (T_3) post exposure (Table 3.1 A and B). Table 3.2 notes the time series regression results of percentage rapid-, slow-, non-progressive and immotile spermatozoa comparing RF-EMF (2.0 and 5.7 W/kg) exposure with their respective controls. Since no interaction between time and dose was present in Tables 3.1 and 3.2 the p-values associated with dose only are reported. Sperm kinetic results are summarized in Figures 3.7 and 3.8. Morphometric results are summarised in Table 3.3, while results comparing morphometric parameters for SAR 2.0 W/kg and SAR 5.7 W/kg are summarized in Tables 3.4 and 3.5 respectively.

3.6.1.1 Percentage progressive motility

Time series regression analysis (Table 3.1) showed no statistically significant effect of RF-EMF exposure on progressive motility of human sperm compared to controls at either of the SAR values ($[p = 0.764]_{2.0\ W/kg}$ and $[p = 0.856]_{5.7\ W/kg}$). When comparing progressive motility in RF exposed sperm for SAR 2.0 W/kg to SAR 5.7 W/kg as a function of time (Mann-Whitney U-test), no significant effect of SAR level on motility was noted at any of the time points; T_1 ($p = 0.910$), T_2 ($p = 0.675$) or T_3 ($p = 0.312$).

Furthermore, a summary of the time series regression analysis results comparing rapid- slow-, non-progressive and immotile categories are given in Table 3.2. There was no statistically significant effect on rapid progressive - a, slow progressive - b, non-progressive - c or immotile categories - d comparing RF exposed spermatozoa at either of the SAR levels with controls. In addition, an increase in SAR had no effect on any of the motility categories.

Table 3.1 Percentage progressive motility after exposure to **(A)** RF-EMF (2.0 W/kg) and **(B)** RF-EMF (5.7 W/kg) in exposed and control spermatozoa determined directly (T_1), 2 h (T_2) and 24 h (T_3) after exposure.

A	Progressive motility	Progressive motility	
Time	**RF-EMF**	**Control**	**p-value***
T_1	86.5 ± 7.44	86.8 ± 5.34	p= 0.764
T_2	87.5 ± 8.57	86.1 ± 8.36	
T_3	70.0 ± 14.51	65.0 ± 16.45	
B	**RF-EMF**	**Control**	**p-value***
T_1	86.6 ± 9.33	87.2 ± 7.32	p = 0.856
T_2	86.2 ± 7.69	84.6 ± 9.18	
T_3	62.71 ± 15.14	65.7 ± 19.15	

* p-value supplied for the time series regression analysis comparing RF exposed with control samples.

Table 3.2 Time series regression results of percentage rapid-, slow-, non-progressive and immotile spermatozoa respectively after RF-EMF (2.0 or 5.7 W/kg) exposure compared to control spermatozoa.

Motile category	SAR 2.0 W/kg	SAR 5.7 W/kg	SAR 2.0 vs. 5.7 W/kg*
Rapid - a	p = 0.401	p = 0.809	p = 0.834
Slow - b	p = 0.518	p = 0.477	p = 0.771
Non-progressive - c	p = 0.765	p = 0.537	p = 0.433
Immotile - d	p = 0.446	p = 0.946	p = 0.469

***** Exposure levels 2.0 and 5.7 W/kg were compared over time after confirmation of equivalent experimental conditions reflected by the homogeneity of the results from controls during the two experiments.

3.6.1.2 Velocity parameters

Comparison between VAP, VSL, and VCL (µm/s) of spermatozoa exposed to RF-RMF (2.0 and 5.7 W/kg) and controls are shown in Figure 3.7 A and B respectively.

For SAR 2.0 W/kg (Figure 3.7 A): No statistical difference (time series regression analysis) was noted in any of the velocity parameters over the three time points comparing RF-EMF exposed sperm at SAR 2.0 W/kg with controls. Directly after exposure both RF-EMF exposed and controls exhibited similar velocities. However

two hours after exposure, RF-EMF exposed sperm displayed more rapid movement in all parameters compared to the controls. This situation was reversed 24 hours after exposure with RF-EMF exposed sperm showing a decrease in all velocity parameters compared to controls.

For SAR 5.7 W/kg (Figure 3.7 B): Time series regression analysis comparing RF-EMF exposed sperm to controls over the three different times noted a statistical significant difference in VSL ($p = 0.05$); the other two velocity parameters were border line significant [VAP ($p = 0.06$) & VCL ($p= 0.09$)]. At all three time points, RF-EMF exposed spermatozoa showed a decrease in all velocity parameters compared to controls. Furthermore, an increase in SAR resulted in a dose related decrease in all velocity parameters with $Velocity_{5.7W/kg} < Velocity_{2.0W/kg}$.

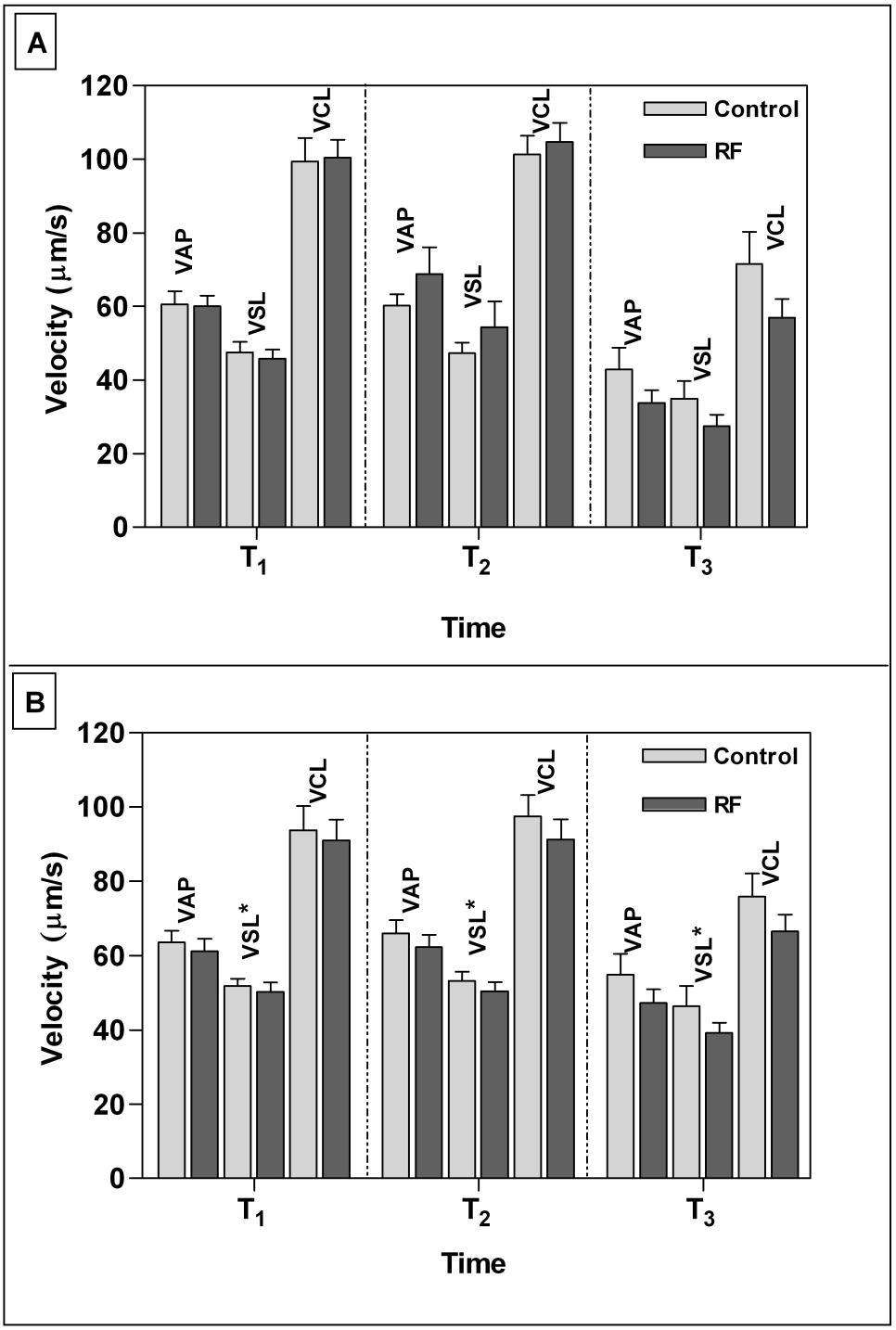

Figure 3.7 Velocity parameters comparing RF-EMF (dark-grey) exposed spermatozoa for SAR 2.0 W/kg (A) and 5.7 W/kg (B) with controls (light-grey) directly (T_1), 2 (T_2), and 24 (T_3) hours after a 1 hour 900 MHz GSM exposure (*$p < 0.05$).

3.6.1.3 Motion parameters

Additional motion kinetics measured by CASA included ALH (µm), BCF (beats/sec), STR (%), LIN (%), and hyper-activated motility. Area (μm^2) and elongation (%), although not part of motion parameters, were also determined. The effect of RF-EMF (SAR 2.0 and 5.7 W/kg) exposure on ALH, BCF, STR, and LIN is illustrated in Figure 3.8 A and B respectively. Time series regression analysis of the effect of RF-EMF on area and elongation is noted separately.

For SAR 2.0 W/kg (Figure 3.8 A): Time series regression analysis between RF-EMF exposed sperm and controls over the three time intervals noted no statistical difference ($p > 0.05$) in ALH, BCF, STR, LIN, or hyper-activated motility. This was also the case for area ($p = 0.08$) and elongation ($p = 0.40$).

For SAR 5.7 W/kg (Figure 3.8 B): There was no statistically significant difference (time series regression analysis) in ALH, STR, LIN, or hyper-activated motility between RF-EMF exposed sperm and controls. However, BCF was significantly higher ($p = 0.04$) in exposed sperm compared to controls. Elongation in exposed sperm did not differ from controls at any of the time points determined ($p = 0.15$), although the area in exposed sperm decreased significantly ($p = 0.38$) as a function of time compared to controls.

3.6.1.4 Morphometric analysis

There was no statistically significant difference in any of the morphology parameters determined by CASA comparing sperm evaluated pre exposure with sperm evaluated directly after a 1 hour RF-EMF exposure. Average morphometric values ± SD of each parameter measured comparing RF exposed (2.0 and 5.7 W/kg) sperm with controls for both normal and abnormal sperm at two time points are given in Tables 3.3 A and B respectively. Time series regression analysis of morphometric parameters comparing RF exposed sperm with controls at both SAR values noted a statistically significant reduction in all the morphometric parameters except elongation (Table 3.4).

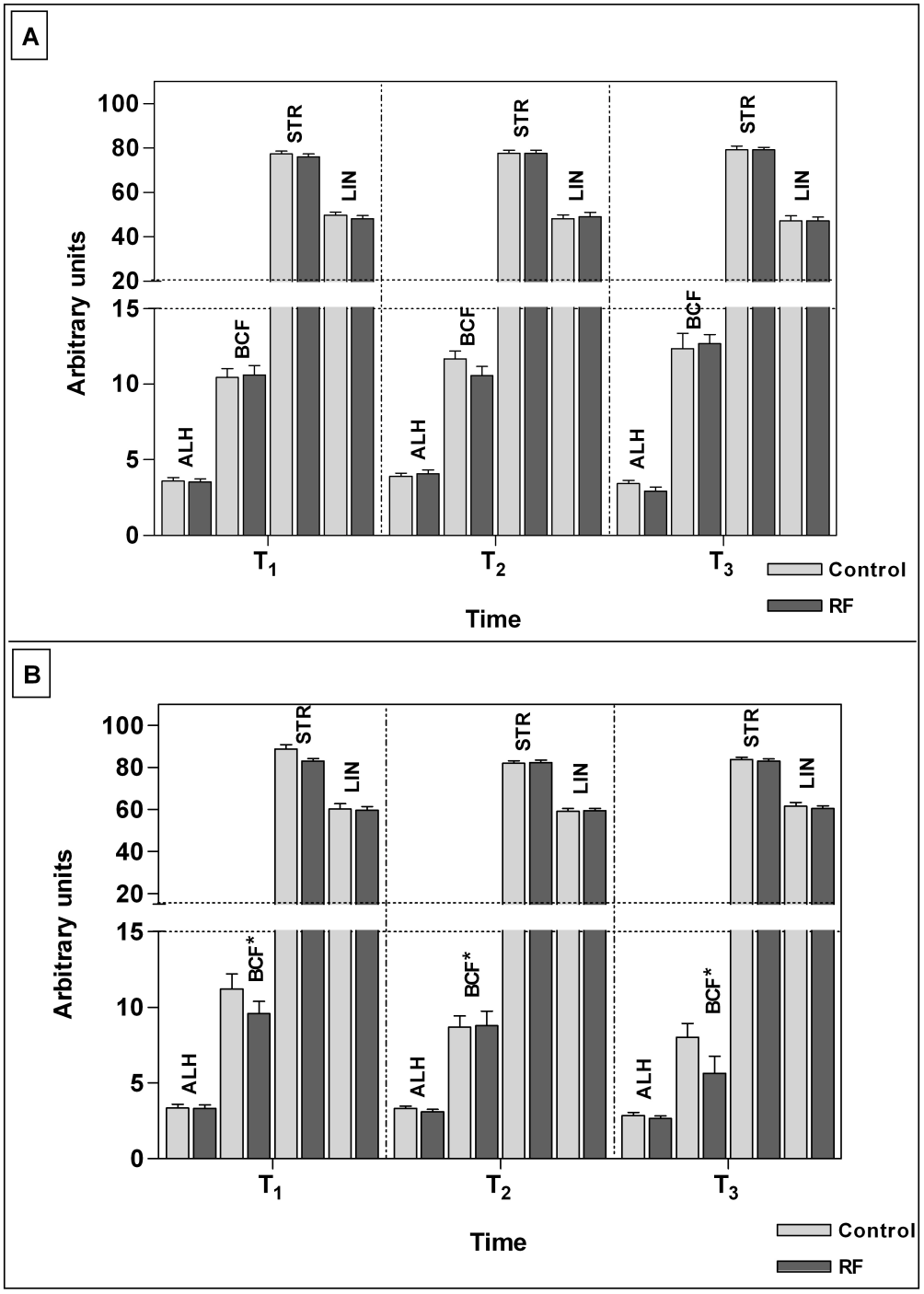

Figure 3.8 Motion parameters comparing RF-EMF (dark grey) exposed spermatozoa for SAR 2.0 W/kg (A) and 5.7 W/kg (B) with controls (light grey) directly (T_1), 2 (T_2), and 24 (T_3) hours after a 1 hour 900 MHz GSM exposure (*$p<0.05$).

Table 3.3 Summary of morphometric results of sperm exposed to **(A)** 2.0 W/kg and **(B)** 5.7 W/kg compared to control values.

A	SAR 2.0 W/kg		Control	
Parameter	**Normal**	**Abnormal**	**Normal**	**Abnormal**
Major axis (μm)	3.53 ± 0.17	5.56 ± 0.73	5.93 ± 0.60	6.02 ± 0.90
Minor axis (μm)	2.39 ± 0.10	3.67 ± 0.38	4.45 ± 0.23	4.08 ± 0.63
Elongation (%)	45.26 ± 2.70	67.22 ± 10.26	75.07± 7.24	68.9 ± 13.31
Area (μm^2)	9.24 ± 0.66	14.80 ± 2.07	18.83 ± 1.37	17.35 ± 3.50
Perimeter (μm)	9.36 ± 0.37	14.82 ± 1.36	16.67± 1.19	16.28 ± 1.97
Acrosome (%)	21.48 ± 3.98	23.53 ± 11.84	22.75 ± 4.85	22.43 ± 9.14
B	**SAR 5.7 W/kg**		**Control**	
Parameter	**Normal**	**Abnormal**	**Normal**	**Abnormal**
Major axis (μm)	3.39 ± 0.38	5.61 ± 0.72	4.125 ± 0.53	5.125 ± 0.735
Minor axis (μm)	2.25 ± 0.24	3.79 ± 0.38	2.875 ± 0.348	3.5 ± 0.573
Elongation (%)	42.66 ± 6.10	68.5 ± 10.61	52.8 ± 7.89	69.93 ± 16.35
Area (μm^2)	9.11 ± 1.61	15.18 ± 1.91	10.85 ± 1.448	12.75 ± 2.45
Perimeter (μm)	9.08 ± 0.93	15.25 ± 1.39	11.28 ± 0.848	13.88 ± 1.48
Acrosome (%)	23.70 ± 4.99	29.56 ± 11.58	26.85 ± 11.01	38.6 ± 14.15

Table 3.4 Summary of p values of the time series regression analysis results of sperm morphology determined by CASA. RF exposed sperm were firstly compared to controls, morphometric parameters were compared directly (T_1) and 2 hours (T_2) after exposure and the number of normal and abnormal forms were compared.

	SAR 2.0 W/kg			SAR 5.7 W/kg		
Parameter	**RF vs. Control**	**T_1 vs. T_2**	**Normal vs. Abnormal**	**RF vs. Control**	**T_1 vs. T_2**	**Normal vs. Abnormal**
Major axis	0.002**	0.842	0.081	0.010*	0.989	0.845
Minor axis	0.022*	0.380	0.857	0.062*	0.865	0.832
Elongation	0.185	0.205	0.592	0.830	0.478	0.963
Area	0.001**	0.810	0.585	0.003**	0.813	0.879
Perimeter	0.004**	0.531	0.243	0.015*	0.882	0.752
Acrosome	0.006*	0.140	0.086	0.011*	0.083	0.218

*$p < 0.05$, **$p < 0.005$

When morphometric parameters of RF exposed sperm at SAR 2.0 W/kg were compared with sperm exposed at SAR 5.7 W/kg, a statistically significant reduction was noted in area and acrosomal region (Table 3.5). There was no statistically significant difference in any of the parameters evaluated comparing T_1 and T_2 as well as number of normal and abnormal forms except when comparing acrosomal region (Table 3.5). Both area and acrosomal region decreased as SAR levels increased.

Table 3.5 Time series regression analysis comparing sperm morphometric parameters of sperm exposed at 2.0 W/kg to sperm exposed at 5.7 W/kg are summarised as p values.

Parameter	2.0 vs. 5.7 W/kg	T_1 vs. T_2	Normal vs. Abnormal
Major axis	0.068	0.784	0.097
Minor axis	0.085	0.350	0.835
Elongation	0.485	0.179	0.620
Area	0.020*	0.616	0.720
Perimeter	0.067	0.465	0.253
Acrosome	0.001**	0.008*	0.051*

*$p < 0.05$, **$p < 0.005$

3.6.2 Acrosome reaction

The flow cytometric evaluation of the two viability dyes (7-AAD and PI) post fixation and permeabilisation is illustrated in Figure 3.9. To ensure the correct loading of the dyes (7-AAD and PSA-FITC), for flow cytometric analysis, stained sperm were visually inspected (Figure 3.10), while positive controls were used to confirm both 7-AAD (Figure 3.11) and PSA-FITC (Figure 3.12) staining. Figure 3.13 (A) depicts flow cytometry fluorescence histograms showing AR as a function of time and Figure 3.13 (B) shows flow cytometry dot plots and projections used to gate acrosome reacted sperm. Flow cytometric results of RF-EMF and control exposed sperm assessed directly, 3 and 24 hr after exposure, are given in Figure 3.14.

3.6.2.1 Comparison between 7-AAD and PI as viability probes for flow cytometry post fixation and permeabilisation

Flow cytometric evaluation of 7-AAD and PI staining post fixation and permeabilisation showed that both the % gated sperm and mean fluorescent intensity of 7-AAD and PI stained spermatozoa decreased exponentially with time (Figure 3.9). Data is presented as log (mean fluorescence) and log (% gated) sperm versus time. Each data point represents the mean of three experiments done in duplicate. In each, 10 000 sperm were analysed by flow cytometry. The difference in slopes between PI and 7-AAD log (mean fluorescence) as well as log (% gated) was shown to be highly significant ($p < 0.0001$).

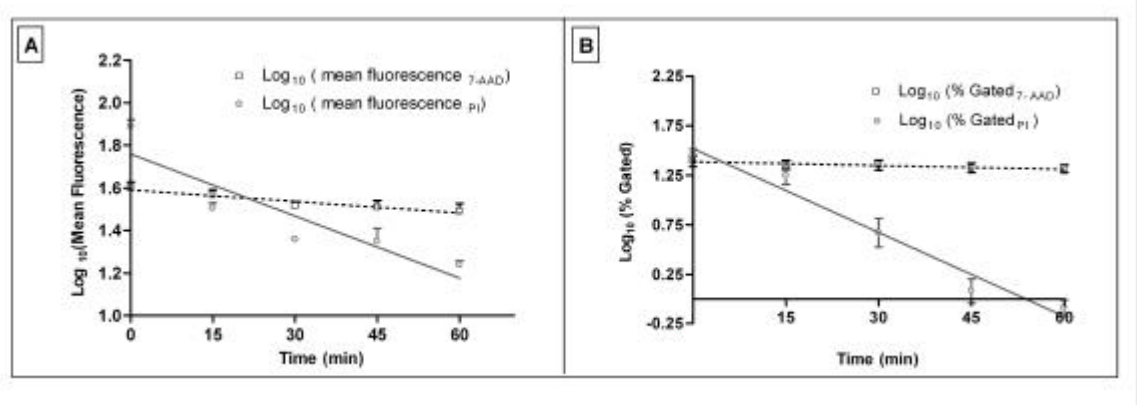

Figure 3.9 **(A)** Linear regression of log (mean fluorescence)$_{7\text{-AAD}}$ ($R^2 = 0.93$) and log (mean fluorescence)$_{PI}$ ($R^2 = 0.83$). **(B)** Linear regression of log (%gated) $_{7\text{-AAD}}$ fluorescence ($R^2 = 0.93$) and log (%gated) $_{PI}$ fluorescence ($R^2 = 0.97$).

3.6.2.2 Visual assessment of the acrosome reaction

Slides made of aliquots taken of spermatozoa stained with PSA-FITC and 7-AAD for flow cytometric evaluation were visually inspected via fluorescence microscopy (Zeiss Confocal Microscope, Germany). PSA-FITC stained the acrosomal contents of acrosome intact spermatozoa bright green (Figure 3.10 A) while no fluorescence was noted in acrosome reacted spermatozoa (Figure 3.10 D). Sperm undergoing the AR, either demonstrated patchy fluorescence in the acrosomal area (Figure 3.10 B) or equatorial staining (Figure 3.10 C). Non-viable spermatozoa stained red (7-

AAD$^+$), as 7-AAD could penetrate their compromised plasma membrane (not shown). For flow cytometric analysis, cells staining 7-AAD$^+$ were excluded in the determination of acrosome status.

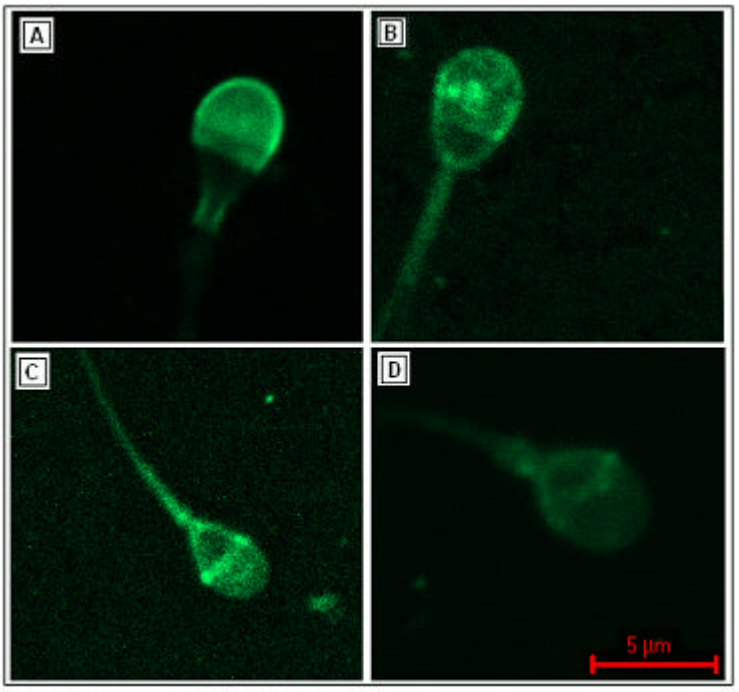

Figure 3.10 ***Fluorescent staining (PSA-FITC) of the human acrosome reaction***: (**A)** Acrosomal cap intact, (**B)** Patchy fluorescence, **(C)** Equatorial staining and **(D)** Acrosome reacted.

3.6.2.3 Assessment of the acrosome reaction by flow cytometry

(i) Evaluation of 7-AAD staining

Figure 3.11 illustrates the staining of human spermatozoa with the viability stain 7-AAD. Unstained cells (background fluorescence) are depicted by the red-brow population, while addition of 7-AAD shifted the population to the right (blue curve). Treatment of cells with Triton X-100 (2 µl / 1 x 10^6 sperm/ml) prior to staining with 7-AAD caused an increase in 7-AAD$^+$ fluorescence (green curve).

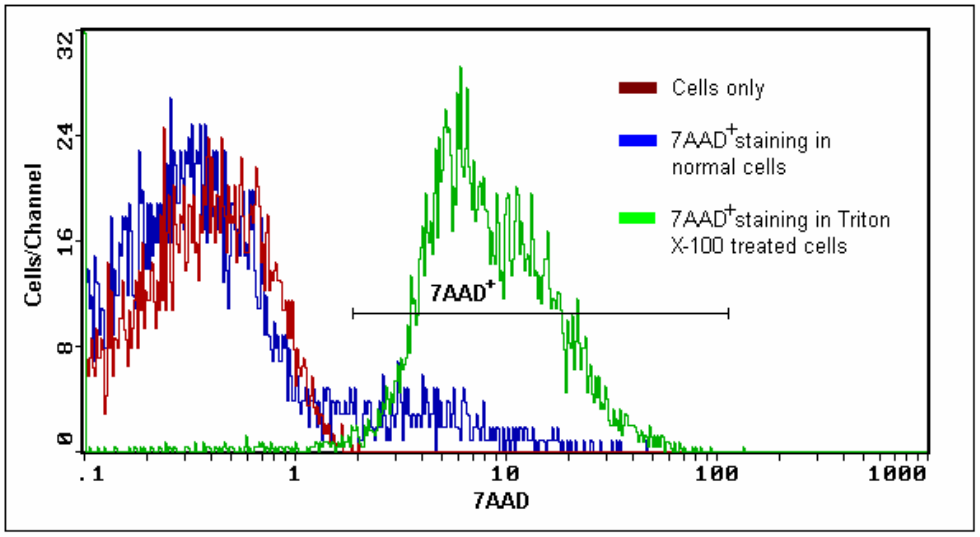

Figure 3.11 7-AAD Viability staining - Flow cytometric histograms showing overlay plots of unstained sperm (red-brown), sperm labelled with 10µl 7-AAD (blue) and sperm treated with 2 µl of Triton x-100 (green) for 15 min. prior to 7-AAD staining.

(ii) Induction of the acrosome reaction

The induced AR assay described by the WHO (1999), was adapted for flow cytometric assessment of the acrosomal status. A typical Log fluorescence histogram of DMSO treated spermatozoa (green curve) versus calcium ionophore (A23187)-induced acrosome reacted sperm (red-brown curve) is illustrated in Figure 3.12. Induction of the AR by calcium ionophore caused a decrease in PSA-FITC fluorescence, shifting the fluorescence intensity to the left. Acrosomal status was assessed in all twelve donors (samples run in duplicate) using 7-AAD to exclude non-viable cells. The mean percentage of spermatozoa that had undergone the AR following calcium ionophore induction was 13.48% ± 3.32.

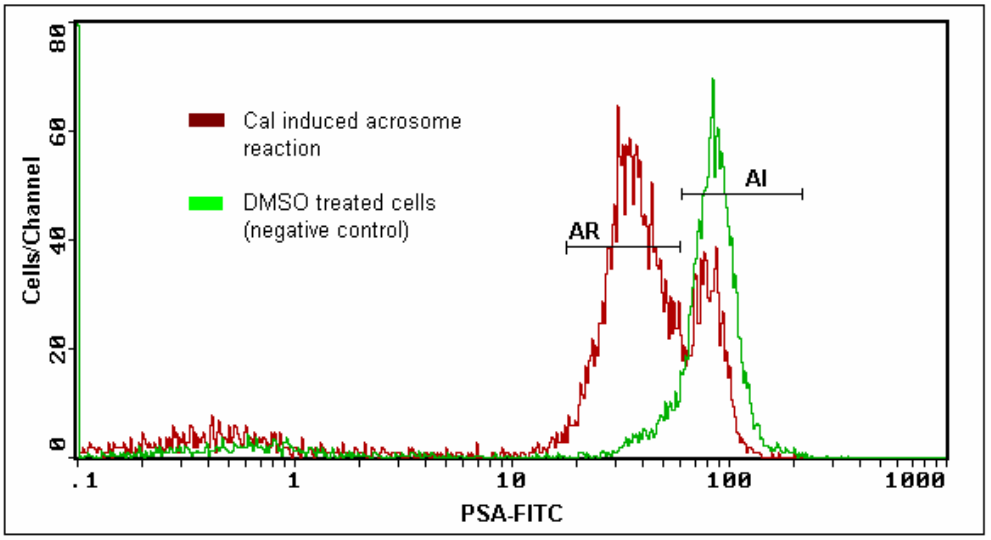

Figure 3.12 PSA-FITC staining - Flow cytometric histograms showing overlay plots of capacitated sperm (24 h) induced to undergo the AR by pre-incubation with A23187 (positive control - red-brown) and sperm treated with DMSO (negative control for calcium ionophore (CaI) stimulation - green) prior to PSA-FITC staining. Fluorescence peaks note the acrosome reacted (AR) and acrosome intact (AI) sperm populations.

The natural progression of the AR in sperm incubated under capacitating conditions is demonstrated in Figure 3.13 A. After 3 hours incubation under capacitating conditions (orange curve) 13.89% ± 8.34 of the cells had spontaneously undergone the AR, this number increased to 27.37% ± 3.48 after 24 hours incubation (green curve). Ionophore challenge (induced AR assay, WHO, 1999) after 24 h capacitation increased the number of acrosome reacted spermatozoa (red-brown curve) to 48.50% ± 11.45.

Typical dot plots and fluorescence histograms of PSA-FITC and 7-AAD staining are illustrated in Figure 3.13 B. The cell population was gated to exclude 7-AAD$^+$ cells, while regions F (acrosome intact) and H (acrosome reacted) were set to gate the differences in PSA-FITC staining.

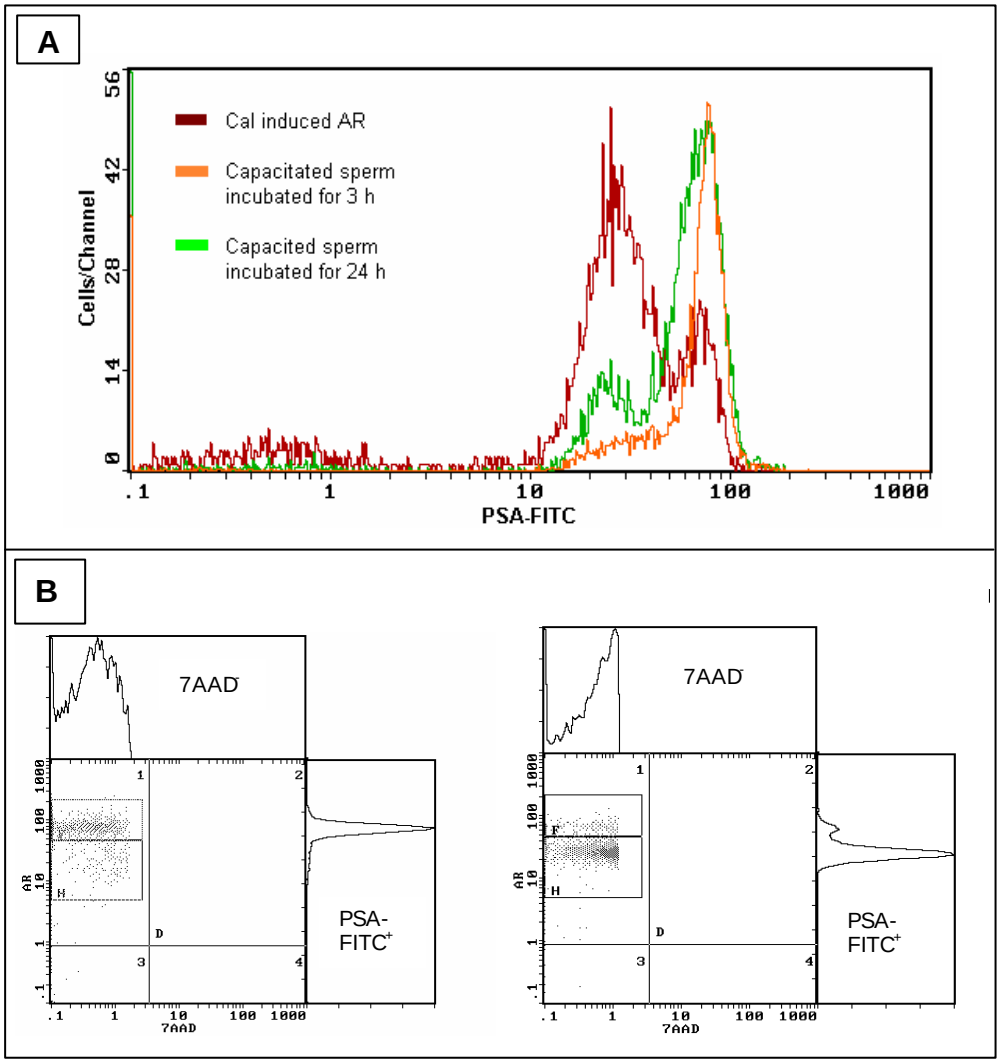

Figure 3.13 PSA-FITC staining - **(A)** Flow cytometric histograms showing overlay plots of capacitated sperm, sperm induced to undergo the AR by pre-incubation with CaI (positive control-red-brown); sperm incubated for 3 hours (orange) and sperm incubated for 24 hours (green) prior to PSA-FITC staining. Gating shows acrosome reacted (AR) and acrosome intact (AI) spermatozoa. **(B)** Flow cytometric dot plots and projections showing gating of PSA-FITC staining in 7-AAD$^-$ (live cells) only, region F denotes acrosome intact spermatozoa and region H acrosome reacted sperm.

(iii) Evaluation of the acrosome reaction post RF-EMF

When evaluating the number of non-viable cells (7-AAD$^+$) at the three different time points (Figure 3.14 A), no statistical difference was seen between RF-EMF exposed (SAR 2.0 W/kg) and control cells ($p = 0.397$). The number of acrosome reacted live (FITC$^+$7-AAD$^-$) spermatozoa increased with time (Figure 3.14 B). However, there was no statistical difference ($p = 0.839$) between RF-EMF exposed and control sperm at any of the time points. In a similar manner, the number of acrosome intact live (FITC$^-$7-AAD$^-$) spermatozoa decreased with time, but again, there was no statistical difference ($p = 0.920$) between exposed sperm and controls. Although not statistically significant, the biggest difference between exposed and control sperm when considering the number of acrosome reacted as well as intact live sperm, were noted at time point T_2 (2 hours post exposure). At this time point, RF-EMF exposure caused a 15% increase in acrosome reacted (decrease in acrosome intact) live sperm compared to control cells.

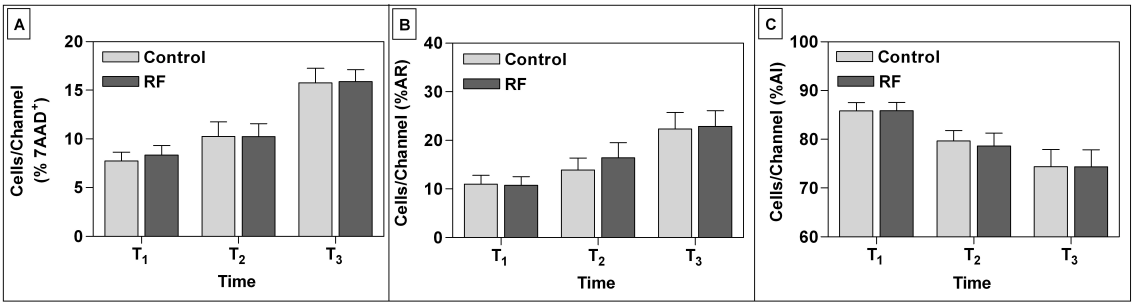

Figure 3.14 Comparison between RF-EMF (dark grey) and control (light grey) sperm assessed by FCM directly, 2 - and 24 - hours after a 1 hour 900 MHz GSM exposure (SAR 2.0 W/kg) **(A)** % 7-AAD$^+$ staining spermatozoa, **(B)** % acrosome intact live cells, **(C)** % acrosome reacted live.

3.6.3 Sperm-oocyte interaction - hemi-zona assay

There was a statistically significant ($p = 0.02$) reduction in zona binding in RF-EMF exposed sperm at SAR 2.0 W/kg compared to controls. Controls bound an average of 31.77 sperm / zona compared to 25.83 sperm / zona of RF-EMF exposed spermatozoa. All donors used in this assay bound on average more than 20 control

sperm/hemi-zona, the minimum criterion for limiting false-negative results with the HZA (Oehninger *et al.*, 1991). Results of the Wilcoxon signed ranks test are illustrated in Figure 3.15.

For comparison, spermatozoa from the two donors that demonstrated the highest difference in binding potential after RF exposure (at 2.0 W/kg) were exposed at the higher SAR of 5.7 W/kg. A total reduction of 27% in binding was noted, with controls binding an average of 32.10 sperm / zona compared to the 23.43 sperm / zona of the RF exposed group.

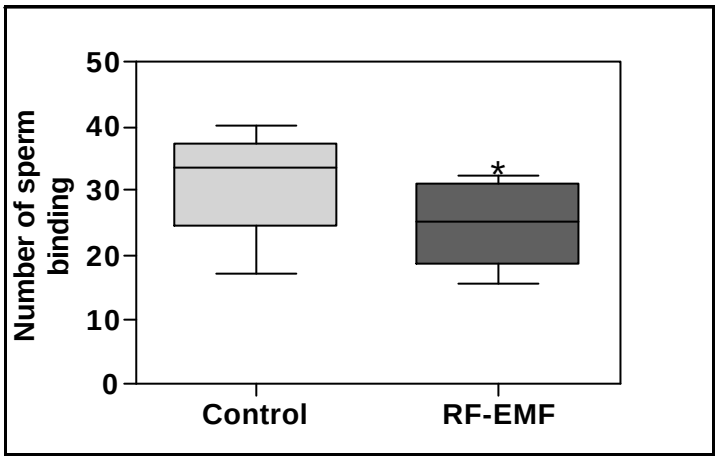

Figure 3.15 Box and whiskers plot (showing medians) of number of sperm binding non-fertilized metaphase II oocytes (5 oocytes per donor, n = 10) after an hour exposure to 900 MHz GSM radiation. RF-EMF exposure caused a significant reduction in sperm bound to the hemi-zonae compared to controls (*p = 0.02).

Morphology was also correlated with the number of sperm binding (Figure 3.16). Although morphology was not significantly correlated with number of sperm bound after RF-exposure (r_s = 0.51, p = 0.13), the greatest reduction (22.4%) in binding ability compared to controls was seen in the group of sperm with the lowest morphology (refer to Annexure C for morphology classification). Category A spermatozoa (5 - 10% normal morphology) showed a reduction of 22.4% in binding ability after RF exposure compared to 16.9% in category B (> 10% normal morphology) and 21.0% in category C (> 15% normal morphology) spermatozoa.

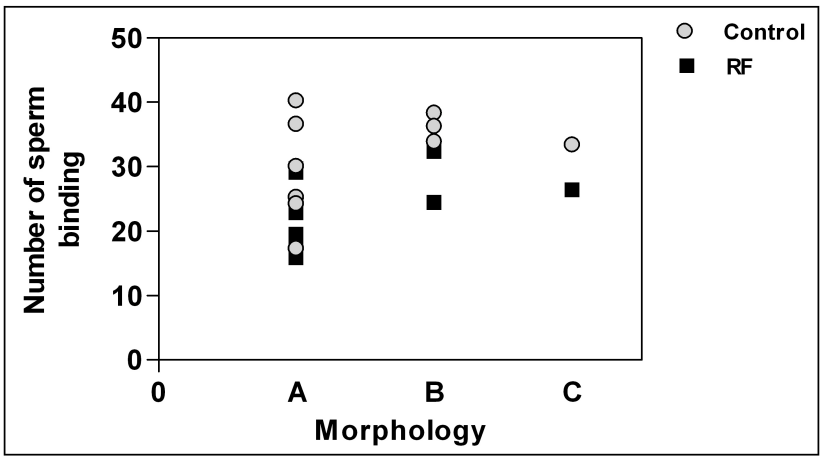

Figure 3.16 Correlation of morphology and number of spermatozoa binding the hemi-zonae after an hour exposure to 900 MHz GSM radiation (■). Number of control (●) spermatozoa is also shown for comparison.

3.7 DISCUSSION

Various studies have recently expounded on the possible influence of RF-EMF on sperm motility (Davoudi *et al.*, 2002; Fejes *et al.*, 2005; Erogul *et al.*, 2006). As with so many studies conducted in this field, some of the findings were criticized due to a lack of dosimetry and not taking confounding risk factors into account (EFCP6 2005). Another possible weakness in the assessment of sperm motility as used by these studies is the lack of the use of an automated system such as CASA to eliminate operator bias in manual motility assessment.

Therefore, in the present study, dosimetry was verified by simulation and temperature rise calculations. In addition, temperature during exposure was regulated at 37°C and did not increase by more than 0.2°C during exposure at SAR 2.0 W/kg, while at SAR 5.7 W/kg the temperature did not increase more than 0.3°C. Furthermore, to avoid the effect of intra- and inter-observer variations in the assessment of sperm kinematic parameters, a computer assisted sperm analysis system for the quantification of sperm motility categories, velocity and motion parameters were used.

RF exposure at neither of the two SAR levels (2.0 and 5.7 W/kg) had any effect on progressive motility assessed by CASA, a finding in agreement with Fejes *et al.* (2005) who also noted no change in overall progressive motility after RF exposure. However, Fejes *et al.* (2005) did observe a decrease in rapid progressive and an increase in slow progressive spermatozoa after RF exposure. On the other hand, Erogul *et al.* (2006) found a decrease in both rapid and slow progressive spermatozoa, while non-progressive and immotile sperm populations increased after exposure. Davoudi *et al.* (2002) only noted a decrease in the proportion of rapid progressive sperm after prolonged exposure (1 month, 6 h/day). One commonality noted in all the studies is a reduction in rapid progressive motility, a result not observed in the present study. Not only did RF exposure at either 2.0 or 5.7 W/kg not affect rapid progressive motility; no effect was seen on slow progressive, non-progressive or immotile spermatozoa. Apart from the use of manual techniques of motility assessment in all of the above studies, motility was assessed in unprocessed semen samples. It is well known that leukocyte contamination significantly contributes to ROS generation (Plante *et al.*, 1994; Whittington and Ford, 1999; Henkel *et al.*, 2003) leading to amongst others a reduction in motility (Plante *et al.*, 1994; Armstrong *et al.*, 1999). It is thus possible that ROS generation and not RF-exposure could have contributed to the decreased progressive motile population observed, explaining the lack of an effect observed in the processed semen sample used in the present study.

During capacitation (which occurs *in vitro* after 2-3 hours of incubation – therefore our choice of assessing at T_2 - 2 hours after exposure), spermatozoa become hyperactivated in preparation of oocyte penetration. As a result, the sperm's velocity increases (determined by VAP, VSL, and VCL) and the motion (determined by ALH BCF, STR, and LIN) becomes more erratic. A change in any of these parameters could thus lead to a decrease in sperm fecundity. In the present study, RF-EMF at both SAR levels had no effect on hyperactivated motility. At a SAR of 2.0 W/kg, RF-EMF did not affect any of the kinematic-parameters (velocity or motion), at any of the time points post irradiation. However, at a SAR of 5.7 W/kg a significant change in VCL and BCF parameters were observed. This result cannot be ascribed to thermal effects, as the temperature rise during the exposure did not exceed 0.3ºC

(confirmed by temperature probe measurements - Annexure A). Therefore, the observed statistically significant change in motility parameters at SAR 5.7 W/kg could possibly be the result of an alternative mechanism, such as a decrease in mitochondrial fecundity or reactive oxygen species generation resulting in depleted ATP levels.

CASA evaluation (Metrix Software) of morphology revealed a statistically significant decline in all morphometric parameters except elongation. Of specific interest was the decrease in area and acrosomal region parameters noted after exposure at both SAR levels. A significant decrease in area was also observed after RF exposure at 5.7 W/kg when computer aided sperm analysis was used in the assessment of sperm motility, which serves as confirmation that RF-exposure causes a decrease in spermatozoa area. Although RF exposure at SAR 2.0 W/kg did not cause a statistically significant decrease in area, shrinkage of spermatozoa with time was none the less observed. If a stress pathway is activated in spermatozoa as a result of RF exposure it is possible that Hsp27 activation, known to be involved in stress fibre stabilisation due to increased actin polymerisation (Landry and Huot, 1995), could result in the shrinkage noted in exposed spermatozoa. This would confirm an observation by Leszczynski *et al.* (2002) who ascribed the shrinkage of endothelial cells, after 900 MHz GSM irradiation, to Hsp27 activation and phosphorylation. In addition, the acrosomal region was also significantly reduced after RF-irradiation. To evaluate if this observation could have an effect on the spermatozoa's ability to undergo the AR, acrosomal status was assessed in RF exposed spermatozoa.

Several methods have been developed to evaluate the acrosomal status of human sperm, including lectin binding protocols - first described by Aitken *et al.* (1984), the triple stain technique (Talbot and Chacon, 1981), indirect immunofluorescence using monoclonal (Wolf *et al.*, 1985) or polyclonal antibodies (Töpfer-Petersen *et al.*, 1986 and Sanchez *et al.*, 1991), chlortetracycline fluorescence assays (Lee *et al.*, 1987), and fluorescein-labelled lectins (Cross *et al.*, 1986). More recently, flow cytometric analysis of human sperm using fluorescein-labelled lectins (Miyazaki *et al.*, 1990; Purvis *et al.*, 1990; and Uhler *et al.*, 1993; Nikolaeva *et al.*, 1998) or monoclonal antibodies (Bronson *et al.*, 1999) have been described as a more accurate, faster,

simpler, dynamic, and more objective method than fluorescence microscopy for the assessment of acrosome-reacted human sperm. The main limitation of assessing acrosomal status by flow cytometry is that detailed information regarding the stage of AR cannot be provided as with the visual method (Nikolaeva *et al*., 1998).

The suitability of using 7-AAD as viability probe for dead cell discrimination during FCM evaluation of the AR evaluation was confirmed. Unlike PI, 7-AAD did not leech from permeabilised, fixed spermatozoa and fluorescence remained stable for up to 1 h post staining. The presence of two distinct fluorescence populations after PSA-FITC labelling of capacitated spermatozoa correspond to acrosome reacted and acrosome intact spermatozoa. These findings are similar to those of Miyazaki *et al*. (1990), Uhler *et al*. (1993), Henley *et al*. (1994), and Nikolaeva *et al*. (1998). In addition, the PSA-FITC staining protocol described here, provided a rapid and precise assessment of acrosome reacted as well as acrosome intact spermatozoa with flow cytometry.

In experiments, no significant difference was noted in the competence of capacitated spermatozoa to initiate the AR after RF exposure. Acrosome reacted sperm increased as a function of time and, similarly, the acrosome intact spermatozoa decreased with time. However no difference was noted between the RF exposed and control populations. On the other hand, calcium ionophore induction lead to a significant increase in acrosome reacted spermatozoa. Flow cytometric results cannot explicate if RF exposure had an effect on the acrosomal region, which can only be confirmed by visual evaluation. Therefore, it is possible that RF exposure could have resulted in a reduction of the acrosomal region as was observed with CASA evaluation of morphology. The only telling way to confirm if these observations could affect sperm fecundity is by evaluating the binding potential of spermatozoa to the human ZP after RF exposure.

The hemi-zona assay plays an essential role in the diagnosis of male factor infertility (Burkman *et al*., 1988; Franken *et al*., 1993; Franken and Oehninger, 2006) and has a high predictive power for fertilisation outcome (Oehninger *et al*., 2000; Franken and Oehninger, 2006). In current experiments, 900 MHz RF-EMF exposure resulted in a statistically significant reduction in sperm binding at a SAR of 2.0 W/kg compared

with controls, a result even more pronounced at the higher SAR level of 5.7 W/kg. Taking into consideration that the number of spermatozoa bound to the ZP correlates with fertilisation rate (Lui *et al.*, 1989; Oehninger *et al.*, 2000; Bastiaans *et al.*, 2003), RF exposure therefore has the potential to affect male fertility and disrupt fertilisation.

However, before RF-EMF can be added to the list of environmental factors affecting male fertility a clearer understanding of the possible mechanism responsible for this effect should be elucidated. It has been noted in literature that RF exposure resulted in an efflux of intracellular calcium $[Ca^{2+}]_i$ in neurological cells (Bawin *et al.*, 1975; Blackman *et al.*, 1985), a process that could potentially affect sperm capacitation where an influx of Ca^{2+} is required in both sperm hyperactivation and the AR. It is unlikely that RF-EMF had an effect on Ca^{2+}, as RF-exposure had no effect on either hyperactivation or the AR. The decreased acrosomal region after RF exposure could be responsible for the reduction in binding observed in the HZA. Alternatively, it is possible that RF exposure could affect the gating of receptors (Chiabrera *et al.*, 2000) on the sperm head, which would explain why fewer exposed sperm bound to the hemi-zona, while no effect was seen on sperm propensity for the AR. If on the other hand, a stress response is initiated in spermatozoa, Hsp activation and phosphorylation could potentially interfere with signalling pathways in preparation of capacitation and sperm-zona pellucida interactions. It has been shown that Hsp70 and 90 are involved in various processes of sperm capacitation as well as zona recognition and fusion (Huang *et al.*, 2000a,b; Matwee *et al.*, 2001; Bohring and Krause, 2003; Huszar *et al.*, 2003; Ecroyd *et al.*, 2003). In particular, antibodies to Hsp70 significantly reduced tight binding of spermatozoa to the zona pellucida (Neuer *et al.*, 1998).

In conclusion, an *in vitro* result can and should not be extrapolated to an *in vivo* situation without additional research and, ultimately, epidemiological confirmation. It is however concerning that RF exposure affected the outcome of the hemi-zona assay, a test that has clinical significance to predicting male fertilising potential.

3.8 REFERENCES

Aitken, R.J., Ross, A., Harfreave, T., Richardson, D., Best, F. 1984. Analysis of human sperm function following exposure to the ionophore. *J Androl.*, 5, 321-9.

Aitken R.J., Buckingham, D.W., Fang, H.G. 1993. Analysis of the response of human spermatozoa to A23187 employing a novel technique for assessing the acrosome eraction. *J Androl*., 14, 132-41.

Andrews, J.C., Nolan, J.P., Hammerstedt, R.H., Bavister, B.D. 1994. Role of zinc during hamster sperm capacitation. *Biol Reprod.*, 51, 1238-47.

Armstrong, J.S., Rajasekaran, M., Chamulitrat, W., Gatti, P., Hellstrom, W.J., Sikka, S.C. 1999. Characterization of reactive oxygen species induced effects on human spermatozoa movement and energy metabolism. *Free Rad Bio Med*., 26, 869-80.

Arnoult, C., Cardullo, R.A., Lemos, J.R., Florman, H.M. 1999. Control of the low voltage-activated calcium channel of mouse sperm by egg ZP3 and by membrane hyperpolatisation during capacitation. *Proc Natl Acad Sci USA.*, 96, 6757-62.

Austin, C.R., Bishop, M.W. 1958. Capacitation of mammalian spermatozoa. *Nature.*, 181, 851-6.

Bai, J.P., Shi, Y.L. 2001. A patch-clamp study of human sperm Cl⁻ channel reassembled into giant liposome. *Asian J Androl.*, 3, 185-91.

Baker, H.W.G., Liu, D.Y., Garrett, C., Martic, M. 2000. The human acrosome reaction. *Asian J Androl.*, 2, 172-8.

Baldi, E., Luconi, M., Bonaccorsi, L., Forti, G. 1998. Non genomic effects of progesterone on spermatozoa: mechanisms of signal transduction and clinical implications. *Front Biosci.*, 3, d1051-9.

Bastiaans, H.S., Windt, M.L., Menkveld, R., Kruger, T.F., Oehninger, S., Franken, D.R. 2003. Relationship between zona pellucida-induces acrosome reaction, sperm morphology, sperm-zona pellucida binding, and *in vitro* fertilization. *Fertil Steril.*, 79, 49-55.

Bawin, S.M., Kaczmarek, L.K., Adey, W.R. 1975. Effects of modulated VHF field on the central nervous system. *Ann NY Acad Sci.*, 247, 74-81.

Benoff, S. 1998. Voltage dependant calcium channels in mammalian spermatozoa. *Front Biosci.*, 3, D1220-40.

Blackman, C.F., Benane, S.G., House, D.E., Joines, W.T. 1985. Effects of ELF (1-120 Hz) and modulated (50 Hz) RF fields on the efflux of calcium ions from brain tissue, *in vitro*. *Bioelectromagnetics.*, 6, 1-11.

Bohring, C., Krause, W. 2003. Characterisation of spermatozoa surface antigens by antisperm antibodies and its influence on acrosomal exocytosis. *Am J Reprod Immunol.*, 50, 411-9.

Breitbart, H. 2002. Role and regulation of intracellular calcium in acrosomal exocytosis. *J Repro Immunol.*, 53, 151-9.

Breitbart, H. 2003. Signalling pathways in sperm capacitation and acrosome reaction. *Cell Mol Biol.*, 49, 321-7.

Bronson, R.A., Peresleni, T., Golighty, M. 1999. Progesterone promotes the acrosome reaction in capacitated human spermatozoa as judged by flow cytometry and CD46 staining. *Mol Hum Reprod.*, 5, 507-12.

Brucker, C., Lipford, G.B. 1995. The human acrosome reaction: physiology and regulatory mechanisms. An update. *Hum Reprod Update.*, 1, 51-62.

Burkman, L.J., Coddington, C.C., Franken, D.R., Kruger, T.F., Rosenwaks, Z., Hodgen, G.D. 1988. The hemi-zona assay (HZA): development of a diagnostic test for the binding of human spermatozoa to the human hemi-zona pellucida to predict fertilization potential. *Fertil Steril.*, 49, 688-97.

Burkman, L.J., Coddington, CC., Franken, D.R., Oehninger, S.C., Hodgen, G.D. 1990. The hemi-zona assay (HZA): assessment of fertilizing potential by means of human sperm binding to the human pellucida. In: B.A. Keel, B.W. Webster, eds. *Handbook of the laboratory diagnosis and treatment of infertility.* Boca Raton, FL: CRC Press, 212-25.

Burkman, L.J. 1991. Discrimination between non-hyperactivated and classical hyperactivated motility patterns in human spermatozoa using computerized analysis. *Fertil Steril.*, 55, 363-71.

Carver-Ward, J.A., Holladers, J.M.G., Jaroudi, K.A., Einspenner, M., Al-Sedairy, S.T., Sheth, K.V. 1996. Progesterone does not potentiate the acrosome reaction in human spermatozoa: flow cytometric analysis using CD46 antibody. *Hum Reprod.*, 11, 121-6.

Chiabrera, A., Bianco, B., Moggia, E., Kaufman, JJ. 2000. Zeeman-stark modelling of the RF-EMF interaction with ligand binding. *Bioelectromagnetics*., 21, 312-24.

Coddington, C.C., Fulgam, D.L., Alexander, N.J., Johnson, D., Herr, J.C., Hodgen, G.D. 1990. Sperm bound to zona pellucida in hemi-zona assay demonstrate reaction when stained with T-6 antibody. *Fertil Steril.*, 54, 50-4.

Cooper, T.G., Neuwinger, J., Bahrs, S., Nieschlag, E. 1992. Internal quality control of semen analysis. *Fertil Steril.*, 58, 172-178.

Corselli, J., Talbot, P. 1986. An in vitro technique to study penetration of hamster oocyte-cumulus complexes by using physiological numbers of sperm. *Gamete Res.*, 13, 293-8.

Cross, N.L., Morales, P., Overstreet, J.W., Hanson, F.W. 1986. Two simple methods for detecting acrosome-reacted human sperm. *Gamte Res.*, 15, 213-26.

Cross, N.L., Morales, P., Overstreet, J.W., Hanson, F.W. 1988. Induction of the acrosome reaction by the human zona pellucida. *Biol Reprod*., 38, 235-44.

Cummins, J.M., Yanagimachi, R. 1986. Development of the ability to penetrate the cumulus oophorus by hamster spermatozoa capacitated in vitro in relation to timing of the acrosome reaction. *Gamete Res.*, 15, 187-94.

Cummins, J.M., Pember, S.M., Jequier, A.M., Yovich, J.L., Hartmann, P.E. 1991. A test of the human sperm acrosome reaction following ionophore challenge: relationship to fertility and other seminal parameters. *J Androl.*, 12, 98-103.

Darszon, A., Labarca, P., Nishigaki, T., Espinosa, F. 1999. Ion channels in sperm physiology. *Physiol Rev.*, 79, 481-510.

Darszon, A., Beltrán, C., Felix, R., Nishigaki, T., Trevino, C.L. 2001. Ion transport in sperm signalling. *Dev Biol.*, 240, 1-14.

Darzynkiewicz, Z., Li, J.G., Gorczyca, W., Muratami, T., Traganos, F. 1997. Cytometry in cell necrobiology: analysis of apoptosis and accidental cell death (necrosis) *Cytometry*., 27, 1-20.

Davoudi, M., Brössner, C., Kuber, W. 2002. The influence of electromagnetic waves on sperm motility. *J Urol Urogynaco*., 9, 18-22.

De Jonge, C.J., Barratt, C. (eds.) 2006. *The Sperm Cell: Production, Maturation, Fertilization, Regeneration.* United Kingdom: Oxford University Press.

De Lamirande, E., Gagnon, C. 1993a. Human sperm hyperactivation in whole semen and its association with low superoxide scavenging capacity in seminal plasma. *Fertil Steril.*, 59, 1291-5.

De Lamirande, E., Gagnon, C. 1993b. A positive role for the superoxide anion in triggering hyperactivation and capacitation of human spermatozoa. *Int J Androl.*, 16, 21-5.

De Lamirande, E., Gagnon, C. 1995. Capacitation-associated production of superoxide anion by human spermatozoa. *Free Rad Biol Med.*, 18, 487-95.

De Lamirande, E., Gagnon, C. 2003. Redox control of changes in protein sulfhydryl levels during human sperm capacitation. *Free Radic Biol Med.*, 35, 1271-85.

De Lamirande, E., Leclerc, P., Gagnon, C. 1997. Capacitation is a regulatory event that primes spermatozoa for the acrosome reaction and fertilization. *Mol Hum Reprod.*, 3, 175-94.

De Lamirande, E., Harakat, A., Gagnon, C. 1998. Human sperm capacitation induced by biological fluids and progesterone, but not by NADH or NADPH, is associated with the production of superoxide anion. *J Androl.*, 19, 215-25.

De Lamirande, E., Yoshida, K., Yoshiike, T.M., Iwamoto, T., Gagnon, C. 2001. Semenogelin, the main protein of semen coagulum, inhibits human sperm capacitation by interfering with the superoxide anion generated during this process. *J Androl.*, 22, 672-9.

Ecroyd, H., Jones, R.C., Aitken, R.J. 2003. Tyrosine Phosphorylation of HSP-90 during mammalian sperm capacitation. *Biol Reprod.*, 69, 1801-07.

Encyclopædia Britannica Online. 2007. Available at http://www.britannica.com/ebc/art-66050**)** [Accessed 07/03/2007].

Erogul, O., Oztas, E., Yildirim, I., Kir, T., Aydur, E., Komesli, G., Irkilata, H.C., Irmak, M.K., Peker, A.F. 2006. Effects of electromagnetic radiation from cellular phone on human sperm motility: an in vitro study. *Arc Med Res.*, 37, 840-3.

ECFP6 (European fast response team on EMF and Health). 2005. *Short-notes on the influence of cellular phones on Human Fertility.* European Commission's Directorate-General for Research. Brussels: The Office for Official Publications of the European Communities.

Evenson, D., Darzynkiewicz, Z., Jost, L., Janca, F., Ballachey, B. 1986. Changes in accessibility of DNA to various fluorochromes during spermatogenesis. *Cytometry*., 7, 45-53.

Fejes, I., Závaczki Z., Szöllõsi, J., Koloszár, S., Daru, J., Kovács, L., Pal, A. 2005. Is there a relationship between cell phone use and semen quality? *Arch Androl*., 51, 385-93.

Florman, H.M., Arnoult, C., Kazam, I.G., Li, C., O'Toole, C.M. 1998. A perspective on the control of mammalian fertilization by egg-activated ion channels in sperm: a tale of two channels. *Biol Reprod*., 59, 12-6.

Florman, H.M., Wassarman, P.M., 1985. O-linked oligosaccharides of mouse egg ZP3 account for its sperm receptor activity. *Cell*., 41, 313-24.

Ford, W.C. 2004. Regulation of sperm function by reactive oxygen species. *Hum Reprod Update*., 10, 387-99.

Franken, D.R., Burkman, L.J., Coddington, C.C., Oehninger, S., Hodgen, G.D. 1990. Human hemi-zona attachment assay. In: A.A. Acosta, R.J. Swanson, S.B. Ackerman, T.F. Kruger, J.A. van Zyl, R. Menkveld, eds. *Human spermatozoa in assisted reproduction*. Baltimore: Williams and Wilkens, 355-71.

Franken, D.R., Kruger, T.F., Oehninger, S., Coddington, C.C., Lombard, C., Smith, K., Hodgen, G.D. 1993. The ability of the hemi-zona assay to predict human fertilization in different and consecutive *in vitro* fertilization cycles. *Human Reprod*., 8, 1240-4.

Franken, D.R. 1998. New aspects of sperm-zona pellucida binding. *Andrologia*., 30, 263-8.

Franken, D.R., Oehninger, S. 2006. The clinical significance of sperm-zona pellucida binding: 17 years later. *Front Biosci*., 11, 1277-33.

García, M.A., Meizel, S. 1999. Progesterone-mediated calcium influx and acrosome reaction of human spermatozoa: pharmacological investigation of T-type calcium channels. *Biol Reprod*., 60, 102-9.

González-Martínez, M.T., Darszon, A. 1987. A fast transient hyperpolarization occurs during the sea urchin sperm acrosome reaction induced by egg jelly. *FEBS Lett*., 218, 247-50.

González-Martínez, M.T., Guerrero, A., Morales, E., De La Torre, L., Darzon, A. 1992. A depolarisation can trigger Ca2+ uptake and the acrosome reaction when preceded by hyperpolarization in L pictus sea urchin sperm. *Dev Biol*., 150, 193-202.

Hammitt, D.G., Syrop, C.H., Walker, D.L., Bennett, M.R. 1993. Conditions of oocyte storage and use of non-inseminated as compared with inseminated, non-fertilized oocytes for the hemi-zona assay. *Fertil Steril*., 60, 131-6.

Harper, C.V., Barratt, C.L., Publicover, S.J. 2004. Stimulation of human spermatozoa with progesterone gradients to simulate approach to the oocyte. Induction of $[Ca(^{2+})]_{(i)}$ oscillations and cyclicaltransitions in flagellar beating. *J Biol Chem.*, 279, 46315-25.

Harris, J.D., Hibler, D.W., Fontenot, G.K., Hsu, K.T., Yurewicz, E.C., Sacco, A.G. 1994. Cloning and characterization of zona pellucida genes and cDNAs from a variety of mammalian species: the ZPA, ZPB and ZPC gene families. *DNA Seq*., 4, 361-93.

Henkel, R., Kierspel, E., Hajimohammed, M., Stalf, T., Hoogendijk, C., Mehnert, C., Menkveld, R., Schill, W.B., Kruger, T. 2003. DNA fragmentation of spermatozoa and assisted reproduction technology. *RBM Online.*, 7, 477-84.

Henkel, R., Müller, C., Miska. W., Gips, H., Schill, W.B. 1993. Determination of the acrosome reaction in human spermatozoa is predictive of fertilization *in vitro*. *Human Reprod*., 8, 2128-32.

Henley, N., Baron, C., Roberts, K.D. 1994. Flow cytometric evaluation of the acrosome reaction of human spermatozoa: a new method using a photoactivated supravital stain. *Int J Androl*., 17, 78-84.

Herrero, M.B., Gagnon, C. 2001. Nitric oxide: a novel mediator of sperm function. *J Androl.*, 22, 349-56.

Ho, H.C., Suárez, S.S. 2001. Hyperactivation of mammalian spermatozoa: function and regulation. *Reprod*., 122, 519-26.

Hoshi, K.H., Sugano, T., Endo, C., Yoshimatsu, N., Yanagida, K., Sato, A. 1993. Induction of the acrosome reaction in human spermatozoa by human pellucida and effect of cervical mucus on zona-induced acrosome reaction. *Fertil Steril*., 60, 149-54.

Huang, S.Y., Kuo, Y.H., Tsou, H.L., Lee, Y.P., King, Y.T., Huang, H.C., Yang, P.C., Lee, W.C. 2000a. The decline of Porcine sperm motility by glendanamycin, a specific inhibitor of heat shock protein 90 (Hsp90). *Theriogenology.*, 53, 1177-84.

Huang, S.Y., Kuo, Y.H., Lee, Y.P., Tsou, H.L., Lin, E.C., Ju, C.C., Lee, W.C. 2000b. Association of heat shock protein 70 with semen quality of boars. *Animal Reprod Science.*, 63, 231-40.

Huszar, G., Ozenci, C.C., Cayli, S., Zavaczki, Z., Hansch, E., Vigue, L. 2003. Hyaluronic acid binding by human sperm indicates cellular maturity: viability and un-reacted acrosomal status. *Fertil Steril.*, 79,1616-24.

Jeyendran, R.S. (ed.). 2000. In: *Interpretation of semen analysis results: A practical guide*. Cambridge: Cambridge University press.

Kruger, T.F., Menkveld, R., Stander, F.S.H. 1986. Sperm morphological features as a prognostic factor in IVF. *Fertil Steril.*, 46, 1118-23.

Landry, J., Huot, J. 1995. Modulation of actin dynamics during stress and physiological stimulation by a signalling pathway involving p38 MAP kinase and heat shock protein 27. *Biochem Cell Biol.*, 73, 703-7.

Leclerc, P., de Lamirande, E., Gagnon, C. 1996. Cyclic adenosine 3',5' monophosphate-dedendant regulation of protein tyrosine phosphorylation in relation to human sperm capacitation and motility. *Biol Reprod.*, 55, 684-92.

Leclerc, P., de Lamirande, E., Gagnon, C. 1997. Regulation of protein-tyrosine phosphorylation and human sperm capacitation by reactive oxygen derivatives. *Free Radical Biol Med.*, 22, 643-56.

Lee, M.A., Trucco, G.S., Bechtol, K.B., Wummer, N., Kopf, G.S., Blasco, L., Storey, B.T. 1987. Capacitation and acrosome reaction in human spermatozoa monitored by chlortetraclycline fluorescence assay. *Fertil Steril.*, 48, 649-54.

Leszczynski, D., Joenväärä, S., Reivinen, J., Kuokka, R. 2002. Non-thermal activation of the hsp27/p38MAPK stress pathway by mobile phone radiation in human endothelial cells: Molecular mechanism for cancer- and blood brain barrier-related effects. *Differentiation.*, 70, 120-9.

Liévano, A., Sánchez, J., Darzon, A. 1985. Single channel activity of bilayers derived from sea urchin sperm plasma membranes at the tip of a patch-clamp electrode. *Dev Biol*., 112, 253-7.

Lui, D.Y., Lopata, A., Johnston, W.I., Baker, H.W.G. 1989. Human sperm-zona pellucida binding, sperm characteristics and in-vitro fertilisation. *Hum Reprod*., 4, 686-701.

Lui, D.Y., Baker, H.W.G. 1990. Inducing the human acrosome reaction with calcium ionophore A23187 decreases sperm-zona pellucida binding with oocytes that failed to fertilize *in vitro*. *J Reprod Fertil*., 89, 127-34.

Matwee, C., Kamaruddin, M., Betts, D.H., Basrur, P.K., King, W.A. 2001. The effects of antibodies to heat shock protein 70 in fertilisation and embryo development. *Mol Hum Reprod*., 7, 829-37.

Meizel, S. 1997. Amino acid neurotransmitter receptor/chloride channels of mammalian sperm and acrosome reaction. *Biol Reprod.*, 56, 569-74.

Miller, D., Brough, S., Al-Harbi, O. 1992. Characterization and cellular distribution of human spermatozoal heat shock proteins. *Hum Reprod*., 7, 637-45.

Miyazaki, R., Funda, M., Takeuchi, H., Itoh, S., Takada, M. 1990. Flow cytometry to evaluate acrosome-reacted sperm. *Arch Androl.*, 25, 243-51.

Morales, E., de la Torre, L., Moy, G.W., Vacquier, V.D., Darzon, A. 1993. Anion channels in sea urchin sperm plasma membrane. *Mol Reprod Dev*., 36, 174-82.

Mortimer, S.T., Swan, M.A., Mortimer, D. 1998. Effect of seminal plasma on capacitation and hyperactivation in human spermatozoa. *Hum Reprod*., 13, 2139-46.

Mortimer, D., Mortimer, S.T. 1999. Laboratory investigation of the infertile male. In: P.R. Brindin, ed. *A textbook of in vitro fertilization and assisted reproduction*, 2nd ed. Cambridge: Parthenon Publishing group, 53-81.

Mujica, A., Neri-Bazan, L., Tash, J.S., Uribe, S. 1994. Mechanism for procaine-mediated hyperactivated motility in guinea pig spermatozoa. *Mol Reprod Dev*., 38, 285-92.

Neuer, A., Mele, C., Liu, H.C., Rosenwaks, Z., Witkin, S.S. 1998. Monoclonal antibodies to mammalian heat shock proteins impair mouse embryo development in vitro. *Hum Reprod*., 13, 987-90.

Nikolaeva, M.A., Golubeva, E.L., Kulakov, V.I., Sukhikh, G.T. 1998. Evaluation of stimulus-induced acrosome reaction by two-colour flow cytometric analysis. *Mol Hum Reprod*., 4, 243-50.

Nunez, R., Murphy, T.F., Huang, H.F., Baron, E. 2004. Use of SYBR14, &-Amino-Actinomycin D, and JC-1 in assessing sperm damage from rats with spinal cord injury. *Cytometry*., 61, 56-61.

O'Brien, M.C., Bolton, W.E. 1995. Comparison of cell viability probes compatible with fixation and permeabilization for combined surface and intracellular staining in flow cytometry. *Cytometry*., 19, 243-55.

Oehninger, S., Franken, D., Kruger, T., Toner, J.P., Acosta, A.A., Hodgen, G.D. 1991. Hemi-zona assay: sperm defect analysis, a diagnostic method for assessment of human sperm-oocyte interactions, and predictive value for fertilization outcome. *Ann NY Acad Sci*., 626, 111-24.

Oehninger, S., Patankar, M., Seppala, M., Clark, G.F. 1998. Involvement of selectin-like carbohydrate binding specificity in human gamete interaction. *Andrologia*., 30, 269-74.

Oehninger, S., Franken, D.R., Sayed, E., Barosso, G., Kolm, P. 2000. Sperm function assays and their predictive value for fertilization outcome in IVF: a meta-analysis. *Hum Reprod Update*., 6, 160-8.

Oehninger, S. 2001. Molecular basis of human sperm-zona pellucida interaction. *Cell Tissue Organ*., 168, 58-64.

Okamura, N., Tajima, Y., Soejima, A., Masuda, H., Sugita, Y. 1985. Sodium bicorbonate in seminal plasma stimulates the motility of mammalian spermatozoa through direct activation of adenylate cyclase. *J Biol Chem*., 260, 9699-705.

Patrat, C., Serres, C., Jouannet, P. 2000. Induction of a sodium ion influx by progesterone in human spermatozoa. *Biol Reprod*., 62, 1380-6.

Philpott, N.J., Turner, A.J.C., Scopes, M., Westby, M., Marsh, J.C.W., Gordon-Smith, E.C., Dalgleish, A.G. 1996. The use of 7-Amino Actinomycin D in identifying apoptosis: Simplicity of use and broad spectrum of application compared with other techniques. *Blood*., 87, 2244-51.

Plante, M., de Lamirande, E., Gagnon, C. 1994. Reactive oxygen species released by activate neutrophils, but not by deficient spermatozoa, are sufficient to affect normal sperm motility. *Fertil Steril*., 62, 387-93.

Purdy, P.H., Graham, J.K. 2004. Effect of adding cholesterol to bull sperm membranes on sperm capacitation, the acrosome reaction, and fertility. *Biol Reprod.,* 71, 522-7.

Purvis, K., Rui, H., Scholberg, A., Hesla, S., Takada, M. 1990. Application of flow cytometry to studies on the human acrosome. *J Androl.*, 25, 245-51.

Riedy, M.C., Muirhead, K.A., Jensen, C.P., Stewart, C.C. 1991. Use of a photolabelling technique to identify nonviable cells in fixed homologous or heterologous cell populations. *Cytometry*., 12, 133-9.

Rossato, M., Di Virgilio, F., Rizzuto, R., Galeazzi, C., Foresta, C. 2001. Intracellular calcium store depletion and acrosome reaction in human spermatozoa: role of calcium and plasma membrane potential. *Mol Hum Reprod*., 7, 119-28.

Sánchez, R., Toepfer-Petersen, E., Aitken, R.J., Schill, W.B. 1991. A new method for evaluation of the acrosome reaction in viable human spermatozoa. *Andrologia*., 23, 197-203.

Sato, Y., Son, J.H., Tucker, R.P., Meizel, S. 2000. The zona pellucida-initiated acrosome reaction: defect to mutations in the sperm glycine receptor Cl channel. *Dev Biol*., 227, 211-8.

Schmid, I., Krall, W.J., Uittenbogaart, C.H., Braun, J., Giorgi, J.V. 1992. Dead cell discrimination with 7-amini-actinomycin D in combination with dual colour immunofluorescence in single laser flow cytometry. *Cytometry*., 13, 201-8.

Siegel, M.S., Paulson, R.J., Graczykowski, J.W. 1990. The influence of follicular fluid on the acrosome reaction, fertilizing capacity and protease activity of human spermatozoa. *Hum Reprod*., 5, 975-80.

Stock, C.E., Bates, R., Lindsay, K.S., Edmonds, D.K., Fraser, L.R. 1989. Human oocyte-cumulus complexes stimulate the acrosome reaction. *J Reprod Fert*., 86, 723-30.

Talbot, P., Chacon, R.S. 1981. A triple-stain technique for evaluating normal acrosome reactions of human sperm. *J Exp Zoology*., 215, 201-8.

Tesarik, J., Mendoza, C. 1993. Sperm treatment with pentoxyfylline improves the fertilizing ability in patients with acrosome reaction insufficiency. *Fertil Steril.*, 60, 141-8.

Töpfer-Petersen, E., Auerbeck, J., Weiss, A., Friess, A.E., Schill, W.B. 1986. The sperm acrosome: immunological analysis using polyclonal and monoclonal antibodies directed against the outer acrosomal membrane of boar spermatozoa. *Andrologia.*, 18, 237-51.

Töpfer-Petersen, E. 1999. Carbohydrate-based interactions on the route of a spermatozoon to fertilization. *Hum Reprod Update.*, 5, 314-29.

Tosti, E., Boni, R. 2004. Electrical events during gamete maturation and fertilization in animals and humans. *Human Reprod Update.*, 10, 153-65.

Trestappen, L.W.M.M., Shah, V.O., Conrad, M.P., Recktenwald, C., Loken, M.R. 1988. Discriminating between damaged and intact cells in fixed flow cytometric samples. *Cytometry.*, 9, 477-84.

Uhler, M.L., Leung, A., Chan, S.Y.W., Schmid, I., Wang, C. 1993. Assessment of human sperm acrosome reaction by flow cytometry: validation and evaluation of the method by fluorescence-activated cell sorting. *Fertil Steril.*, 60, 1076-81.

Visconti, P.E., Westbrook, V.A., Chertihin, O., Demarco, I., Sleight, S., Diekman, A.B. 2002. Novel signalling pathways involved in sperm acquisition of fertilizing capacity. *J Reprod Immunol.*, 53, 133-50.

Wassarman, P.M., Litscher, E.S. 1995. Sperm-egg recognition mechanisms in mammals. *Curr Top Dev Bio.*, 30, 1–19.

Whittington, K., Ford, W.C. 1999. Relative contribution of leukocytes and of spermatozoa to reactive oxygen species production in human sperm suspensions. *Int J Androl.*, 22, 229-35.

Wolf, D.P., Boldt, J., Byrd, W., Bechtol, K.B. 1985. Acrosomal status evaluation in human ejaculated sperm with monoclonal antibodies. *Biol Reprod.*, 32, 1157-62.

WHO (World Health Organisation). 1999. *WHO laboratory manual for the examination of human semen and sperm-cervical mucus interaction*. 4th ed. Cambridge: Cambridge University Press.

Yanagimachi, R. In: R.H Asch, J.P. Balmaceda, I. Johnston, eds. 1990. *Gamete Physiology*. Serono Symposia, USA.

Yanagimachi, R. 1994. Mammalian Fertilisation. In: E. Knobil, J. Neill, eds. *The physiology of reproduction*. 2nd ed. New York: Raven Press., 189-317.

Zini, A., Finelli, A., Phang, D., Jarvi, K. 2000. Influence of sperm processing technique on human sperm DNA integrity. *Urology*., 56, 1081-4.

CHAPTER 4

APOPTOTIC STATUS OF HUMAN SPERMATOZOA

4.1 INTRODUCTION

The ability of fully differentiated human spermatozoa to initiate apoptosis is not conclusive at this point (Oehninger *et al*., 2003; Taylor *et al*., 2004). Some attribute the presence of apoptotic markers such as morphological changes (Baccetti *et al*., 1996; Gandini *et al*., 2000), loss of asymmetric distribution of PS at the plasma membrane (Barroso *et al*., 2000; Oosterhuis *et al*., 2000), FAS positivity (Sakkas, 1999; Pentikainen *et al*., 1999), and DNA fragmentation (Barroso *et al*., 2000; Gandini *et al*., 2000) to failed apoptosis during spermatogenesis (Sakkas *et al*., 1999, 2002, 2003; Said *et al*., 2004; Almeida *et al*., 2005). On the other hand, other studies hypothesise a sperm specific apoptotic pathway (Weng *et al*., 2002) independent of caspase activation (Weng *et al*., 2002; Tesarik *et al*., 2004).

Regardless of whether human spermatozoa are able to initiate apoptosis or not, many physiological processes in spermatozoa are mediated by organelles/molecules that also serve as biomarkers for apoptosis. For instance, loss of mitochondrial membrane potential could result in the release of cytochrome-c into the cytosol triggering the caspase-9 dependant apoptotic pathway (Kroemer and Reed, 2000). However, in human spermatozoa, loss of mitochondrial membrane potential has a direct effect on sperm motility (Marchetti, 2002). Therefore, change in mitochondrial membrane potential as a result of RF-EMF exposure could provide a sensitive marker for sperm fecundity.

Another process known to occur in the early stages of apoptosis is the externalisation of the phospholipid, phosphatidylserine. PS externalisation is governed by scramblase activity (Vermes *et al*., 1995), and it is also associated with bicarbonate-mediated phospholipid scrambling during capacitation of human spermatozoa (Gadella and Harrison, 2002; de Vries *et al*., 2003; Martin *et al*., 2005). Thus, PS externalisation not only indicates the initiation of early apoptosis, but it also signifies that membrane changes required for capacitation are operational in human spermatozoa. Capri *et al*. (1995) reported on the RF-field effects on scramblase

activity, therefore necessitating the investigation of the effect of RF-EMF on PS externalisation in human spermatozoa.

Furthermore, Leszczynski *et al*. (2002) reported that RF-EMF inhibits apoptosis through the caspase-3 dependant apoptotic pathway. In human sperm, the role for caspases is still questionable. However, Weng *et al*. (2002), de Vries *et al*. (2003) Paasch *et al*. (2003) and Taylor *et al*. (2004) recently reported the presence of active and inactive forms of caspases in low and highly motile fractions of human sperm. The possibility that RF-EMF could influence caspase activity therefore had to be investigated.

Lastly, it has been proposed that a caspase independent pathway could be operational in sperm; therefore if RF-EMF could initiate apoptosis in spermatozoa it should be confirmed by investigating DNA fragmentation. Various studies have claimed a genotoxic effect of RF exposure (Lai and Singh, 1995, 1996, 1997; Maes *et al*., 1996; Tice *et al*., 2002; Mashevich *et al*., 2003). In addition, ROS generation as a consequence of RF-EMF could also contribute to DNA fragmentation. Irmak *et al*., (2002) reported that RF exposure lead to an increase in oxidative stress. Hence, the generation of ROS and DNA fragmentation required investigation.

This section therefore focused on the detection of cellular stress in RF-EMF exposed human spermatozoa by determining changes in various apoptotic markers (PS externalisation, mitochondrial membrane potential changes, caspase activation, and DNA fragmentation, as well as reactive oxygen species generation).

4.2 EXPERIMENTAL PROTOCOL

To determine the effect of RF-RMF on early- (PS externalisation, $\triangle\psi m$, and caspase activation) and late- apoptotic markers (DNA fragmentation), as well as factors that could affect apoptotic markers (endogenous generation of ROS), RF-EMF exposed and control spermatozoa were subjected to a variety of assays. A diagram outlining the experimental approach is shown in Figure 4.1.

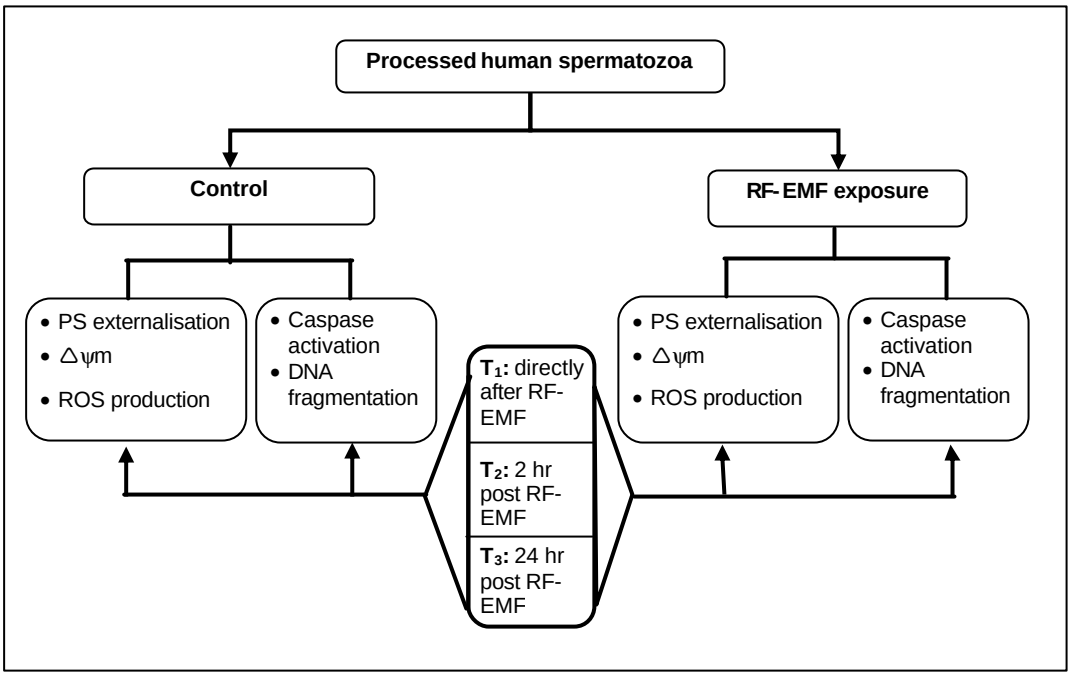

Figure 4.1 RF-EMF exposure protocol: Assessment of the apoptotic status post RF-EMF and control exposure.

Apoptosis detected by Annexin V staining (PS externalisation), Δψm by MitoTracker® Red uptake and ROS generation by conversion of hydroethidine (HE) to ethidium were all assessed on the same day at three different time points over a period of 4 weeks for all twelve donors. Similarly, caspase activation and DNA fragmentation were assessed at a later date, again on the same day at three different time points over a period of 4 weeks for all twelve donors. This was necessary due to the fact that it was not practicably possible to simultaneously evaluate all apoptotic parameters at each time point. Appropriate solvent controls were used as positive and negative controls for each biomarker.

Semen collected from the donors were purified by density gradient centrifugation (as described in Chapter 3) and seeded at a concentration of to 20 x 10^6 sperm/ml in petri dishes marked for RF-EMF exposure or controls (2 petri dishes each). Directly after the control/RF-EMF exposure, spermatozoa were gently recovered from the petri dishes, transferred to separate conical test tubes (Lasec) and concentrations were adjusted to 20 x 10^6/ml by centrifugation (300 g for 5 min). Spermatozoa were then incubated under capacitating conditions (5% CO_2 at 37°C) and assessed at different

time points (directly (T_1), 2 (T_2) and 24 (T_3) hours post-exposure) for apoptosis. All tests were run in duplicate.

Flow cytometric analysis was performed on a Coulter Epics® XL.MCL flow cytometer (XL.MCL) equipped with an air cooled argon laser (Beckman Coulter) for the analysis of all SAR 2.0 W/kg samples, while a Coulter Epics® Altra flow cytometer (Altra) equipped with a water cooled coherent enterprise laser (Beckman Coulter) was used for analysis of all SAR 5.7 W/kg samples unless otherwise stated. Appropriate controls were used to confirm the results from the different flow cytometers. The sperm population was identified using forward-angle light scatter, while side-angle light scatter was used to exclude electronic noise and debris. A total of 10 000 events were acquired for each endpoint. Analysis was done with System II software when using the XL.MCL and EXPO 32 software when using the Altra. The results are expressed as the mean cell number with SD.

4.3 ASSESSMENT OF THE APOPTOTIC STATUS IN SPERMATOZOA

4.3.1 Phosphatidylserine externalisation determined by the Annexin V assay

Early phases of apoptosis are marked by the loss in plasma membrane asymmetry resulting in the translocation of the membrane phospholipid PS from the inner to the outer plasma membrane leaflet, thereby exposing PS to the external environment. Annexin V is 35-36 kDa Ca^{2+}-dependant phospholipid-binding protein with a high affinity for PS, therefore it serves as a sensitive probe for detecting sperm within a population that are actively undergoing apoptosis (Koopman *et al*., 1994; Vermes *et al*., 1995; Martin *et al*., 1995). Annexin V is conjugated with FITC for easy detection.

PI is a standard flow cytometric viability probe and can be used to distinguish viable from non-viable sperm (Koopman *et al*., 1994; Vermes *et al*., 1995; Martin *et al*., 1995; O'Brein and Bolton, 1995). Viable sperm with intact membranes will exclude PI whereas damaged or dead sperm will be permeable to PI. Using Annexin V-FITC in conjunction with PI, one can distinguish between viable sperm (Annexin V-FITC and PI negative), sperm that are in early apoptosis (Annexin V-FITC positive and PI

negative), sperm that are in late apoptosis or already dead (Annexin V-FITC and PI positive), and nonviable sperm (sperm that have already undergone apoptotic death and those that have died as a result of a necrotic pathway).

To determine PS externalisation, BD Bioscience's Annexin V-FITC apoptosis detection kit II (BD Biosciences) was used. The Annexin V-FITC staining protocol of the manufacturer was followed, with minor adjustments.

4.3.1.1 Annexin V-FITC staining protocol

Aliquots (100 µl) taken from the control and RF exposed spermatozoa were re-suspended in 2 ml cold Dulbecco's PBS (Sigma Chemical Co.) and washed by centrifugation (300 g for 5 min). Spermatozoa were re-suspended in 400 µl Annexin V binding buffer (BD Biosciences) (10 mM Hepes/NaOH (pH 7.4), 140 mM NaCl, 2.5 mM $CaCl_2$) at a concentration of 5 x 10^6 sperm/ml. A 100 µl of the solution was then transferred to a 5 ml flow tube to which 5 µl Annexin V-FITC (BD Biosciences) and 5 µl of PI (BD Biosciences) were added. The sperm were gently vortexed and left to incubate for 15 min at room temperature (25°C) in the dark.

After the incubation time, 400 µl of the Annexin V binding buffer was added to each tube and the spermatozoa were analysed by flow cytometry within 20 min. A minimum of 10 000 spermatozoa were examined for each test. The sperm population was gated by using forward-angle light scatter, while side-angle light scatter was used to exclude electronic noise and debris. The FITC-labelled Annexin V positive sperm were measured in the FL1 channel. PI fluorescence is detected in the far-red range of the spectrum (650 nm long pass filter) (Schmid *et al*., 1992; O'Brein and Bolton, 1995) and PI-labelled sperm were measured in the FL2 channel of the flow cytometer. All tests were run in duplicate.

To ensure specificity of Annexin V-FITC binding, appropriate controls were used. Recombinant Annexin V provided a negative control while, staurosporine used to induce apoptosis, provided a positive control for Annexin V-FITC labelling.

4.3.1.2 Annexin V blocking by recombinant Annexin V

Recombinant Annexin V was provided as part of the BD Bioscience Annexin V-FITC apoptosis detection kit II. Pre-incubation of cell samples with purified recombinant Annexin V serves to block Annexin V-FITC binding sites, thereby demonstrating the specificity of Annexin V-FITC staining. The protocol provided by the manufacturers was followed.

Sperm were washed twice by centrifugation (300 g for 5 min) with cold Dulbecco's PBS and then re-suspended in Annexin V binding buffer at a concentration of 1 x 10^6 sperm/ml. Of this cell suspension, 100 µl was transferred to a 5 ml flow tube. Purified recombinant Annexin V (10 µg) was then added to the suspension and the sperm were gently mixed and left to incubate for 15 min at room temperature. Annexin V-FITC (5µl) was added and the sperm incubated for a further 15 min in the dark after which 400 µl of the Annexin V binding buffer was added to each tube and the spermatozoa were analysed by flow cytometry within 20 min.

4.3.1.3 Induction of apoptosis by staurosporine

Cells induced to undergo PCD by staurosporine die with the characteristic morphological features of apoptosis followed by caspase activation (Weil *et al.*, 1998). Although the exact activation mechanism is still unknown, staurosporine acts as a protein kinase inhibitor, and induced cell death can be repressed by either the over-expression of the PCD-suppressor gene Bcl-2 or petide caspase inhibitors (Jacobson *et al.*, 1993, 1994, 1996; Bertrand *et al.*, 1994). It has previously been demonstrated that staurosporine induces apoptosis in human spermatozoa (Weng *et al.*, 2001; Morshedi *et al.*, 2003) and specifically increases PS translocation (Morshedi *et al.*, 2003).

Staurosporine (Sigma Chemical Co.) was stored as aliquots at a stock concentration of 1 mM at -20ºC. To establish optimal agonist concentrations, induction of apoptosis assessed by the Annexin V assay was performed for a range of concentrations for staurosporine. Directly before experimentation, aliquots were diluted in BSA free Ham's F-10 medium and added to sperm (1 x 10^6/ml) at final concentrations of 1 µM, 5 µM, and 10 µM. Sperm were incubated for 15 min with

the different staurosporine concentrations after which 0.5% BSA was added to the sperm suspension. The sperm were left to incubate for a further 2 hours in a humidified CO_2 incubator at 37°C, washed twice by centrifugation (300 g for 5 min) with cold PBS before proceeding with Annexin V-FITC staining protocol and flow cytometric analysis.

4.3.2 Mitochondrial membrane potential

Baseline $\Delta\psi m$ was determined by the method described by Marchetti *et al*. (2004a) with minor adjustments. Mitochondria were stained with the mitochondrial selective stain MitoTracker® Red CMXRos (Molecular Probes, Eugene, USA). The MitoTracker® Red probe passively diffuses across the plasma membrane and accumulates in active mitochondria. MitoTracker® Red CMXRos is excited at a frequency of 579 nm and emits at 599 nm. Mitochondrial membrane depolarisation is thus associated with a decrease in fluorescence.

4.3.2.1 MitoTracker® Red CMXRos staining procedure

MitoTracker® Red CMXRos was stored as a stock concentration of 1 mM at -20°C, dilutions were made directly before staining and MitoTracker® was added to sperm at a final concentration of 150 nM per 1 x 10^6 sperm/ml in 0.5% BSA supplemented Ham's F-10 medium. Sperm suspensions were then incubated for 15 min in a humidified (5% CO_2) incubator at 37°C. After incubation, sperm were washed (5 min at 300 g), the supernatant removed and the sperm re-suspended in 1 ml warm medium (37°C) before being analysed by flow cytometry. MitoTracker® Red CMXRos fluorescence was detected in FL3.

4.3.2.2 Abolishment of $\Delta\psi m$ by Carbamoylcyanide m-chlorophenylhydrazone

Carbamoylcyanide m-chlorophenylhydrazone (mClCCP) has previously been used to abolish the mitochondrial membrane potential of spermatozoa (Marchetti *et al.*, 2002). Spermatozoa (1 x 10^6/ml) were incubated in the presence of 50 µmol/l mClCCP for 15 min at 37°C in a humidified incubator (5% CO_2) before proceeding with the MitoTracker® Red CMXRos staining procedure to determine $\Delta\psi m$.

4.3.3 Detection of superoxide

ROS in semen are either produced by the infiltration of leukocytes as a result of genitourinary inflammation (Wolff, 1995) or is a consequence of damaged and immature spermatozoa (Aitken *et al.*, 1988). Spermatozoa are highly susceptible to peroxidative damage due to the abundance of polyunsaturated fatty acids in their plasma membrane (Aitken *et al.*, 1989). The primary product of ROS production in human spermatozoa is the superoxide anion radical ($O_2^{-\cdot}$) which subsequently dismutases to H_2O_2 in the presence of intracellular superoxide dismutase (Aitken and Fisher, 1994). Intrinsic ROS production has been linked to DNA damage in spermatozoa (Griveau and Le Lannou, 1997; Henkel *et al.*, 2004). For this reason, ROS production was evaluated not only as a possible consequence of RF-EMF exposure but also to determine its effect on DNA damage. Furthermore, the presence of leucocytes in the ejaculate also contributes to ROS production therefore a leukocyte specific antigen (CD45) was used to firstly identify and quantify leukocytes in the sperm population of all donors and secondly to correctly gate the sperm population.

4.3.3.1 Detection of $O_2^{-\cdot}$ with hydroethidine

The methods described by Marchetti *et al.* (2002) and Henkel *et al.* (2004) for the detection of the superoxide anion radical in human spermatozoa was adapted. Hydroethidine (Molecular Probes Inc.) an uncharged cell-permeant compound is converted to cationic ethidium by superoxide oxidation. Ethidium (E^+) is cell impermeant and intercalates with the DNA.

Hydroethidine was stored as stock solutions of 1 mM in DMSO at -20ºC. Directly prior to use, HE (2 µmol/l) was added to spermatozoa in BSA free Ham's F-10 medium recovered from the RF exposed and control petri-dishes (1 x 10^6 sperm/ml). Sperm suspensions were then incubated for 15 min at 37°C in a humidified incubator (5% CO_2), washed by centrifugation (300 g for 5 min) with 2 ml PBS, and re-suspended in 1 ml PBS before FCM analysis. Ethidium fluorescence was detected in FL1.

It has previously been shown that cytofluorometric analysis of white blood cells (WBC) and seminal leukocytes are comparable (Ricci *et al*., 2000). Therefore, to correctly identify and gate different WBC subpopulations a known number (2 x 10^6 white blood cells / 1 x 10^6 sperm/ml) of peripheral blood leukocytes (obtained from heparinized blood of healthy donors), were added to normal semen samples devoid of leukocytes. CD 45 labelling as outlined above was then used to correctly gate the different leukocyte regions.

4.3.3.2 Determination of leukocyte contamination in processed spermatozoa

The presence of leukocytes in seminal plasma contributes to the inhibition of both sperm movement and ATP production (Armstrong *et al*., 1999; Henkel *et al*., 2004). Therefore, to eliminate the effect of leukocytes on spermatozoa, leukocyte presence in processed sperm were detected by labelling leukocytes with a monoclonal CD45 antibody to enable the correct gating of the sperm population for flow cytometry.

The CD45 leukocyte antigen conjugated with FITC (BD Bioscience) reacts with the 180, 190, 205, and 220 KDa isoforms of the leukocyte antigen present on all human leukocytes including lymphocytes, monocytes, granulocytes, eosinophils, and thymocytes (Knapp *et al*., 1989). The antibody was stored at 4°C.

The percentage leukocyte contamination present in each of the twelve donor's processed sample was determined by adding 20 µl of the CD45 solution to 1 x 10^6 sperm/ml suspensions and incubating samples for 20 min at room temperature in the dark. After incubation, samples were analysed by flow cytometry. The FITC signal was measured on FL 1 through a 530/30 nm band pass filter.

4.3.4 Caspase-3 activation.

Caspase-3 is a key protease that is activated during the early stages of apoptosis. Active caspase-3 (aCp3), is a marker for cells that are actively undergoing apoptosis, and once activated, proteolytically cleaves and activates other caspases as well as relevant targets within the cytoplasm, namely D4-GDI, Bcl-2, and poly-ADP-ribose polymerase (PARP) in the nucleus (D'Amours *et al*., 1999).

Active caspase-3 consists of a heterodimer of 17 and 12 kDa subunits derived from the 32 kD proenzyme. BD Pharmingen (BD Bioscience) supplies a PE-conjugated monoclonal rabbit-anti active caspase-3 antibody apoptosis kit containing essential reagents for measuring apoptosis by flow cytometric analysis. The PE-conjugated monoclonal rabbit-anti active caspase-3 antibody recognises both human and mouse aCp3. The antibodies were raised against a sequence corresponding to active human caspase-3 and are affinity purified using Protein G and conjugated with PE under optimal conditions (contains no unconjugated antibody). The antibodies are solubilized in phosphate buffer (pH 7.2) with 500 mM NaCl, 0.09% (w/v) sodium azide and 0.2% (w/v) BSA and are stored at 4°C.

Reagents supplied with the kit include, Cytofix/Cytoperm™ Solution and Perm/Wash™ Buffer. The Cytofix/Cytoperm™ Solution (neutral pH-buffered saline, saponin and 4% (w/v) paraformaldehyde) was used for the simultaneous fixation and permeabilization of sperm prior to intracellular staining and was stored at 4°C. Perm/Wash™ Buffer was used to permeabilise sperm for intracellular staining, and also serves as an antibody diluent and cell wash buffer. The buffer contains foetal bovine serum (FBS), sodium azide and saponin and is stored at 4°C.

4.3.4.1 Active caspase-3 PE staining protocol

Sperm recovered from the RF exposed petri dishes were first labelled with MitoTracker® Red CMXRos before being washed twice with cold PBS, re-suspended in Cytofix/Cytoperm™ solution at a concentration of 1 x 10^6 sperm/0.5 ml, and incubated for 20 min on ice. Sperm were then pelleted (centrifuge at 300 g for 5 min) and the supernatant discarded after which sperm were washed twice (300 g for 5 min) with Perm/Wash™ buffer at a volume of 0.5 ml buffer/1 x 10^6 sperm at room temperature. Next, sperm were re-suspended in a 100 µl Perm/Wash™ buffer per 20 µl antibody containing solution and incubated for 30 min at room temperature. After incubation, spermatozoa were again washed in 1 ml Perm/Wash™ buffer and finally re-suspended in 0.5 ml Perm/Wash™ buffer before flow cytometric analysis.

4.3.4.2 Caspase inhibition by CaspACE™ FITC-VAD-FMK

CaspACE™ FITC-VAD-FMK (Promega Corporation, Madison, USA) is used as an *in situ* marker for apoptosis. The marker is a FITC conjugate of the cell permeable caspase inhibitor VAD-FMK. This structure allows delivery of the inhibitor into the cells where it binds to activated caspases. CaspACE™ FITC-VAD-FMK *in situ* marker is supplied as a 5 mM solution in DMSO.

RF-EMF and control cells (1 x 10^6/ml) were washed (300 g for 5 min) with 2 ml PBS before the pellet was re-suspended in 1 ml PBS and 5 µM CaspACE™ FITC-VAD-FMK was added to the suspension. Cells were then incubated for 20 min at room temperature in the dark before being washed twice, re-suspended in 1 ml PBS, and analysed by FCM. FITC fluorescence was detected in FL1.

4.3.5 DNA fragmentation

One of the later steps of apoptosis resulting from the activation of endonucleases during PCD is DNA fragmentation (Enari *et al*., 1998; Sakahira *et al*., 1998). These nucleases degrade the higher order chromatin structure into fragments of ~300 kb and subsequently into even smaller fragments of about 50 bp in length (Walker *et al*., 1993). The APO-DIRECT™ kit (BD Bioscience) is a single step method for labelling DNA breaks with FITC-dUTP (TUNEL – Terminal deoxynucleotidyl transferase-mediated dUTP nick end labelling).

The kit comprises of two parts. Part A contains the PI/RNase staining buffer (5 µg/ml PI, 200 µg/ml RNase), reaction buffer (containing cacodylic acid [dimethylarsenic]), rinsing buffer (containing 0.05% sodium azide), and wash buffer (containing 0.05% sodium azide). Part B contains FITC-dUTP (0.25 nMol/reaction containing 0.05% sodium azide), negative control cells and positive control cells (both containing 70% (v/v) ethanol) as well as TdT enzyme ([S.A. = 100,000 U/mg] 200 µg/ml in 50% (v/v) glycerol solution). The control cells were derived from a human lymphoma cell line and have already been fixated.

4.3.5.1 Fixation protocol for APO-Direct™ samples

Spermatozoa recovered from the RF exposed and control petri dishes were re-suspended at a concentration of 2 x 10^6 sperm/ml in 1% (w/v) paraformaldehyde

(Sigma Chemical Co.) in PBS (pH 7.4). The cell suspension was incubated on ice for 30 min before the sperm were centrifuged for 5 min at 300 g and the supernatant discarded. Sperm were washed in 5 ml of PBS and again pelleted by centrifugation before the wash procedure was repeated. The cell pellet was then re-suspended in the residual PBS by gentle vortexing and adjusted to 1 x 10^6 sperm/ml in 70% ice-cold ethanol. Sperm were frozen at -20°C until assessment at a later stage.

4.3.5.2 APO-Direct™ staining protocol

Frozen sperm were left to thaw at room temperature before commencing with the labelling step. The sperm were re-suspended by gently swirling the tubes after which the cell suspensions were centrifuged for 5 min at 300 g. The supernatant containing the 70% (v/v) ethanol was removed by gentle aspiration and the sperm re-suspended in 1 ml of the wash buffer. The cell suspension was washed twice more by centrifuging (300 g, 5 min) before the supernatant was discarded and the sperm re-suspended in 50 µl of the staining solution (10 µl reaction buffer, 0.75 µl TdT Enzyme, 8 µl FITC-dUTP and 32.25 µl distilled H_2O/ assay).

The samples suspended in the staining solution were incubated for 60 min at 37°C after which they were washed twice in 1 ml of the rinse buffer (300g, 5 min). After removing the supernatant by gentle aspiration, the cell pellet was re-suspended in 0.5 ml of the PI/RNase staining buffer. The sperm were incubated for 30 min at room temperature in the dark after which DNA fragmentation was assessed by flow cytometry. For each determination, at least 10 000 spermatozoa were examined by using flow cytometry. The FITC-labelled dUTP-positive spermatozoa were measured in the FL 1 channel of the flow cytometer.

4.3.5.3 Induction of DNA fragmentation by DNase

A positive control sample was prepared by the additional treatment of each sample with RQ1 RNase-Free DNase (Promega Corporation, Madison, WI, USA). RQ1 (RNA-Qualified) RNase-Free DNase is a DNase 1 (endonuclease) that degrades both double-stranded and single-stranded DNA producing 3′-OH oligonucleotides (Moore, 1981). After fixation and permeabilization of spermatozoa in preparation of the APO-Direct™ protocol, sperm (1 x 10^6 sperm/ml) were pelleted and re-

suspended in 10 µl of the 10x reaction buffer (40 mM Tris-HCL [pH 8.0], 10 mM $MgSO_4$ and 1 mM $CaCl_2$ – Promega Corp.) to which 2 IU RQ1 RNase-Free DNase was added. Spermatozoa were incubated for 15 min at 37°C. After incubation, the reaction was stopped by incubating the samples in 10 µl (20 mM) RQ1 DNase stop solution (pH 8.0) for 10 min at 65°C. Samples were washed twice with PBA (PBS + 0.5% BSA) before commencing with the labelling step of the APO-Direct™ protocol described above.

4.4 STATISTICAL ANALYSIS

To determine the effect of different concentrations of staurosporine on sperm viability assessed using the Annexin V-FITC and PI assay, data were analysed using a two-tailed paired t-test with GraphPadPrism® version 4.01 software (GraphPadSoftware, San Diego, CA, USA).

The effect of RF exposure on various apoptotic parameters was determined by analysing the data with Stata Statistical Software Release 8.0 (Stata Corp.) using a within subject design considering two treatments, control vs. RF-EMF (SAR 2.0 or 5.7 W/kg), at three time points (T_1 - directly after exposure, T_2 - 2 hours after exposure and T_3 - 24 hours after exposure), for a total of 12 donors. Results were analysed using time series regression under the random effect option. Data is presented as mean values ± SD for all twelve donors with each test run in duplicate. Repeatability of duplicate tests was confirmed with the intraclass correlation coefficient for assays = 0.92. Correlations between different apoptotic markers were computed using the Pearson's correlation coefficient. All statistical tests were two-sided and statistical significance was considered when $p < 0.05$.

4.5 RESULTS

4.5.1 Phosphatidylserine externalisation determined by the Annexin V assay

Results of Annexin V staining specificity using recombinant Annexin V and induction of PS externalisation using staurosporine are shown in Figures 4.2 and 4.3 respectively. A typical flow cytometric dot plot and fluorescence histograms after

Annexin V and PI staining are shown in Figure 4.4. The effect of 900 MHz GSM (SAR of 2.0 and 5.7 W/kg) irradiation on PS externalisation are summarised in Figures 4.5 and 4.6 respectively.

4.5.1.1 Annexin V blocking by recombinant Annexin V

Figure 4.2 shows a typical fluorescence histogram of the total Annexin V (16.5%) staining (red) in a density purified sperm sample. After addition of 10 µg purified recombinant Annexin V to 1 x 10^6 /ml sperm suspensions, Annexin V staining was completely blocked (blue).

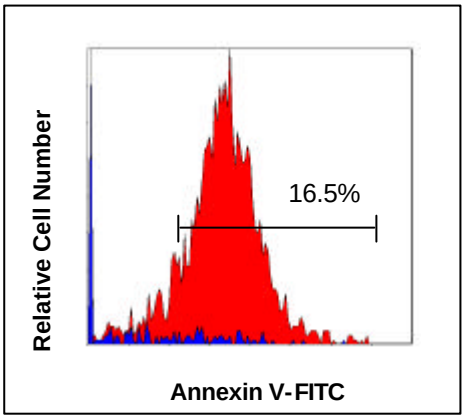

Figure 4.2 Flow cytometric histograms of total Annexin V before (red) and after (blue) addition of recombinant Annexin V- demonstrating the specificity of Annexin V staining.

4.5.1.2 Induction of apoptosis by staurosporine

The percentage PI^+, Annexin V^+, and apoptotic (Annexin V^+ PI^-) cells after addition of different concentrations of staurosporine are depicted in Figure 4.3. The percentage PI positive stained cells increased from 20.65 ± 0.35 for control cells to 92.380 ± 0.09 after 2 hour exposure to 10 µM staurosporine. Using a lower concentration (1 µM), no statistical significant difference in viability was noted between control cells and staurosporine treated cells after 2 hours. The total amount of PS externalised after a 2 hour exposure to 10 µM staurosporine was highly significant ($p < 0.0001$) compared to control cells. When comparing PS

externalisation (Annexin V^+) after staurosporine treatment in viable cells (PI^-), there was no statistical significant difference in $\%AV^+/PI^-$ control and 1 µM staurosporine treated cells. However $\%AV^+/PI^-$ control cells differed significantly from 5 µM ($p < 0.05$) and 10 µM ($p < 0.005$) staurosporine treated cells.

Spermatozoa treated with 1 µM staurosporine were again analysed by flow cytometry after a further incubation period of 2 hours (4 hours after addition of staurosporine). The number of non-viable cells (PI^+) differed significantly ($p < 0.005$) as well as the total amount of PS externalised (Annexin V^+) ($p < 0.005$) compared with the 2 hour viability and PS assessment. However, no statistically significant difference in percentage Annexin V^+/PI^- sperm after the additional 2 hour assessment was noted.

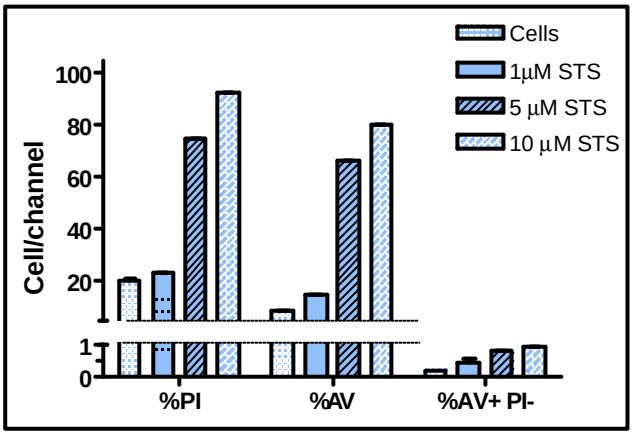

Figure 4.3 The percentage PI, Annexin V and Annexin V^+/PI^- sperm after a 2 hour exposure to 1 µM, 5 µM and 10 µM staurosporine (STS), each datum represents the mean ± SD of three determinations.

4.5.1.3 The effect of 900 MHz GSM irradiation on phophatidylserine externalisation

Figure 4.4 shows a typical dot-plot with fluorescence histograms of the flow cytometric analysis of PS externalisation in spermatozoa. PI fluorescence is used to distinguish viable and non-viable cells in the sperm population. The dot-plot regions

respectively correspond to necrotic cells - $AV^- PI^+$, dead cells - $AV^+ PI^+$, unlabelled sperm population - $AV^- PI^-$, and apoptotic cells - $AV^+ PI^-$. The population gated by C in histogram A notes the total Annexin V fluorescence. PI fluorescence, shown in histogram B and gated by E, gives the total population of dead cells in the sample. In some samples, a secondary peak of weaker fluorescence (gated by D in histogram B), were noted.

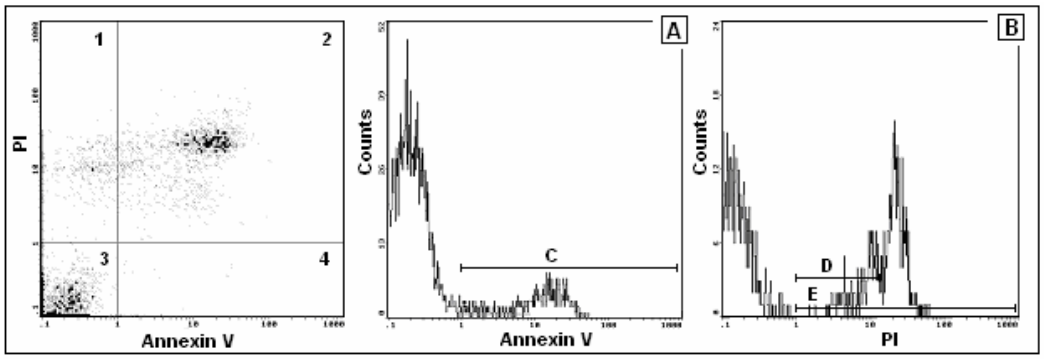

Figure 4.4 Dot plot and fluorescence histograms of **(A)** Annexin V and **(B)** PI staining of human spermatozoa.

When considering the total Annexin V staining after 1 hour RF-EMF exposure at a SAR value of 2.0 W/kg (Figure 4.5 A_1) no difference ($p = 0.406$) was seen between RF exposed and control cells assessed directly after exposure (T_1), 2 hours after exposure (T_2), or 24 hours after exposure (T_3). Similarly, no difference was seen in total PI fluorescence ($p = 0.144$) (Figure 4.5 A_2) and number of apoptotic cells ($p = 0.784$) (Annexin $V^+ PI^-$ Figure 4.5 A_3). There was also no difference in the number of apoptotic necrotic ($p = 0.407$) (Annexin $V^+ PI^+$ Figure 4.6 A_1) and dead cells ($p = 0.651$) (Annexin $V^- PI^+$ Figure 4.6 A_2).

For a SAR of 5.7 W/kg, no difference ($p = 0.448$) between RF exposed and control cells determined directly (T_1), 2(T_2) and 24 hours (T_3) after exposure were noted when total Annexin V staining (Figure 4.5 B_1) was assessed. This was also the case with total PI fluorescence ($p = 0.323$) (Figure 4.5 B_2) and number of apoptotic cells ($p = 0.711$) (Annexin $V^+ PI^-$) (Figure 4.5 B_3). The total number of apoptotic necrotic

($p = 0.457$) (Annexin V^+ PI^+ Figure 4.6 B_1) and dead cells ($p = 0.841$) (Annexin V^- PI^+ Figure 4.6 B_2) were also not significantly affected. Interestingly, for both SAR values Annexin V^+ PI^- cells decreased at T_2 (Figure 4.6 A_3 and B_3).

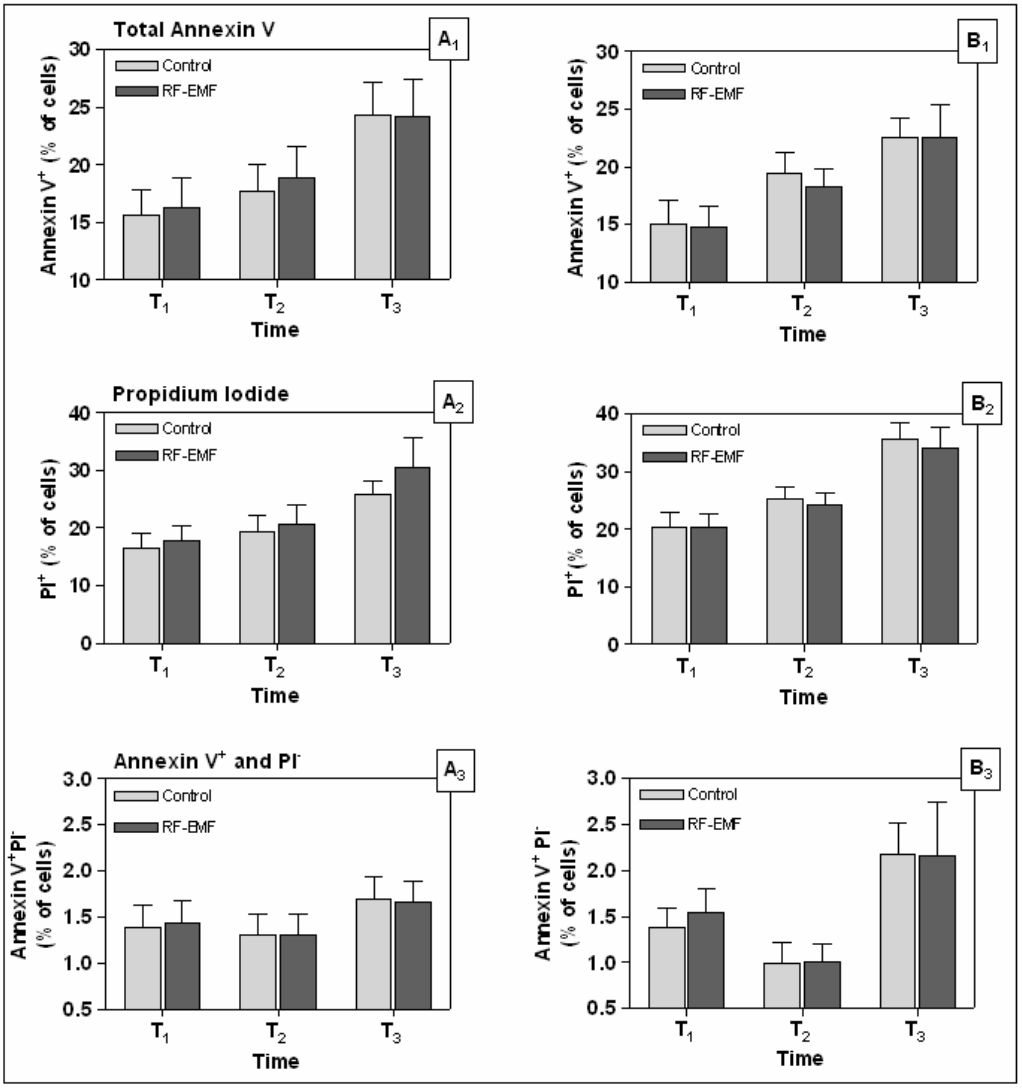

Figure 4.5 In **A_1** (2.0 W/kg) and **B_1** (5.7 W/kg) the total percentage Annexin V staining is noted as a function of time. **A_2** (2.0 W/kg) and **B_2** (5.7 W/kg) depict the total percentage of non-viable cells (PI^+) as a function of time. **A_3** (2.0 W/kg) and **B_3** (5.7 W/kg) show the total percentage Annexin V^+ viable cells (PI^-) as a function of time.

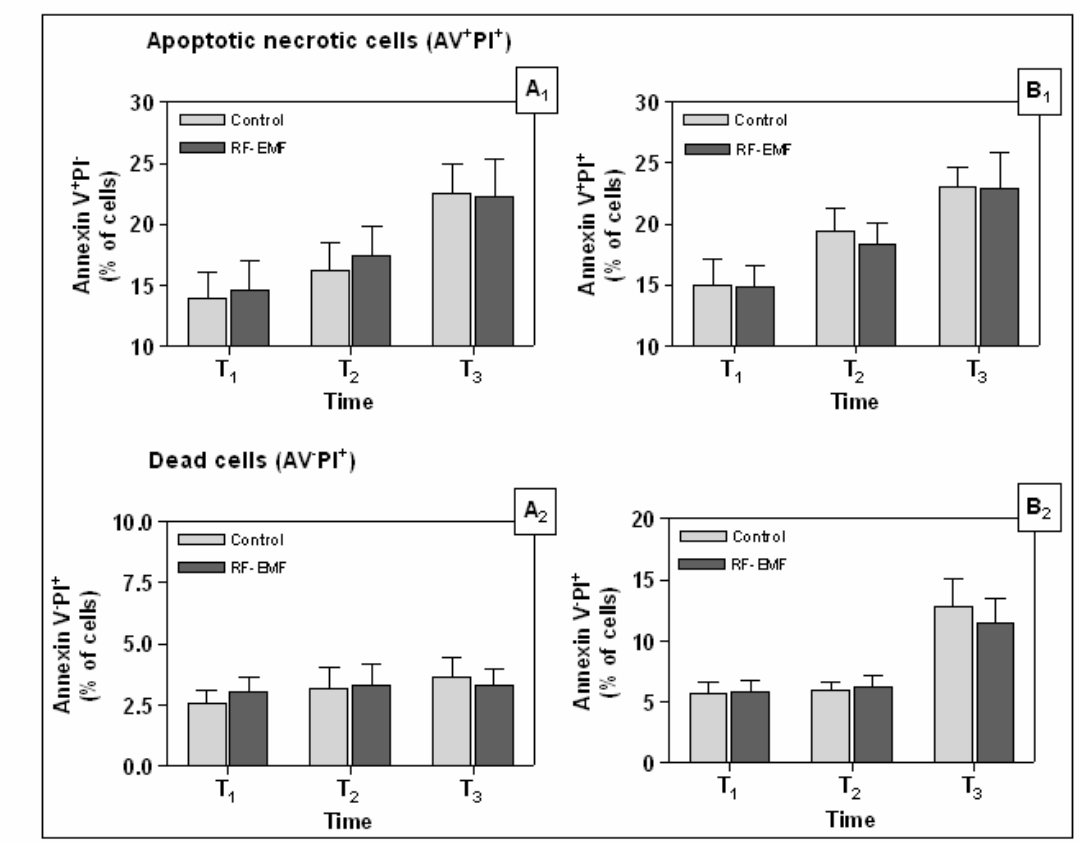

Figure 4.6 In Figures **A_1** (2.0 W/kg) and **B_1** (5.7 W/kg) the total number of apoptotic necrotic (Annexin V^+ PI^+) staining is noted as a function of time. **A_2** (2.0 W/kg) and **B_2** (5.7 W/kg) depict the total percentage of dead cells (Annexin V^- PI^+) as a function of time.

To determine the effect of the increased exposure dose on cell viability (PI fluorescence) and PS externalisation (Annexin V fluorescence), total Annexin V fluorescence, total PI fluorescence, and percentage apoptotic cells (Annexin V^+ PI^-) of RF-exposed sperm at all three time points at 2.0 W/kg were also compared with sperm exposed at 5.7 W/kg. This was possible, as control values for the different SAR levels did not differ significantly between experiments. Using Stata statistical software a paired t-test was performed at each time point for each SAR level. No statistical difference in total Annexin V fluorescence, total PI fluorescence, or percentage apoptotic cells determined at any of the time points were observed (Table 4.1).

Table 4.1 Summary of paired t-test results comparing viability (PI-fluorescence) and PS externalisation (Annexin V fluorescence) of RF-exposed spermatozoa at SAR 2.0 W/kg with SAR 5.7 W/kg.

Biomarker	T_1	T_2	T_3
Propidium Iodide	p = 0.391	p = 0.241	p = 0.885
Annexin V	p = 0.673	p = 0.798	p = 0.504
Annexin V^+ PI^-	p = 0.767	p = 0.297	p = 0.985

Investigating the progression of apoptosis in RF-EMF exposed cells (SAR 2.0 W/kg), a Pearson's correlation test was used to correlate the percentage early apoptotic cells (Annexin V^+ PI^-) with late apoptotic-necrotic cells (Annexin V^+ PI^+), as well as percentage dead cells (Annexin V^- PI^+) (Table 4.2). Similar correlations and statistical significance were observed for control cells (data not shown) as well as RF-EMF exposed cells (SAR 5.7 W/kg).

Table 4.2 Comparison between Annexin V^+ PI^-, Annexin V^+ PI^+ and Annexin V^- PI^+ staining cells as a progression of time.

	Biomarker	Annexin V^+ PI^-	Annexin V^+ PI^+	Annexin V^- PI^+
T_1				
	Annexin V^+ PI^-		r = 0.523, p = 0.121	r = 0.496, p = 0.145
	Annexin V^+ PI^+			r = 0.857, p < 0.005**
T_2				
	Annexin V^+ PI^-		r = 0.520, p =0.101	r = 0.698, p < 0.05*
	Annexin V^+ PI^+			r = 0.863, p < 0.005**
T_3				
	Annexin V^+ PI^-		r = 0.718, p < 0.05	r = 0.464, p = 0.129
	Annexin V^+ PI^+			r = 0.794, p < 0.005**

* significant, ** highly significant

There was a significant positive correlation between late apoptotic necrotic cells (Annexin V^+ PI^+) and early apoptotic cells (Annexin V^+ PI^-) after 24 hours (Table 4.2). However no correlation was seen between early apoptotic (Annexin V^- PI^+) and dead cells (Annexin V^- PI^+), except at T_2 - 2 hours after exposure. This corresponds

with the decrease seen in Annexin V^+ PI^- staining. A highly significant correlation existed at all three time points between apoptotic necrotic (Annexin V^+ PI^+) and dead spermatozoa (Annexin V^- PI^+).

4.5.2 Mitochondrial membrane potential

A typical flowcytometric representation of MitoTracker® Red CMXRos staining is shown in Figure 4.7. Depolarisation of the mitochondrial membrane potential is associated with a shift in fluorescence. The effect of 900 MHz GSM irradiation on mitochondrial membrane potential with SAR values of 2.0 and 5.7 W/kg respectively are summarised in Figure 4.8.

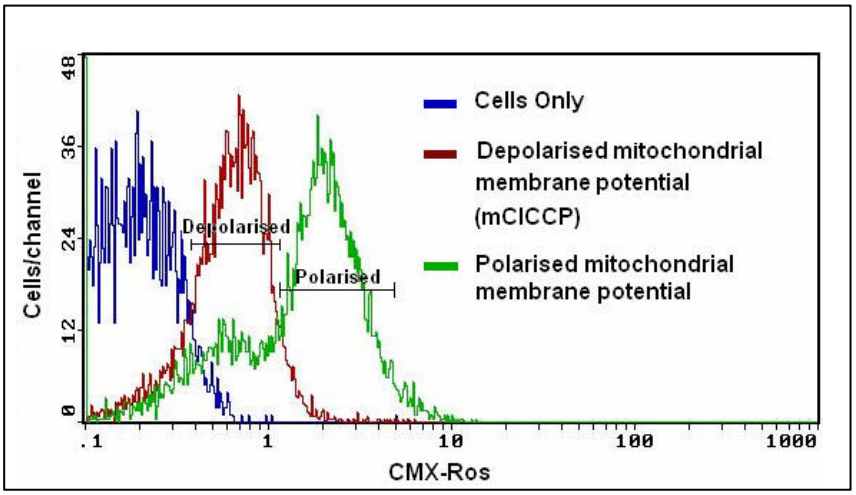

Figure 4.7 Cytofluorometric analysis of the depolarisation of the mitochondrial membrane potential showing a frequency histogram of processed spermatozoa (blue) stained with, MitoTracker® Red CMXRos before treatment (green) with the mitochondrial membrane potential abolisher mClCCP (red-brown).

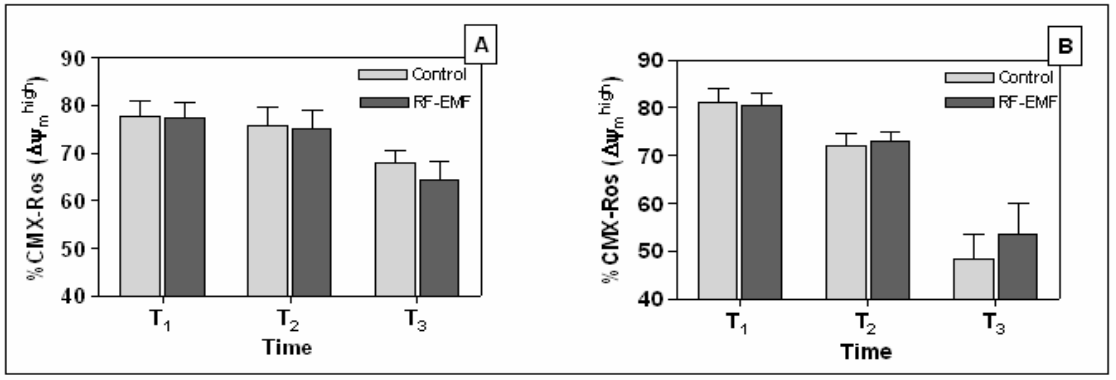

Figure 4.8 The percentage of MitoTracker® Red CMXRos (150 nM) staining in RF-EMF exposed sperm at a SAR of (A) 2.0 W/kg and (B) 5.7 W/kg compared to control samples determined as a function of time.

For both 2.0 W/kg and 5.7 W/kg the mitochondrial membrane potential decreased significantly ($p < 0.05$) over time (Figure 4.8 A and B). However this decrease was not significant ($p = 0.272$ and $p = 0.751$) between RF exposed compared with control sperm at SAR values 2.0 and 5.7 W/kg respectively (Figure 4.8 A and B). Furthermore there was no interaction observed between exposed (SAR 2.o ơ 5.7 W/kg) and control spermatozoa.

From Figure 4.8 it is evident that a dose (SAR 2.0 vs. 5.7 W/kg) effect was not present since at all the respective time points control and SAR values displayed similar polarised mitochondrial membrane percentages ($\Delta\psi_m^{high}$).

4.5.3 Detection of ROS

4.5.3.1 Detection of leukocyte contamination in processed spermatozoa

Cytofluorometric dot plots of gated white blood cells in a processed sperm sample (population C) are depicted in Figure 4.9. The population of cells gated by D note the total population of lymphocytes, E notes the population of monocytes and F notes the population of granulocytes. After addition of 2 x 10^6 white blood cells/ml to the processed sperm sample (Figure 4.9 B), the percentage of $CD45^+$ labelled white blood cells normalized to the gated population increased 50 fold for lymphocytes and monocytes and 96 fold for granulocytes.

When analysing the total number of white blood cell (population D + E + F) contamination in the processed sample of each of the twelve donors, the percentage $CD45^+$ labelled cells normalised to the total sperm population was less than 0.62%.

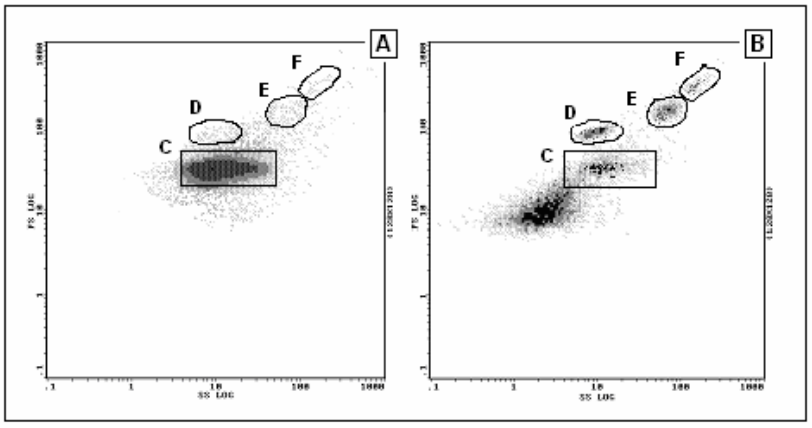

Figure 4.9 Cytofluorometric dot plot showing **(C)** gated sperm population, **(D)** lymphocytes, **(E)** monocytes and **(F)** granulocytes in **(A)** a processed sperm population and **(B)** a processed sperm population spiked with 2 x 10^6 white blood cells.

4.5.3.2 Detection of O_2^- with hydroethidine

A typical fluorescence histogram of HE staining is depicted in Figure 4.10. ROS generation, specifically O_2^- production, increased with the addition of white blood cells, shown in Figure 4.10 as an increase in HE fluorescence.

A statistical significant increase ($p < 0.05$) in O_2^- production was noted after 24 hours in both RF exposed and control sperm for both SAR values (Figure 4.11). However, there was no difference in O_2^- production in spermatozoa exposed at SAR 2.0 W/kg ($p = 0.641$) or 5.7 W/kg ($p = 0.402$) compared to control cells determined directly (T_1), 2 (T_2) and 24 hours (T_3) after exposure.

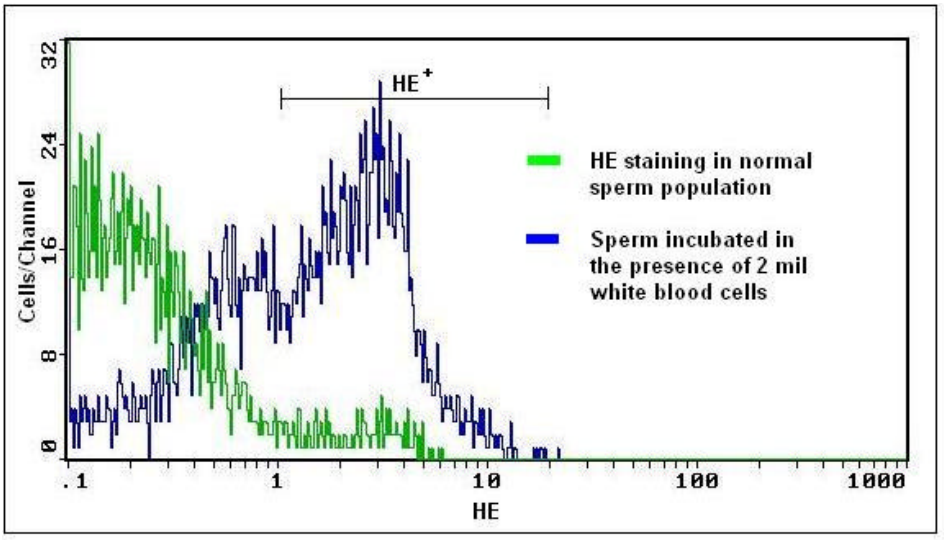

Figure 4.10 Cytofluorometric analysis of O_2^- production in human spermatozoa using hydroethidine (HE). Frequency histogram notes the increased production of ethidium (E^+) due to superoxide oxidation in processed spermatozoa incubated in the presence of 2 x 10^6/ml white blood cells (blue) compared to normal sperm (green).

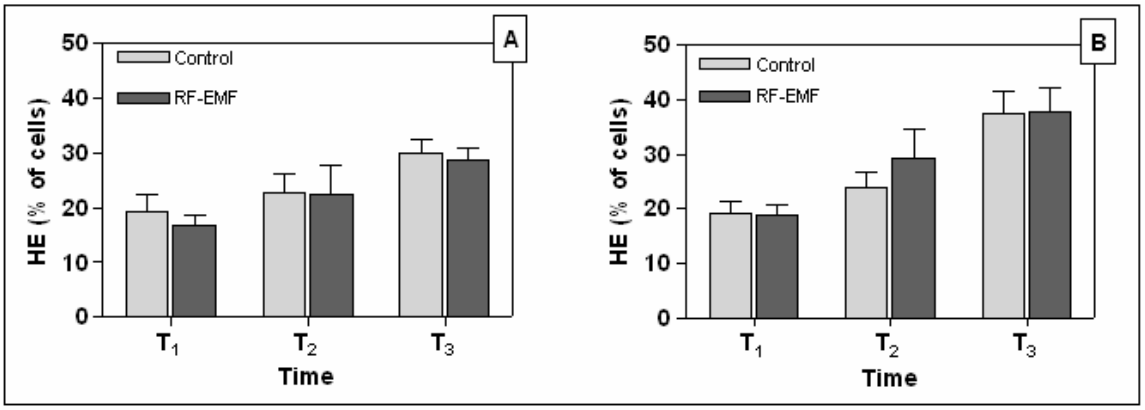

Figure 4.11 The percentage of hydroethidine staining in sperm exposed to RF-EMF at **(A)** SAR 2.0 W/kg and **(B)** SAR 5.7 W/kg compared to control samples determined directly after exposure (T_1), 2 hours after exposure (T_2) and 24 hours after exposure (T_3).

4.5.4 Caspase activation

4.5.4.1 Detection of active caspase-3

In all samples (n =12) analysed, active caspase-3 activity was less than 1% after density gradient purification (Figure 4.12). There was also no statistically significant difference in time series regression analysis (p = 0.320) assessing caspase-3 activity after RF-EMF exposure at 2.0 W/kg compared to controls (Figure 4.12). Due to the low yield in active caspase-3 activity, a biomarker FITC-VAD-FMK, directed against all active caspase activity, was used to assess the effect of RF fields at SAR's 2.0 and 5.7 W/kg on total caspase activation.

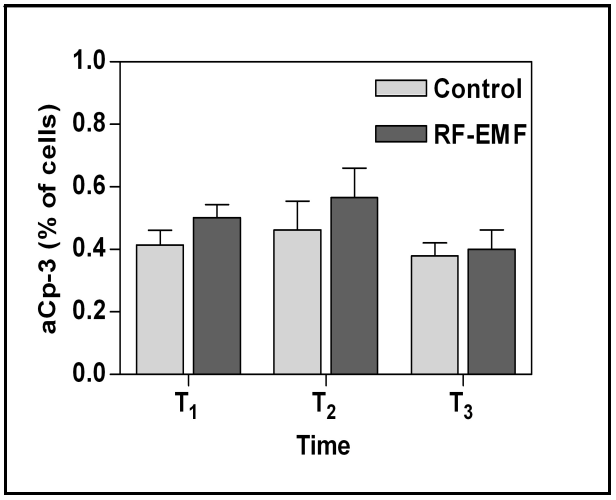

Figure 4.12 The percentage of cells staining positive for activated caspase-3 determined for control and RF-EMF (SAR 2.0 W/kg) exposed cells detected at T_1 (directly after exposure), T_2 (2 hours after exposure) and T_3 (24 hours after exposure).

4.5.4.2 FITC-VAD-FMK detection of activated caspases

Figure 4.13 shows the fluorescent intensity profile over time of a processed sperm sample labelled with FITC-VAD-FMK measured by flow cytometry. The cytofluorometric profiles show a major population presenting FITC-VAD^- (or unlabeled cells), while a smaller sub-population denotes the FITC-VAD^+ cell population. The unstained population (brown) shifted after FITC-VAD-FMK staining, the secondary population (smaller peak) shows the positive FITC-VAD-FMK staining.

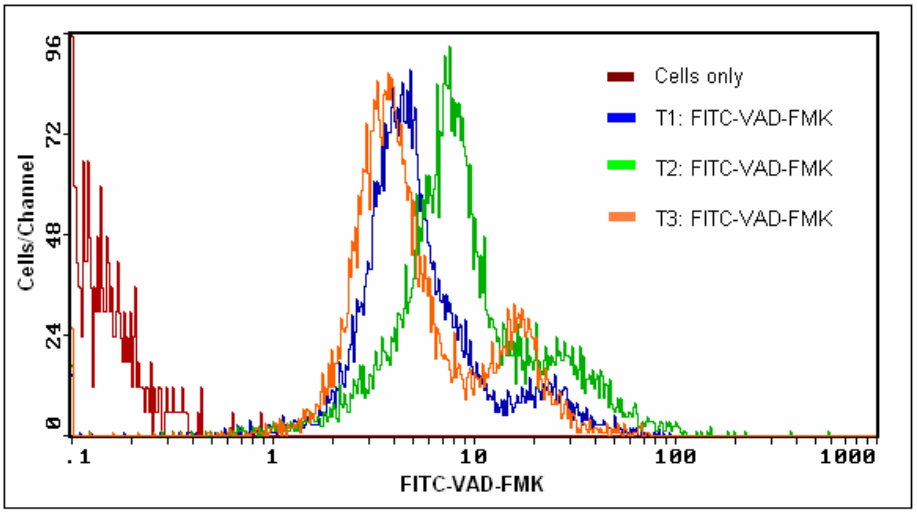

Figure 4.13 Cytofluorometric analysis of the frequency histogram of processed spermatozoa (red-brown) stained with, FITC-VAD-FMK directly after RF-EMF exposure (blue), 2 hours after exposure (green) and 24 hours after exposure (orange).

Statistical analysis of active caspase activation after 1 hour RF-EMF irradiation (SAR 2.0 W/kg) determined for both RF exposed and control cells at T_1 (directly after exposure), T_2 (2 hours after exposure) and T_3 (24 hours after exposure) note a decrease in activated caspases (Figure 4.14 A). However, the decrease in activated caspases in RF-exposed sperm did not differ statistically from control sperm ($p = 0.395$) as determined over the 24 hour period. Similarly, at a SAR level of 5.7 W/kg, there was no difference in caspase activation comparing RF exposed and control sperm ($p = 0.537$) (Figure 4.14 B).

However, caspase activation determined in RF exposed sperm (SAR 2.0 W/kg) decreased over time, whereas an increase over time was noted in RF exposed sperm at SAR 5.7 W/kg. Bearing in mind that only three donors were used at the higher SAR level, it is quite plausible that the differences in caspase activation noted for the different SAR values could be due to the relatively small sample size and large variances at the higher SAR value and not a true reflection of caspase activation for all twelve donors as noted at the SAR of 2.0 W/kg.

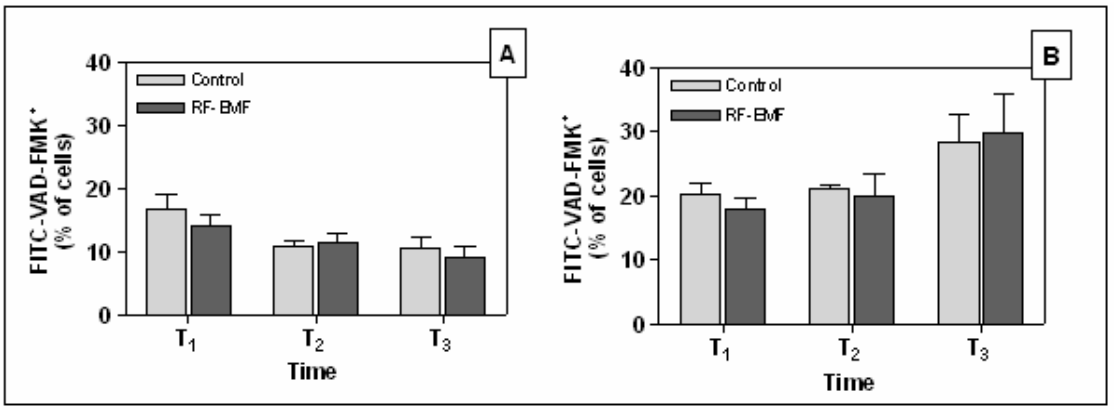

Figure 4.14 The percentage of cells staining positive for FITC-VAD-FMK determined for control and RF-EMF **(A)** SAR 2.0 W/kg and **(B)** SAR 5.7 W/kg exposed cells detected at T_1 (directly after exposure), T_2 (2 hours after exposure) and T_3 (24 hours after exposure).

4.5.5 DNA fragmentation

Figure 4.15 illustrates the fluorescent staining of fragmented DNA detected by TUNEL (FITC-dUTP) labelling. After DNase treatment, the unlabeled cell population (red-brown) shifted completely to the right demonstrating an increase of $TUNEL^+$ staining. A smaller fraction of fragmented DNA (green population) is noted in normal processed spermatozoa.

In Figure 4.16 A, the percentage TUNEL positive stained cells after 1 hour RF-EMF (SAR 2.0 W/kg) exposure is compared to control cells at different time points (directly after exposure - T_1, 2 hours after exposure - T_2 and 24 hours after exposure - T_3). The percentage $TUNEL^+$ control cells increased more rapidly over time compared to RF exposed cells, however, this difference was not statistically significant ($p = 0.298$). There was also no statistical difference ($p = 0.122$) in percentage $TUNEL^+$ sperm at the higher SAR level (5.7 W/kg) noted between RF exposed and control sperm shown in Figure 4.16 B.

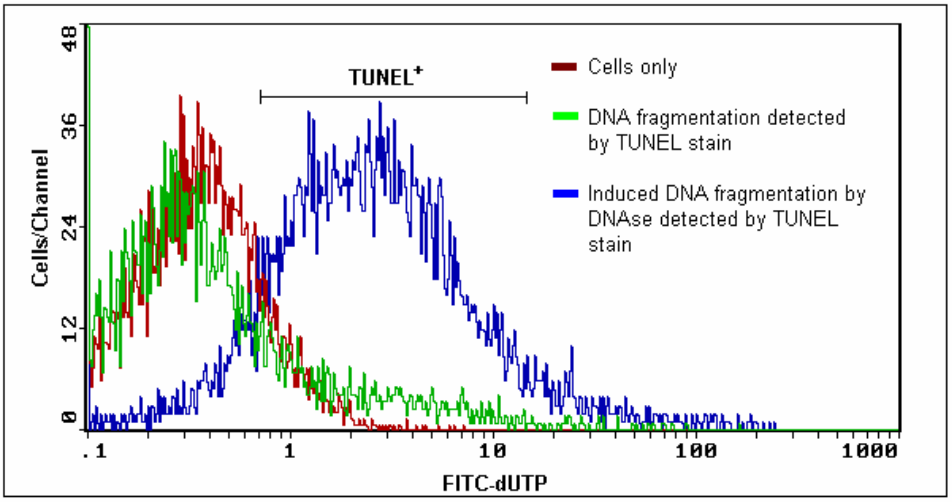

Figure 4.15 Cytofluorometric analysis of the frequency histogram of processed unstained spermatozoa (red-brown), before TUNEL staining (green) and induction of DNA damage using DNAse (blue).

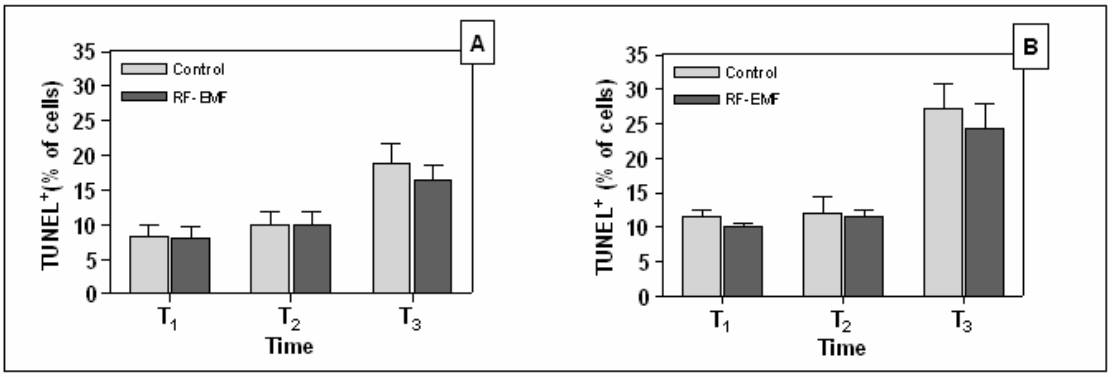

Figure 4.16 The percentage of cells staining positive for TUNEL determined for control and RF-EMF **(A)** SAR 2.0 W/kg and **(B)** SAR 5.7 W/kg exposed cells detected at T_1 (directly after exposure), T_2 (2 hours after exposure) and T_3 (24 hours after exposure).

4.5.6 Correlation between apoptotic markers and ROS

Table 4.3 A and B summarises the correlation coefficients (Pearson's) of apoptotic markers after RF-EMF exposure at SAR 2.0 W/kg and SAR 5.7 W/kg respectively.

Table 4.3 A Correlations between apoptotic biomarkers of RF-EMF (SAR – 2.0 W/kg) exposed spermatozoa evaluated directly (T_1), 2 hours (T_2) and 24 hours (T_3) after exposure.

T_1	$AV^+ PI^-$	CMXRos	F-VAD-FMK	TUNEL	HE
$AV^+ PI^-$		r = -0.618; p < 0.05*	r = -0.775; p < 0.005**	r = 0.111; p = 0.732	r = 0.466; p = 0.175
CMXRos			r = 0.470; p = 0.123	r = -0.157; p = 0.626	r = -0.015; p = 0.968
F-VAD-FMK				r = -0.347; p = 0.269	r = 0.018; p = 0.962
TUNEL					r = -0.100; p = 0.783
HE					
T_2					
$AV^+ PI^-$		r = -0.660; p < 0.05*	r = -0.327; p = 0.326	r = 0.065; p = 0.849	r = -0.399; p = 0.374
CMXRos			r = 0.319; p = 0.312	r = -0.261; p = 0.412	r = -0.374; p = 0.408
F-VAD-FMK				r = -0.107; p = 0.739	r = -0.442; p = 0.321
TUNEL					r = -0.489; p = 0.266
HE					
T_3					
$AV^+ PI^-$		r = -0.283; p = 0.428	r = -0.009; p = 0.984	r = -0.158; p = 0.684	r = -0.449; p = 0.225
CMXRos			r = -0.552; p = 0.199	r = -0.361; p = 0.339	r = -0.032; p = 0.935
F-VAD-FMK				r = -0.264; p = 0.492	r = -0.192; p = 0.680
TUNEL					r = -0.635; p = 0.066
HE					

AV = Annexin V; PI = Propidium iodide; F-VAD-FMK = FITC-VAD-FMK; TUNEL = Terminal deoxynucleotidyl transferase-mediated dUTP nick end labelling; HE = hydroethidine.

Table 4.3 B Correlations between apoptotic biomarkers of RF-EMF (SAR – 5.7 W/kg) exposed spermatozoa evaluated directly (T_1), 2 hours (T_2) and 24 hours (T_3) after exposure.

T_1	$AV^+ PI^-$	CMXRos	F-VAD-FMK	TUNEL	HE
$AV^+ PI^-$		r = 0.652; p = 0.548	r = 0.784; p = 0.427	r = -0.317; p = 0.795	r = 0.955; p = 0.191
CMXRos			r = 0.982; p = 0.121	r = -0.926; p = 0.247	r = -0.398; p = 0.739
F-VAD-FMK				r = -0.838; p = 0.368	r = 0.565; p = 0.618
TUNEL					r = -0.837; p = 0.368
HE					
T_2					
$AV^+ PI^-$		r = -0.863; p = 0.337	r = 0.974; p = 0.144	r = -0.051; p = 0.967	r = 0.969; p = 0.157
CMXRos			r = -0.727; p = 0.481	r = -0.460; p = 0.696	r = -0.960; p = 0.180
F-VAD-FMK				r = -0.274; p = 0.823	r = 0.890; p = 0.301
TUNEL					r = -0.194; p = 0.876
HE					
T_3					
$AV^+ PI^-$		# correlations not possible because TUNEL and F-VAD data only collected for 3 donors, not 12			
CMXRos					
F-VAD-FMK					
TUNEL					
HE					

AV = Annexin V; PI = Propidium iodide; F-VAD-FMK = FITC-VAD-FMK; TUNEL = Terminal deoxynucleotidyl transferase-mediated dUTP nick end labelling; HE = hydroethidine

4.6 DISCUSSION

In recent years, flow cytometry has become the method of choice for analysis of apoptosis in a variety of cell systems as it provides a rapid, accurate, and quantitative analysis of a high number of cells (Telford *et al*., 1994; Darzynkiewicz *et al*., 1997). This application is also currently widely used in assessing apoptosis in human spermatozoa (Ricci *et al*., 2000; D'Cruz *et al*., 2000; Oosterhuis *et al*., 2000; Sakkas *et al*., 2002; Marchetti *et al*., 2004a,b; Erenpreiss *et al*., 2004; Eley *et al*., 2005).

Although there are many conflicting reports on whether apoptosis is possible in fully differentiated spermatozoa, the classical approach of investigating the effect of a possible "toxic" agent entails the study of cell proliferation, apoptosis, and the possibility of a dose related effect. Using this approach we embarked on a comprehensive study of the effect of 900 MHz RF-EMF on early and late apoptotic markers in human spermatozoa.

PS externalisation is an early upstream indicator of apoptosis as its presence on the outer leaflet of the plasma membrane precedes other alterations such as DNA fragmentation, changes in nuclear and cytoplasmic organisation, and cellular fragmentation into apoptotic bodies (van Blerkom and Davis, 1998). In an attempt to induce apoptosis in spermatozoa using staurosporine, concentrations of 5 µM and 10 µM, although significantly increasing the amount of PS externalisation, also effectively killed the spermatozoa. A lower concentration (1 µM) did not cause a marked increase in cell death (PI^+), but even though the total amount of PS (Annexin V^+) increased significantly, this was not accompanied by a significant increase in apoptotic cells (Annexin V^+ PI^-). Bearing in mind that apoptosis can take place in a few hours or even minutes (Wyllie *et al*., 1980; Majno and Joris, 1995; Uchiyama, 1995; Vaux and Korsmeyer, 1999), and that it progresses rapidly, it is difficult to detect cells in early stages of apoptosis (Schwartzman and Cidlowski, 1993). This was also demonstrated in a study of Ramos and Wetzels (2001), were Annexin V binding of sperm following addition of H_2O_2 increased in conjunction with an increase in dead cells (PI^+), resulting in almost all cells being in apoptotic necrosis (Annexin V^+ PI^+) after a 60 min incubation with H_2O_2. Thus, very few cells were

detected in early apoptosis, which is in agreement with findings of the current study after staurosporine treatment. Eley *et al*. (2005) recently reported that staurosporine (1 mM) did significantly induce early apoptosis in human spermatozoa, although this was accompanied by a substantial increase in necrotic cells. These results should be interpreted with caution as other biomarkers for apoptosis have to confirm a positive result.

The percentage of early apoptotic live (Annexin V^+ PI^-) cells reported is closer in agreement with that found by Ricci *et al*. (2002) than what was previously published (Glander and Schaller, 1999; Oosterhuis *et al*., 2000; Barosso *et al*., 2000). This is probably due to the method employed to accurately select the sperm population. Similarly to Ricci and co-workers (2002), a leukocyte specific antibody (CD45) was used to accurately gate the sperm population for flow cytometry. At no time during experimentation (i.e. treatment with staurosporine or exposure to RF-EMF), was a significant increase in early apoptotic cells seen. There were also no statistical difference between RF-EMF exposed and control cells comparing number of dead cells (PI^+) and total PS externalisation (Annexin V^+) assessed directly, 2 and 24 hours after exposure. Hence it can be concluded that an hour exposure of human spermatozoa *in vitro* to 900 MHz GSM radiation does not adversely effect PS externalisation. This finding is consistent with results from a recent paper by Hook *et al*. (2004) that also found no evidence of an effect on Molt-4 cells after *in vitro* exposure to RF-EMF.

If PS externalisation in human spermatozoa were an exclusive marker for early apoptosis, a linear response of Annexin V^+ PI^- staining with time could be expected. This was not seen in the current results, with PS externalisation decreasing for both exposed and control cells 2 hours post RF-EMF exposure while increasing again 24 hours after exposure irrespective of the SAR level used. It is thus possible that PS externalisation accompanied by Annexin V staining changes with alterations in the plasma membrane fluidity due to capacitation and is not an exclusive marker of apoptosis. Several studies have reported conflicting results with Annexin V staining (Glander and Schaller, 1999; Osterhuis *et al*., 2000; Marchetti *et al*., 2004). Interestingly, Ricci *et al*. (2002) reported that mature sperm are indeed able to

undergo apoptosis, leading to the exposure of PS on the outside of the plasma membrane. They hypothesised that Annexin V^- PI^+ cells are unable to bind Annexin V due to the high degree of membrane disorganisation in this group of cells, and that these cells are actually in the latter stage of apoptosis. In accordance with Ricci and co-workers (2002), two populations staining PI^+, one fraction staining Annexin V^+, while the other Annexin V^- were observed in the present study. The natural progression of cells in apoptosis would entail an increase of cells in early apoptosis (Annexin V^+ PI^-) followed by an accumulation of cells in apoptotic necrosis (Annexin V^+ PI^+) with time, whereas cells staining Annexin V^- PI^+ are generally considered dead. If the cells in this latter group were actually in late apoptosis, this would mean that Annexin V^+ PI^- sperm should inversely correlate with Annexin V^- PI^+ sperm over time. The current data does not support this hypothesis. In fact, at no time point was a negative correlation between early apoptotic and dead cells noted.

Taking all this evidence into consideration, it would seem that Annexin V staining on its own as an indicator of apoptosis, at least for human spermatozoa, is not an unambiguous gauge of apoptosis. Recent studies concluded that PS externalisation in human spermatozoa does not correlate with apoptosis but is rather associated with plasma membrane changes after cryostorage (Glander and Schaller, 1999), as well as capacitation (Gadella and Harrison, 2002; de Vries *et al*., 2003; Martin *et al*., 2005).

Analyses of the mitochondrial function by means of determining changes in the inner mitochondrial membrane potential can serve as a sensitive indicator for the energetic state of the mitochondria and the cell. It can also be used in the assessment of mitochondrial respiratory chain activity, electron transport systems, and the activation of the mitochondrial permeability transition (Ly *et al*., 2003). In human spermatozoa reduced mitochondrial membrane potential correlates with diminished motility and fertility (Donnely *et al*., 2000; Marchetti *et al*., 2002; Piasecka and Kawiak, 2003; Wang *et al*., 2003). Recently, Marchetti *et al*. (2004a) compared different fluorochromes for the detection of $\Delta\psi m$ in human spermatozoa, the authors noted that Mitotracker® RedCMX-Ros provides a simple, sensitive method for the assessment of $\Delta\psi m$.

Although, the mitochondrial membrane potential decreased over time, no significant difference between RF-EMF exposed and control spermatozoa were noted. The lack of an effect on mitochondrial membrane potential observed directly, 2 hours and 24 hours after RF-EMF irradiation for both SAR 2.0 W/kg and 5.7 W/kg correlates well with that reported by Capri and co-workers (2004) who also found that *in vitro* exposure of human lymphocytes to 900 MHz had no effect on the mitochondrial membrane potential assessed at different time points. It is thus unlikely that RF-EMF could have an effect on the electron transport chain and the proton pump machinery in mitochondria.

Disruption of the mitochondrial membrane potential could result in the release of cytochrome c into the cytosol where it binds apoptotic protease activating factor-1 (Apaf-1) resulting in the activation of a family of cysteine proteases, called caspases. Caspases exist in cells as inactive zymogens and become proteoliticly activated by apoptotic signals from the cell (Sinha Hikim *et al*., 2003). Caspase activation entails the activation of initiator caspase 9 followed by executioner caspases 3, 6, and 7 activation. Activation of caspase-3 is seen as the point of no return in the execution of apoptosis. However, we failed to detect significant levels of activated caspase-3 activity in the highly motile fraction of mature spermatozoa. This result is in agreement with what has been reported by others (Weil *et al*., 1998; de Vries *et al*., 2003). On the other hand, Almeida *et al*. (2005) recently reported caspase-3 activity in human spermatozoa after swim-up preparation. This finding could be explained because swim–up prepared sperm contain more sperm with DNA damage compared with sperm separated by density-gradient (Host *et al*., 2000). Caspases are not completely removed during undisturbed spermatogenises (Paasch *et al*., 2003) but are present in cytoplasmic droplets in spermatids and immature spermatozoa (Weil *et al*., 1998; Blanco-Rodríguez and Martínez-García, 1999) as well as in the cytoplasm localised in the midpiece region (Weng *et al*., 2002; Paasch *et al*., 2003; Marchetti *et al*., 2004b). It is thus possible that there would be more sperm presenting caspases after swim-up preparation compared to density gradient separation. Furthermore, Marchetti *et al*. (2004b) also detected active caspase-3 by western blot but only in semen samples with the highest percentage of FITC-VAD-FMK^{+} cells. In addition, Taylor *et al*. (2004) observed higher caspase catalytic activity in low motility

fractions compared to high motility sperm fractions. It is thus not surprising that such low levels of active caspase-3 were detected in the highly motile density gradient purified spermatozoa used in the present study.

Noting that Weng *et al.* (2002) postulated a sperm-specific apoptotic pathway that may not include caspase-3 activation, a cell-permeable fluorescent derivative of the inhibitor peptide VAD-FMK able to detect the overall caspase activation status in human spermatozoa was used in experiments. First described by Paasch *et al.* (2003), Marchetti and co-workers (2004b) confirmed that FITC-VAD-FMK could be utilized for the flow cytometric analysis of activated caspases in human sperm. Current results are comparable with that reported by Marchetti *et al.* (2004b). When considering the total caspase activation (FITC-VAD-FMK^{+}) after RF-EMF exposure, no difference between RF exposed and control cells at any time point irrespective of the SAR level was observed.

Leszczynski *et al.* (2002) reported that RF-EMF inhibited apoptosis through the caspase-3 dependant apoptotic pathway. It is thus not surprising that this effect was not observed in the highly motile fraction of density gradient separated spermatozoa. Firstly as negligible amounts of caspase-3 activity were observed and furthermore it has not conclusively been demonstrated that caspases are involved in the execution of apoptosis in human sperm.

One of the final phases of apoptosis is the degradation of DNA through the activation of an endonuclease that cleaves DNA between regularly spaced nucleosomal units (Boatright *et al.*, 2003; Said *et al.*, 2004). There are many conflicting reports regarding the ability of RF-EMF to induce DNA damage. Whereas genotoxic effects were observed in certain cell types (Maes *et al.*, 1996; Tice *et al.*, 2002; Mashevich *et al.*, 2003), in other cell types RF-EMF did not appear to induce DNA damage (Maes *et al.*, 1997; Malyapa *et al.*, 1997; Li *et al.*, 2001, Zeni *et al.*, 2003). If on the other hand RF-EMF does exert a genotoxic effect on human cells, post-meiotic male germ cells would be particularly sensitive to DNA damage, as they have lost their capacity for DNA repair. During spermatogenesis male germ cells are supported by Sertoli cells. However, once these cells mature they lose most of their cytoplasm containing antioxidants that protect them from oxidative stress making them highly

susceptible to any genotoxic agent (Aitken, 1999). Aitken *et al*. (2005) reported that a 7-day exposure of male mice to RF-EMF significantly induced DNA damage in both the nuclear and mitochondrial genomes of spermatozoa recovered from the cauda epididymis.

Using the TUNEL assay, we examined the induction of DNA fragmentation in spermatozoa exposed to SAR levels of 2.0 and 5.7 W/kg. The percentage of DNA fragmentation in density gradient purified fractions reported here corresponds with previous findings where flow cytometry and the TUNEL assay were used to assess DNA damage (Ramos and Wetzels, 2001; Marchetti *et al*., 2004b). Although DNA fragmentation increased over time, there were no significant differences detected between RF-EMF exposed and control sperm.

Aitken and co-workers (2005) assessed DNA damage after an *in vivo* exposure period of 7 days, whereas in the present study, DNA damage was assessed directly after a one-hour exposure period. It is thus possible that DNA damage is cumulative as was suggested by Fejes *et al*. (2005) and not observable after an exposure time of one hour. The current approach on the other hand was to expose sperm *in vitro* to a worst-case scenario to see of RF-EMF could elicit a genotoxic response after an hour RF-EMF exposure to SAR levels of 2.0 and 5.7 W/kg. Based on results shown here, RF exposure at either of the SAR levels did not induce DNA fragmentation. Similar findings reporting a lack of DNA damage after RF-EMF exposure of Molt-4-T-lymphoblastoid cells (Hook *et al*., 2004) as well human lymphocytes (Meas *et al*., 1997; Vijayalaxmi *et al*., 2000) have been reported.

Reactive oxygen species generation by human spermatozoa as a result of aerobic metabolism is not just of significance because of peroxidative damage caused to the sperm plasma membrane due to the relative lack of antioxidant protection by cytoplasmic antioxidant enzymes (Aitken and Baker, 2002), but also due to the structural and chemical damage they cause to proteins and target DNA (Riley and Behrman, 1991; Aitken *et al*., 1998; Ramos and Wetzels, 2001; Henkel *et al*., 2004). The presence of leukocytes in the purified highly motile fraction of spermatozoa could contribute significantly to increased ROS generation. Therefore, a leukocyte specific antibody (CD45) was used to gate the sperm population correctly to enable

the quantification of intrinsic ROS generation only. The total percentage $CD45^+$ cells were less than 0.62% of the total sperm population after density separation and, according to the WHO (1999), not pathological.

To determine intrinsic ROS production within the spermatozoa, a redox probe hydroethidine, which is specifically oxidized by O_2^- to form the membrane impermeant polynucleotide stain ethidium (Gallop *et al*., 1984), was used. Unlike current ROS probes (luminol and lucigenen) that decompose with the omission of light (Aitken *et al*., 2003), hydroethidine intercalates with the DNA (Rothe and Valet, 1990), which makes it ideal for flow cytometric detection. Recently, Henkel *et al*. (2004) and Marchetti *et al*. (2002) used hydroethidine to evaluate ROS production in human spermatozoa. RF-EMF had no effect on ROS generation in human spermatozoa when comparing RF-EMF exposed sperm with control sperm, directly after RF-EMF exposure as well as 2 and 24 hours after exposure for both SAR 2.0 and 5.7 W/kg.

When assessing the correlation between apoptotic indicators, a high mitochondrial membrane potential inversely, though not significantly, correlated with ROS generation and DNA fragmentation at all time points after initial RF exposure (2.0 W/kg). This result was consistent with previous reports regarding the correlation of these apoptotic markers in human spermatozoa (Marchetti *et al*., 2002). A negative correlation also existed between ROS generation and DNA fragmentation as was expected (Aitken *et al*., 1998). In addition, the correlation between DNA damage and PS externalisation, as well as caspase activation, was investigated. Results indicate that these markers were not significantly correlated. Considering that Marchetti *et al*. (2002) found that sperm prepared by density gradient removed most of the damaged cells resulting in the lack of correlation between ROS, DNA fragmentation, and loss of viability, it confirms what was observed in the current study. However, the objective of this study was to establish if RF-EMF could induce apoptosis in human spermatozoa *per se*, irrespective of the current dispute in academia questioning the ability of fully differentiated spermatozoa to initiate apoptosis.

Sakkas *et al*. (2003, 2004) and others (Gandini *et al*., 2002; Tesarik *et al*., 2004) are of the opinion that the presence of apoptotic markers in human spermatozoa are due to an abortive apoptotic program during spermatogenesis and the failure of elimination of these cells before ejaculation. These authors further hypothesise that the presence of DNA damage could be the result of incorrect nuclear remodelling due to problems arising directly from protamine deposition during spermatogenesis. Based on the results presented here, we are in agreement with these authors as apoptotic markers in human spermatozoa did not correlate with apoptosis.

In conclusion, the study encompassed a wide variety of both early and late apoptotic markers as well as considering ROS generation as a function of time. This study not only provides evidence that an hour RF-EMF exposure of human spermatozoa *in vitro* does not significantly affect any of the apoptotic indicators investigated here, but also sheds light on the apoptotic behaviour of fully differentiated sperm over time.

4.7 REFERENCES

Aitken, R.J., Clarkson, J.S. 1988. Significance of reactive oxygen species and antioxidants in defining the efficacy of sperm preparation techniques. *J Androl.*, 9, 367-76.

Aitken, R.J., Clarkson, J.S., Fishel, S. 1989. Generation of reactive oxygen species, lipid peroxidation, and human sperm function. *Biol Reprod.*, 41, 183-97.

Aitken, R.J., Fisher, H. 1994. Reactive oxygen species generation and human spermatozoa: the balance of benefit and risk. *Bio Essays.*, 16, 259-67.

Aitken R.J., Gordon, E., Harkiss, D., Twigg, J.P., Milne, P., Jennings, Z., Irvine, D.S. 1998. Relative impact of oxidative stress on the functional competence and genomic integrity of human spermatozoa. *Biol Reprod.*, 59, 1037-46.

Aitken, R.J. 1999. The Amoroso lecture. The human spermatozoa-a cell in crisis. *J Reprod Fertil.*, 115, 1-7.

Aitken, R.J, Baker, M.A. 2002. Reactive oxygen species generation by human spermatozoa: a continuing enigma. *Int J Androl.*, 25, 191-4.

Aitken, R.J, Ryan, A.L., Curry, B.J., Baker, M.A. 2003. Multiple forms of redox activity in populations of human spermatozoa. *Mol Hum Reprod.*, 9, 645-61.

Aitken, R.J, Bennetts, L.E, Sawyer, D., Wiklendt, A.M., King, B.V. 2005. Impact of radiofrequency electromagnetic radiation on DNA integrity in the male germline. *Int J Androl.*, 28, 171-9.

Almeida, C., Cardoso, M.F., Sousa, M., Viana, P., Goncalves, A., Sliva, J., Barros, A. 2005. Quantitative study of caspase-3 activity in semen and after swim-up preparation in relation to sperm quality. *Hum Reprod.*, 20, 1307-13.

Armstrong, J.S., Rajasekaran, M., Chamulitrat, W., Gatti, P., Hellstrom, W.J., Sikka, S.C. 1999. Characterization of reactive oxygen species induced effects on human spermatozoa movement and energy metabolism. *Free Rad Bio Med.*, 26, 869-80.

Baccetti, B., Collodel, G., Piomboni, P. 1996. Apoptosis in human ejaculated sperm cells. *J Submicrosc Cytol Pathol.*, 28, 587-96.

Blanco-Rodríguez, J., Martínez-García, C. 1999. Apoptosis is physiologically restricted to a specialized cytoplasmic compartment in rat spermatids. *Biol Reprod.*, 61, 1541-7.

Barroso, G., Morshedi, M., Oehninger, S. 2000. Analysis of DNA fragmentation, plasma membrane translocation of phophatidylserine and oxidative stress in human spermatozoa. *Human Reprod*., 15, 1338-44.

Bertrand, R., Solary, E., O'Connor, P., Kohn, K.W., Pommier, Y. 1994. Induction of a common pathway of apoptosis by staurosporine. *Exp Cell Res*., 211, 314-321.

Boatright K.M., Renatus, M., Scott, F.L., Sperandio, S., Shin, H., Pedersen, I.M., Ricci, J.E., Edris, W.A., Sutherlin, D.P., Green, D.R., Salvesen, G.S. 2003. A unified model for apical caspase activation. *Mol Cell*, 11, 529-41.

Capri, M., Scarcella, E., Fumelli, C., Bianchi, E., Salvioli, S., Mesirca, P., Agostini, C., Antonili, A., Schiavoni, A., Catellani, G., Bersani, F., Franceschi, C. 2004. *In vitro* exposure of human lymphocytes to 900 MHz CW and GSM modulated radiofrequency: studies of proliferation, apoptosis and mitochondrial membrane potential. *Rad Res*., 162, 211-8.

D'Amours, D., Desnoyers, S., D'Silva, I., Poirier, G.G. 1999. Poly(ADP-ribosyl) action reactions in the regulation of nuclear functions. *Biochem J*., 342, 249-68.

D'Cruz, O.J., Vassilev, A., Uckun, F.M. 2000. Studies in humans on the mechanism of potent spermicidal and apoptosis inducing activities of Vanadocene complexes. *Biol Reprod*., 62, 939-49.

Darzynkiewicz, Z., Juan, G., Li, X., Gorczyca, W., Murakami, T., Traganos, F. 1997. Cytometry in cell necrobiology: analysis of apoptosis and accidental cell death (necrosis). *Cytometry*., 27, 1-20.

de Vries, K.J., Wiedmer, T., Sims, P.J., Gadella, B.M. 2003. Caspase-independent exposure of aminophospholipids and tyrosine phosphorylation in bicarbonate responsive human sperm cells. *Boil Reprod*., 68, 2122-34.

Donnelly, E.T., O'Connell, M., McClure, N., Lewis, S.E. 2000. Differences in nuclear DNA fragmentation and mitochondrial integrity of semen and prepared human spermatozoa. *Hum Reprod*., 15, 1552-61.

Eley, A., Hosseinzadeh, S., Hakimi, H., Geary, I., Pacey, A.A. 2005. Apoptosis of ejaculated human sperm is induced by co-incubation with Chlamydia trachomatis lipopolysaccharide. *Hum Reprod*., 20, 2601-7.

Enari, M., Sakahira, H., Yokoyyama, H., Okawa, K., Iwamatsu, A., Nagata, S. 1998. A caspase-activated DNase that degrades DNA during apoptosis and its inhibitor ICAD. *Nature*., 391, 43-50.

Erenpreiss, J., Jepson, K., Giwercman, A., Tsarev, I., Erenpreisa, J., Spano, M. 2004. Toluidine blue cytometry test for sperm DNA conformation: comparison with flow cytometric sperm chromatin structure and TUNEL assay. *Hum Reprod.*, 19, 2277-82.

Fejes, I., Závaczki, Z., Szöllõsi, J., Koloszár, S., Daru, J., Kovács, L., Pal, A. 2005. Is there a relationship between cell phone use and semen quality? *Arch Androl.*, 51, 385-93.

Gadella, B.M., Harrison, R.A. 2002. Capacitation induces cyclic adenosine 3',5'-monophosphate-dependent, but apoptosis-unrelated, exposure of aminophospholipids at the apical head plasma membrane of boar sperm cells. *Biol Reprod.*, 67, 340-50.

Gallop, P.M., Paz, M.A., Henson, E., Latt, S.A. 1984. Dynamic approaches to the delivery of reporter reagents into living cells. *Biotechniques.*, 3, 32-6.

Gandini, L., Lombardo, F., Paoli, D., Caponecchia, L., Familiari, G., Verlengia, C., Dondero, F., Lenzi, A. 2000. Study of apoptotic DNA fragmentation in human spermatozoa. *Hum Reprod.*, 15, 830-9.

Glander, H.J., Schaller, J. 1999. Binding of annexin V to plasma membranes of human spermatozoa: a rapid assay for detection of membrane changes after cryostorage. *Mol. Human Reprod.*, 5, 109-15.

Griveau, J.F., Le Lannou, D. 1997. Reactive oxygen species and human spermatozoa: physiology and pathology. *Int J Androl.*, 20, 61-9.

Henkel, R., Kierspel, E., Stalf, T., Mehnert, C., Menkveld, R., Tinneberg, H.R., Schill, W.B., Kruger, T.F. 2004. Effect of reactive oxygen species produced by spermatozoa and leukocytes on sperm functions in non-leukospermic patients. *Fertil Steril.*, 83, 635-42.

Hook, G.J., Zhang, P., Lagroye, J., Li, L., Higashikubo, R, Moros, H.G., Straube, W.L., Picard, W.F., Baty, J.D., Roti Roti, J.L. 2004. Measurement of DNA damage and apoptosis in Molt-4 cells after *in vitro* exposure to radiofrequency radiation. *Rad Res.*, 161, 193-200.

Host, E., Lindenberg, S., Smidt-Jensen, S. 2000. The role of DNA strand breaks in human spermatozoa used fro IVF and ICSI. *Acta Obstet Gynaecol Scand*., 79, 559-63.

Irmak, M.K., Fadilhoglu, E., Güleç, M., Erdogan, H., Yagmurca, M., Akyol, Ö. 2002. Effects of electromagnetic radiation from cellular telephone on the oxidant and antioxidant levels in rabbits. *Cell Biochem Funct*., 20, 279-83.

Jacobson, M.D., Burne, J.F., King, M.P., Miyashita, T., Reed, J.C., Raff, M.C. 1993. Bcl-2 blocks apoptosis in cells lacking mitochondrial DNA. *Nature*., 361, 365-9.

Jacobson, M.D., Burne, J.F., Raff, M.C., 1994. Programmed cell death and Bcl-2 protection in the absence of a nucleus. *EMBO J*., 13, 1899-910.

Jacobson, M.D., Weil, M., Raff, M.C. 1996. Role of Ced-3/ICE-family proteases in staurosporine-induced programmed cell death. *J Cell Biol.*, 133, 1041-51.

Knapp, W., Dorken, B., Rieber, E.P., (eds.). 1989. *Leukoocyite Typing IV: White cell differentiation antigens*, New York: Oxford University Press.

Koopman, G., Reutelingsperger, C.P., Kuijten, G.A., Keehnen, R.M., Pols, S.T., Van Oers, M.H. 1994. Annexin V for flow cytometric detection of phosphatidylserine expression on B cells undergoing apoptosis. *Blood*., 84, 1415-20.

Kroemer, G., Reed, J.C. 2000. Mitochondrial control of death. *Nature Med*., 6, 513-9.

Lai, H., Singh, N.P. 1995. Acute low-intensity microwave exposure increases DNA single-strand breaks in rat brain cells. *Bioelectromagnetics*., 16, 207-10.

Lai, H., Singh, N.P. 1996. Single- and double-strand DNA breaks in rat brain cells after acute exposure to radiofrequency electromagnetic radiation. *Int J Rad Biol.*, 69, 513-21.

Lai, H., Singh, N.P. 1997. Melatonin and a spin-trap compound block radiofrequency electromagnetic radiation-induced DNA strand breaks in rat brain cells. *Bioelectromagnetics.*, 18, 446-54.

Leszczynski, D., Joenväärä, S., Reivinen, J., Kuokka, R. 2002. Non-thermal activation of the hsp27/p38MAPK stress pathway by mobile phone radiation in human endothelial cells: Molecular mechanism for cancer and blood brain barrier-related effects. *Differentiation*., 70, 120-29.

Li, L., Bisht, K.S., LaGroye, I., Zhang, P., Straube, W.L., Moros, E.G., Roti Roti, J.L. 2001. Measurement of DNA damage in mammalian cells exposed in vitro to radiofrequency fields at SARs of 3-5 W/kg. *Rad Res.*, 156, 328-32.

Ly, J.D., Grubb, D.R., Lawen, A. 2003. The mitochondrial membrane potential (deltapsi(m)) in apoptosis: an update. *Apoptosis*., 8, 115-28.

Maes, A., Collier, M., Slaets, D., Verschaeve, L. 1996. 954 MHz microwaves enhance the mutagenic properties of mitomycin C. *Environ Mol Mutagen*., 28, 26-30.

Maes, A., Collier, M., van Gorp, U., Vandoninck, S., Verschaeve, L. 1997. Cytogenic effects of 935.2 MHz (GSM) micro-waves alone and in combination with mitomycin C. *Mutat Res*., 393, 151-6.

Majno, G., Joris, I. 1995. Apoptosis, oncosis and necrosislan overview of the cell death. *Am J Pathol*., 146, 3-15.

Malyapa, R.S., Ahem, E.W., Straube, W.L., Moros, E.G., Picard, W.F., Roti Roti, J.L. 1997. Measurement of DNA damage after exposure to 2450 MHz electromagnetic radiation. *Rad Res.*, 148, 608-17.

Marchetti, C., Obert, G., Defossez, A., Formstecher, P., Marchetti, P. 2002. Study of mitochondrial membrane potential, reactive oxygen species, DNA fragmentation and cell viability by flow cytometry in human sperm. *Hum Reprod*., 17, 1257-65.

Marchetti, C., Jouy, N., Leroy-Martin, B., Defossez, A., Formstecher, P., Marchetti, P. 2004a. Comparison of four fluorochromes for the detection of the inner mitochondrial membrane potential in human spermatozoa and their correlation with sperm motility. *Hum Reprod.*, 19, 2267-76.

Marchetti, C., Gallego, M.A., Defossez, A., Formstecher, P., Marchetti, P. 2004b. Staining of human sperm with fluorochrome-labelled inhibitor of caspases to detect activated caspases: correlation with apoptosis and sperm parameters. *Hum Reprod*., 19, 1127-34.

Martin, G., Sabido, O., Durand P., Levy, R. 2005. Phophatidylserine externalisation in human sperm induced by calcium ionophore A23187: relationship with apoptosis, membrane scrambling and the acrosome reaction. *Hum Reprod*., 20, 3459-68.

Martin, S., Reutelingsperger, C.P.M., McGahon, A., Rader, J.A., van Schie, R., LaFace, D.M. 1995. Early redistribution of plasma membrane phosphatidylserine is a general feature of apoptosis regardless of the initiating stimulus: inhibition of over expression of Bcl-2 and Ab-l. *J Exp Med*., 182, 1545-56.

Mashevich, M., Folkman, D., Kesar, A., Barbul, A., Korenstein, R., Jerby, E., Avivi, L. 2003. Exposure to human peripheral blood lymphocytes to electromagnetic fields associated with cellular phones leads to chromosomal instability. *Bioelectromagnetics*., 24, 82-90.

Moore, S. 1981. Pancreatic DNase *In*: P.D. Boyer, ed. *The Enzymes*. Vol. 14 A. New York: Academic Press, 281.

Morshedi, M.S., Taylor, S.L., Weng, S.L., Duran, H., Beebe, S.J., Oehninger, S. 2003. Roles of caspases in human spermatozoa: A marker for sperm quality? *Fertil Steril*., 80, 30-1.

O'Brein, M.C., Bolton, W.E. 1995. Comparison of cell viability probes compatible with fixation and permeabilization for combined surface and intracellular staining in flow cytometry. *Cytometry*., 19, 243.

Oehninger, S., Morshedi, M., Weng, S.L., Taylor, S., Duran, H., Beebe, S. 2003. Presence and significance of somatic cell apoptosis markers in human ejaculated spermatozoa. *RBM Online*., 7, 469-476.

Oosterhuis, G.J., Mulder, A.B., Kalsbeek-Batenburg, E., Lambalk, C.B., Schoemaker, J., Vermes, I. 2000. Measuring apoptosis in human spermatozoa: a biological assay for semen quality? *Feritl Steril*., 74, 245-50.

Paasch, U., Grunewald, S., Fitzl, G., Glander, H.J. 2003. Deterioration of plasma membrane is associated with activated caspases in human spermatozoa. *J Androl*., 24, 246-52.

Pentikäinen,V., Erikkilä, K., Dunkel, L. 1999. Fas regulates germ cell apoptosis in the human testis *in vitro*. *Am J Phys*., 276, E310-16.

Piasecka, M., Kawiak, J. 2003. Sperm mitochondria of patients with normal sperm motility and with asthenozoospermia: morphological and functional study. *Fiola Hstochem Cytobiol*., 41, 125-39.

Ramos, L., Wetzels, A.M.M. 2001. Low rates of DNA fragmentation in selected motile human spermatozoa assessed by TUNEL assay. *Hum Reprod*., 16, 1703-07.

Ricci, G., Presani, G., Guaschino, S., Simeone, R., Perticarari, S. 2000. Leukocyte detection in human semen using flow cytometry. *Hum Reprod*., 50, 1329-37.

Ricci, G., Perticarari, S., Fragonas, E., Giolo, E., Conova, S., Pozzobon, C., Guaschino, S., Presani, G. 2002. Apotosis in human sperm: its correlation with semen quality an the presence of leukocytes. *Hum Reprod*., 17, 2665-72.

Riley, J.C.M., Behrman, H.R. 1991. Oxygen radicals and reactive oxygen species in reproduction. *Pro Soc Exp Biol Med*., 198, 781-91.

Rothe, G., Valet, G. 1990. Flow cytometry analysis of repiratory burst activity in phagocytes with hydroethidine and 2',7'-dichlorofluorescien. *J Leukoc Biol*., 27, 440-8.

Said, T.M., Paasch, U., Glander, H.S., Agarwal, A. 2004. Role of caspases in male infertility. *Hum Reprod Update.*, 10, 39-51.

Sakahira, H., Enari, M., Nagata, S. 1998. Cleavage of CAD inhibitor in CAD activation and DNA degradation during apoptosis. *Nature*., 391, 96-9.

Sakkas, D., Mariethoz, E., St. John, J.C. 1999. Abnormal sperm parameters in humans are indicative of an abortive apoptotic mechanism linked to the Fas-mediated pathway. *Exp Cell Res.*, 251, 350-5.

Sakkas, D. 1999. Origin of DNA damage in ejaculated human spermatozoa. *Rev Reprod*., 4, 31-7.

Sakkas, D., Moffatt, O., Manicardi, G.C., Mariethoz, E., Tarozzi, N. 2002. Nature of DNA damage in ejaculated human spermatozoa and the possible involvement of apoptosis. *Biol Reprod*., 66, 1061-7.

Sakkas, D., Seli, E., Bizzaro, D., Tarozzi, N., Manicardi, G.C. 2003. Abnormal spermatozoa in the ejaculate: abortive apoptosis and faulty nuclear remodelling during spermatogenesis. *Reprod Biomed Online*., 7, 428-32.

Sakkas, D., Seli, E., Manicardi, G.C., Nijs, M., Ombelet, W., Bizzaro, D. 2004. The presence of abnormal spermatozoa in the ejaculate: did apoptosis fail? *Hum Fertil*., 7, 99-103.

Schmid, I., Kral, W.J., Uittenbogaart, C.H. 1992. Dead cell discrimination with 7-Amino-Actinomycin D in combination with dual colour immunofluorescence in single laser flow cytometry. *Cytometry*., 13, 204-10.

Schwartzman, R.A., Cidlowski, J.A. 1993. Mechanism of tissue-specific induction of internucleosomal deoxyribonucleic acid cleavage activity and apoptosis by glucocorticoids. *Endocrinology*., 33, 591-9.

Sinha Hikim, A.P., Lue, Y., Diaz-Romero, M., Yen, P.H., Wang, C., Swerdloff, R.S. 2003. Deciphering the pathways of germ cell apoptosis in the testis. *J Steroid Biochem Mol Biol.*, 85, 175-82.

Taylor, S.L., Weng, S.L., Fox, P., Duran, E.H., Morshedi, M.S., Oehninger, S., Beebe, S.J. 2004. Somatic cells apoptosis markers and pathways in human ejaculated sperm: potential utility as indicators of sperm quality. *Mol Hum Reprod*., 10, 825-34.

Telford, W.G., King, L.E., Fraker, P.J. 1994. Rapid quantification of apoptosis in pure and heterogeneous cell populations using flow cytometry. *J Immunol Meth.*, 172, 1-6.

Tesarik, J., Ubaldi, F., Rienzi, L., Martinez, F., Iacobelle, M., Mendoza, C., Greco, E. 2004. Caspase-dependant and –independent DNA fragmentation in Sertoli and germ sperm from men with primary testicular failure: relationship with histological damage. *Hum Reprod*., 19, 254-61.

Tice, R.R., Hook, G.G., Donner, M., McRee, D.I., Guy, A.W. 2002. Genotoxicity of radiofrequency signals. I. Investigation of DNA damage and micronuclei induction in cultured human blood cells. *Bioelectromagnetics*., 23, 113-26.

Uchiyama, Y., (ed.). 1995. Apoptosis. Morphological approaches and biological significance. *Arch Histol Cytol*., 58 (Special Issue), 127-264.

Van Blerkom, J., Davis, P.W. 1998. DNA strand breaks and phosphatidylserine redistribution in newly ovulated and cultured mouse and human oocytes: occurrence and relationship to apoptosis. *Hum Reprod*., 13, 1317-24.

Vaux, D.K., Korsmeyer, S.J. 1999. Cell death in development. *Cell*., 96, 245-54.

Vermes, I., Haansen, C., Steffens-Nakken, H., Reutelingsperger, C. 1995. A novel assay for apoptosis. Flow cytometric detection of phophatidylserine expression on

early apoptotic cells using fluorescien labelled Annexin V. *J Immunol Methods*., 184, 39-51.

Vijayalaxmi, Z.D., Leal, B.Z., Szilagyi, M., Prihoda, T.J., Meltz, M.L. 2000. Primary DNA damage in human blood lymphocytes exposed in vitro to 2450 MHz radiofrequency radiation. *Rad Res.*, 153, 479-86.

Walker, R.P., Kokileva, L., LeBlanc, J., Sikorska, M. 1993. Detection of the initial stages of DNA fragmentation in apoptosis. *Biotechniques.*, 15, 1032-36.

Wang, X., Shara, R.K., Gupta, A., George, V., Thomas, A.J., Falcone, T., Agrawal, A. 2003. Alterations in mitochondria membrane potential and oxidative stress in infertile men: a prospective observational study. *Fertil Steril.*, 80, 844-50.

Weil, M., Jocobson, M.D., Raff, M.C. 1998. Are caspases involved in the death of sperm with a transcriptionally inactive nucleus? Sperm and chicken erythrocytes. *J Cell Science*. 111, 2702-15.

Weng, S.L., Schuffner, A., Morshedi, M.S., Beebe, S.J., Taylor, S., Oehninger, S. 2001. Caspase-3 activity is present at low levels in ejaculated human spermatozoa. *Fertil Steril*., 76, Supplement 1, S193.

Weng, S.L., Taylor, S.L., Morshedi, M., Schuffner, A., Duran, E.H., Beebe, S., Oehninger, S. 2002. Caspase activity and apoptotic markers in ejaculated human sperm. *Mol Hum Reprod*., 8, 984-91.

Wolff, H. 1995. The biological significance of white blood cells in semen. *Fertil Steril*., 63, 1143-57.

Wyllie, A.H., Kerr, J.F.R., Currie, A.R. 1980. Cell death: the significance of apoptosis. *Int Rev Cytol*., 68, 251-306.

Zeni, O., Chiavoni, A.S., Sannino, A., Antolini, A., Forgio, D., Bersani, F., Scarfi, M.R. 2003. Lack of genotoxic effects (micronucleus induction) in human lymphocytes exposed *in vitro* to 900 MHz electromagnetic fields. *Rad Res.*, 160, 152-8.

CHAPTER 5

ACTIVATION OF HEAT SHOCK PROTEINS IN HUMAN SPERMATOZOA

5.1 INTRODUCTION

The activation of a cellular stress response is designed to prevent and to repair damage incurred by exposure to a stressor. This stress response is immediately detectable in changes in the phosphorylation level of various proteins. Stress proteins have been widely studied as biomarkers of effect (Kreps *et al*., 1997) and under this category the highly conserved heat-shock proteins (Hsps) have received much attention. Hsps are expressed or phosphorylated due to a variety of cellular injuries and as such their activation can be used as an indicative response of cellular stress.

Several recent studies have indicated that RF-EMF increases expression or phosphorylation of certain stress response proteins (Daniells *et al*., 1998; Leszczynski *et al*., 2002, 2004; Czyz *et al*., 2004; Lee *et al*., 2005; Nylund and Leszczynski, 2006). Therefore, by examining changes in protein synthesis and phosphorylation levels in reply to a cellular stress response, it is possible to determine whether cells can respond to the very low energy emitted by mobile phones.

Various heat shock proteins have been identified in mature human spermatozoa (discussed in Chapter 2). Whether these Hsps are up-regulateable is uncertain, as mature sperm cells lack the operative mechanism for *de novo* protein synthesis (Díez-Sánchez *et al*., 2003; Moustafa *et al*., 2004; Grunewald *et al*., 2005; Lalancette *et al*., 2006). However, the presence of mRNAs in ejaculate human spermatozoa are well established (Kramer and Krawetz, 1997; Ostermeier *et al*., 2002), and it was initially thought that these mRNAs are remnants of untranslated stores during spermatogenesis (Miller, 2000; Grunewald *et al*., 2005). Grunewald *et al*. (2005) concluded that although no novel RNA transcription in human spermatozoa is possible, mRNAs present in spermatozoa are still functional. This finding was supported by Ostermeier *et al*. (2004), who demonstrated that paternal mRNAs were

transferred to the oocyte at fertilization, as transcripts coding for specific proteins were detected in early embryos after fertilization, while they were not found in the oocyte. Grunewald *et al.* (2005) also noted that RNA from spermatozoa could be reverse transcribed which is in agreement with data of Giordano *et al.* (2000). Furthermore, transcripts for Hsp70 and 90 have recently been found in ejaculate human spermatozoa (Miller, 2000; Dadoune *et al.*, 2005).

Hsp70 is up-regulateable as a result of stress (Hahn and Li, 1990; Senisterra *et al.*, 1997) whereas Hsp90 is activated by phosphorylation (serine/threonine/tyrosine) (Lees-Miller and Anderson, 1989a, b; Harris *et al.*, 2000; Brouet *et al.*, 2001). Hsp27 exists as an oligomeric structure and is also activated by phosphorylation after serine residues (Ser82, Ser78, and Ser15) (Rogalla *et al.*, 1999) through the p38 mitogen-activated protein kinase (MAPK) stress pathway (Landry *et al.*, 1992; Rouse *et al.*, 1994; Huot *et al.*, 1995). In human spermatozoa, MAPKs, also known as extracellular signal regulated kinases (ERKs) involved in the phosphorylation of specific proteins during capacitation, have been identified (Luconi *et al.*, 1998). In addition, several papers have identified sequentially activated kinase cascades in human spermatozoa that phosphorylate proteins after tyrosine, serine and, threonine residues (Naz, 1999; Baldi, *et al.*, 2002; Visconti *et al.*, 2002; Lalancette *et al.*, 2006; Martinez-Heredia *et al.*, 2006). In particular, Ficarro *et al.* (2003) noted that Hsp90 becomes tyrosine phosphorylated during human sperm capacitation.

In addition, Hsp70 plays an important role in fertilisation and early embryo development (Matwee *et al.*, 2001) since the presence of antibodies to Hsp70 significantly reduced tight binding of spermatozoa to the ZP and decreased blastocyte development (Neuer *et al.*, 1998, 2000). Hsp70 is thought to be involved in protein folding and translocation of proteins across the membrane during acrosomal excocytosis (Bohring and Krause, 2003) and prevents apoptosis during early development (Bloom *et al.*, 1998; Muscarella *et al.*, 1998). Consequently, Hsp70 transcripts, amongst others, could be the male gametes contribution to early embryogenesis. If RF-EMF could cause the premature translation of these transcripts, this could lead to disruption of fertilisation and early embryonic development.

Hsp27 is a known regulator of F-actin polymerisation (Huot *et al*., 1996; Rosseau *et al*., 1997). Furthermore, actin has been identified in various areas in human sperm, most notably the acrosome, post-acrosomal area, neck, and principal tail-piece (Fouquet and Kann, 1992). It is thought that actin polymerisation plays a role in acrosomal exocytosis as the sperm plasma membrane undergoes complex modifications during sperm-ZP interaction including changes in plasma membrane fluidity (Liu *et al*., 1999, Brener *et al*., 2003). Liu *et al*. (2002) confirmed this by demonstrating that an anti-actin mAb prevented actin polymerisation resulting in the inhibition of the AR of ZP bound spermatozoa. Thus, Hsp27 phosphorylation as a result of RF-EMF could affect F-actin polymerisation, which in turn could potentially have an effect on the human sperm AR. This would justify studying the status of F-actin polymerisation in human spermatozoa after RF-EMF.

Spermatozoa posses the ability not only to translate mRNA by means of transverse scriptase but could also activate proteins through kinase activity. Whether Hsps present in spermatozoa would recognise RF-EMF as a stressor and launch a stress response remains to be demonstrated. Therefore, this section focuses on the detection of cellular stress in RF-EMF exposed human spermatozoa by investigating the expression and/or phosphorylation of Hsps 70 and 27, in particular, as well as F-actin polymerisation

5.2 EXPERIMENTAL PROTOCOL

Ejaculated density gradient purified human spermatozoa were exposed for an hour to 900 MHz GSM (SAR 2.0 W/kg) irradiation inside a specially constructed waveguide (characterised in Chapter 3), while controls were kept at 37ºC in a humidified CO_2 incubator. Depending on the experiment, spermatozoa were heat shocked for up to an hour at 43ºC in a water bath to provide a positive control for Hsp expression/phosphorylation or F-actin activation.

The ability of RF-RMF and/or heat shock to elicit a cellular stress response in human spermatozoa was examined by determining phosphorylation and expression status of different heat shock proteins. A diagram outlining the experimental approach is shown in Figure 5.1. Hsp70 and 27 expression and/or phosphorylation were assessed

by flow cytometric analysis while slides were prepared for visualisation (immunofluorescence) and F-actin activation on the same day at three different time points or directly after exposure over a period of 4 weeks for all twelve donors. As an additional control, cellular stress due to RF-EMF and heat shock was determined in a breast cancer cell line (MCF-7). F-actin accumulation in MCF-7 cells was visually inspected after an hour exposure to either RF-EMF or 43ºC.

Western Blot analysis (WB) analysis of Hsps 70 and 27 directly after RF-EMF or heat shock were assessed at a later date using two donors (category A and B morphology as outlined in Annexure C) only. In addition, the expression of Hsps 110, 90, 75, 60, and 40 in the same two donors were analysed to determine if other Hsps could be affected by RF-EMF. The human epithelial cell line AE.hy926 heat shocked for 1 hour at 43ºC provided a positive control for the WB analysis of Hsps 70 and 27.

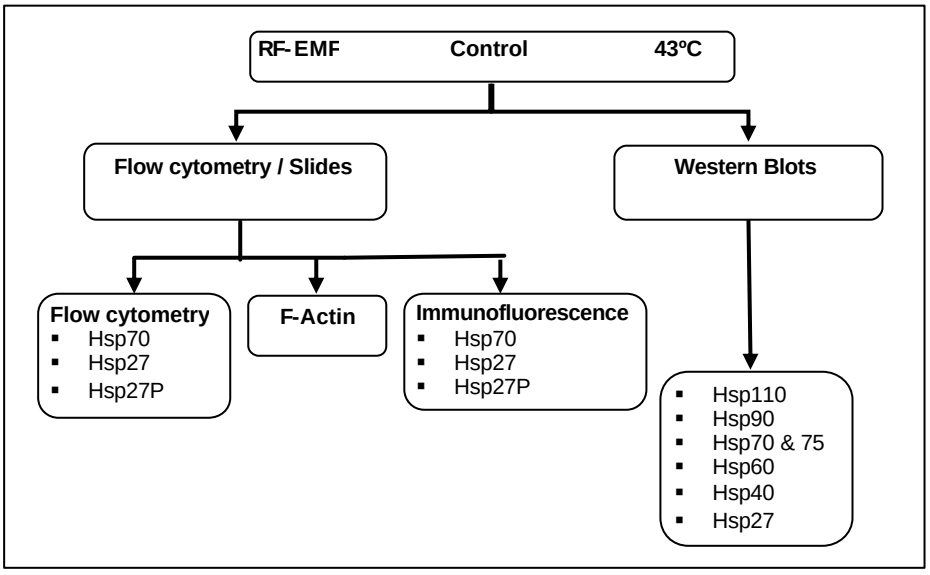

Figure 5.1 RF-EMF exposure protocol. Assessment of cellular stress in human spermatozoa post RF-EMF exposure and heat shock at 43ºC.

5.3 DETERMINATION OF HEAT SHOCK PROTEIN EXPRESSION AND PHOSPHORYLATION

5.3.1 Flow cytometric analysis of Hsp70 and Hsp27 expression and/or phosphorylation

Fixation, permeabilisation, Hsp detection, and staining were adapted from the method described by Bachelet *et al.* (1998). Fixation was performed with a freshly prepared paraformaldehyde solution: 0.37 g paraformaldehyde (Sigma Chemical Co.) solubilised in 10 ml PBS by heating the mixture at 70°C. After cooling the solution to room temperature, the pH was adjusted to 7.4. Cell extracts equivalent to 1-2 x 10^6 spermatozoa per sample were re-suspended in 100 µl paraformaldehyde solution, incubated for 10 min on ice and washed twice by centrifugation (300 g for 5 min) in 1 ml PBS. Cell membranes were permeabilised with 0.5% Triton X-100 in PBS for 10 min at room temperature.

Spermatozoa were then washed (300 g, 5 min) with PBA (PBS supplemented with 0.5% BSA) to block non-specific binding. Primary monoclonal antibody staining was performed with three different heat shock proteins, Hsp70-directed against its inducible form (BD Biosciences), Hsp27 (Calbiochem, CA, USA) and Hsp27P-phosphorylated Hsp27 at Ser 82 (Calbiochem). Spermatozoa were incubated for 30 min at room temperature with anti-Hsp70, anti-Hsp27 and anti-Hsp27P diluted to 1:100 in PBA, after which the cells were washed in PBA (300 g, 5 min). Secondary antibody staining was performed by incubating cells for 30 min at room temperature with FITC-conjugated rat anti-mouse IgG_1 (for Hsp70 and 27) and IgG_{2a} (for Hsp27P), (BD Biosciences) diluted to 1:100 in PBA. Cells were then washed (300 g for 5 min) in PBA, re-suspended in 1 ml PBS/BSA, and kept on ice directly after labelling until flow cytometric analysis. Cells kept on ice remained stable, as no difference in fluorescence intensity was noted in cells kept on ice for up to 4 hours after initial labelling. To determine non-specific binding of the secondary antibody (FITC-conjugated rat anti-mouse IgG_1 or IgG_{2a}), spermatozoa were prepared as described above but the primary antibody labelling was omitted.

Flow cytometric analysis was performed on a Coulter Epics® XL.MCL flow cytometer (XL.MCL) equipped with an air cooled argon laser and System II software

(Beckman Coulter). A total of 10 000 events were acquired for each endpoint and all tests were run in duplicate. The results are expressed as the mean cell number. Aliquots were also taken directly after exposure to visually assess Hsp distribution within the sperm cell (for visual assessment primary and secondary antibodies were diluted to 1:50 in PBA). Spermatozoa were visualised under 100x oil magnification and images were acquired using a Zeiss fluorescence microscope (Axioskop40, Axiocam camera and Axiovision AC software V4.5, Carl Zeiss (Pty)Ltd.).

5.3.2 Western Blot analysis of Hsps 110, 90, 75, 70, 60, 40, and 27 expression

5.3.2.1 Protein extraction

Following 900 MHz GSM exposure, petri dishes containing control samples and RF-EMF exposed samples (20 x 10^6 cells) were placed directly onto ice and the cells were transferred to sterile test tubes (Greiner Bio-One, Germany) by gently washing the petri dishes with 3 ml of ice cold PBS containing 1 mM sodium orthovanadate (Sigma Chemical Co.) and 1 % protease inhibitors (Sigma Chemical Co.). Cells were then centrifuged for 10 min at 300 g, the supernatant removed, and the pellet re-suspended in 1 ml ice-cold PBS mixture (containing 1 mM sodium orthovanadate and 1% protease inhibitors). Sperm-suspensions were then transferred to eppendorph tubes (Sigma Chemical Co.) and centrifuged (230 g) at 4ºC for 10 min after which the supernatant was removed and the pellet stored at -80ºC until further analysis.

After thawing, pellets were lysed with 50 µl lysis buffer (containing 2% SDS - sodium dodecyl sulphate; 1% 0.1 M sodium orthovanadate (Sigma Chemical Co.), and 1% Protease inhibitor cocktail (Sigma Chemical Co.)) for 60 min on ice. Cells were then boiled on a heater block (100°C) for 5 minutes. Cell extraction was accomplished by aspiration through a needle (22G, at least 10 times). Non-soluble debris was removed by centrifugation (10 min at 300 g). Protein content was determined using the Bradford method (Bio-Rad's DC protein Assay) (Bradford 1976). In addition, results were confirmed using the LOWRY method (results not shown) with a cell concentration of 20 x 10^6 cells/ml producing approximately 50 µg of proteins.

5.3.2.2 Electrophoresis

Sperm extracts containing 50 µg of proteins were loaded onto Invitrogen Nupage 10% Bis-Tris gel 1.0 mm x 10 wells. Running conditions were 200 V for 55 minutes using MOPS/SDS running buffer (1.0 M MOPS, 1.0 M TrisBase, 69.3 mM SDS, 20.5 mM EDTA, free acid).

5.3.2.3 Blotting

Directly after electrophoresis, blots of the 1 D-gels were performed. Proteins were blotted on PVDF membranes (Bio-Rad, UK) using a 10% Towbin buffer as a transfer buffer (25 mM Tris, 192 mM glycine, 10% MeOH) with Bio-Rad's mini wet-blot equipment. Running conditions were 80 V for 60 min. Membranes were blocked at room temperature in TBS (Tris- buffered Saline, 20mM TrisBase, 137mM NaCl, adjusted with concentrated HCl to pH 7.6) containing 3% BSA for 1 hour. Hsps were detected in the membranes using appropriate antibodies (Stress Gen, Canada). All antibodies used were rabbit polyclonal and Hsp27 and Hsp70 were diluted 1/3000 while all other antibodies were diluted 1/2000 in 3% BSA. Membranes with antibodies were left overnight in 4ºC. The following day membranes were washed 3 times with TBS containing 0.05% Tween for 5-10 minutes each wash. Directly afterwards the secondary antibody was added, Goat-anti-rabbit (DAKO), diluted 1/30 000 in 3% BSA and membranes were left for 2 hours. Membranes were then washed 3 times with TBS (0.05% Tween), where after Hsps were detected by enhanced chemiluminescence (Millipore Immobilon western Chemilumenescent HRP- substrate). Analysis of Hsps, were performed using Non-linear Dynamics Phoretics 1D version 2003.02 software.

5.3.2.4 Western Blot analysis of Hsp70 and Hsp27 in EA.hy926 cells

EA.hy926 cells (kindly donated by Dr. Cora-Jean S. Edgell, North Carolina University, NC, USA) were grown in Dulbecco's MEM, supplemented with antibiotics, 10% foetal bovine serum, L-glutamine and HAT-supplement (all supplements were from GIBCO). For experiments, cells were trypsinated (GIBCO, 0.25% trypsin 1mM EDTA) and reseeded at a density of 400 000 cells per petri dish (NUNC). Cells were left to adhere overnight before confluent monolayers of EA.hy926 were heat shocked for 1 hour at 43°C in a CO_2 incubator. Control samples

were kept at 37°C for the duration of the exposure. Protein extraction, electrophoresis and blotting were performed as described for spermatozoa.

5.4 PHYSIOLOGICAL EFFECTS OF HSP ACTIVATION

5.4.1 Detection of stress fibres in human spermatozoa

Directly after RF-EMF exposure, cells (1 x 10^6/ml) were washed twice with PBS (300 g, 5 min) and fixed in 3.7% paraformaldehyde (Sigma Chemical Co.). These cells were then washed a further three times by centrifugation (300 g, 5 min) in PBS before being permeabilised with 0.1% Triton X-100 (Sigma Chemical Co.). Droplets were then made on a slide and the cells allowed to air dry. The dry slides were rinsed three times with PBS and incubated for 30 min at room temperature in a 1% BSA-PBS solution. Cells were then overlaid with 5 µl Alexa Fluor 488 Phalloidin (BD Biosciences) in 200 µl PBS and incubated for 30 min at room temperature. The stained slides were rinsed three more times with PBS and once with distilled water, before mounting the slides with mounting medium (Sigma Chemical Co.). Once mounted, slides were analysed using a Zeiss fluorescence microscope (Axioskop40, Carl Zeiss (Pty) Ltd.) and images were acquired with an AxioCam digital camera using Axiovision AC V4.5 software.

5.4.2 Detection of stress fibres in MCF-7 cells

To confirm the methodology of stress fibre detection, a human breast cancer cell line MCF-7, exposed to RF-EMF as well as heat shock (43ºC) for 1 hour, was used. MCF-7 cells were grown to confluency in tissue culture flasks and were trypsinated (Trypsin/Versene, Highveld Biological, SA) the day before exposure. Cells were counted and seeded at a concentration of 350 x 10^3 cells/coverslip which was placed at the bottom of a glass petri dish overlaid with 3 ml complete medium (Dulbecco's-MEM, Gibco, Scientific Group, USA) supplemented with 10% foetal bovine serum (Highveld Biological) and Penstrep-Fungizone (Highveld Biological) and left to adhere overnight. The following day, the medium was replaced with 3 ml complete medium (kept at 37ºC) and cells were exposed for a period of 1 hour to 900 MHz GSM radiation or heat shocked at 43ºC in a warm oven, while control cells were maintained at 37ºC in a humidified CO_2 incubator. F-actin accumulation was

detected with Alexa Fluor-Phalloidin using the same method described for visual assessment of stress fibre stabilisation in sperm, except that staining was performed on cells adherent to cover-slips.

5.5 STATISTICAL ANALYSIS

Statistical analysis was done with Stata Statistical Software Release 8.0 (Stata Corp., 2003, USA) using a within subject design considering two treatments, control and RF-EMF (SAR 2.0 W/kg), at three time points for a total of 12 donors. Flow cytometric results were analysed using time series regression under the random effect option. Western Blot data (for two donors only) was analyzed using a Wilcoxon matched pairs signed ranks test due to the relative small sample size (n = 6 per donor). All data is presented as mean values ± SD.

5.6 RESULTS

5.6.1 Flow cytometric analysis and visualisation of Hsp70 and 27 expression and phosphorylation

Baseline expression of Hsp27 in human spermatozoa as determined by flow cytometry and the phosphorylation thereof detected by the monoclonal antibody anti-Hsp27P are noted in Figure 5.2 A, while indirect immunofluorescence detection of Hsp27P in sperm is depicted in Figure 5.2 B. Hsp70 expression determined by flow cytometry, and indirect immunofluorescence detection thereof is shown in Figure 5.3 A and B.

5.6.1.1 Flow cytometric analysis of Hsp27 expression and phosphorylation

Hsp27 fluorescence produced a stronger fluorescence signal compared to phosphorylated Hsp27 (Figure 5.2 A). In flow cytometric analysis of Hsp27 phosphorylation, non-specific binding of the secondary antibody (FITC) resulted in a background fluorescence of 1.12 ± 0.92 cells/channel. Hsp27 phosphorylation detected by the anti-Hsp27P antibody decreased significantly ($p < 0.05$) as a function of time (Figure 5.2). However no significant difference in Hsp27 phosphorylation after RF-EMF exposure at any of the time points was detected compared to control

spermatozoa. Hsp27P increased slightly in 43°C exposed spermatozoa, but this increase was not significantly different from spermatozoa maintained at 37°C (controls). Figure 5.2 B depicts typical Hsp27P staining in control (I) and RF-EMF exposed (II) spermatozoa, Hsp27P fluorescence was mainly located in the neck and principle tail-piece of spermatozoa. No significant increase in fluorescence intensity after RF exposure was noted.

5.6.1.2 Flow cytometric analysis of Hsp70 expression

In flow cytometric analysis of Hsp70 expression, non-specific binding of the secondary antibody (FITC) resulted in a background fluorescence of 1.80 ± 0.91 cells/channel. Hsp70 expression decreased as a function of time (Figure 5.3 A) with fluorescence decreasing below background fluorescence after 24 hours (data not shown). Hsp70 expression after RF-exposure was slightly elevated, however, no significant difference was noted at any of the time points compared to control spermatozoa. There was also no difference in Hsp70 expression between RF-EMF exposed, control, or heat shocked spermatozoa determined respectively after 1 hour RF-EMF or 43°C exposure. Hsp70 fluorescence (Figure 5.3 B) was detected mainly in the neck area of spermatozoa, and no difference was noted in fluorescence intensity between control (I) and RF-exposed (II) sperm.

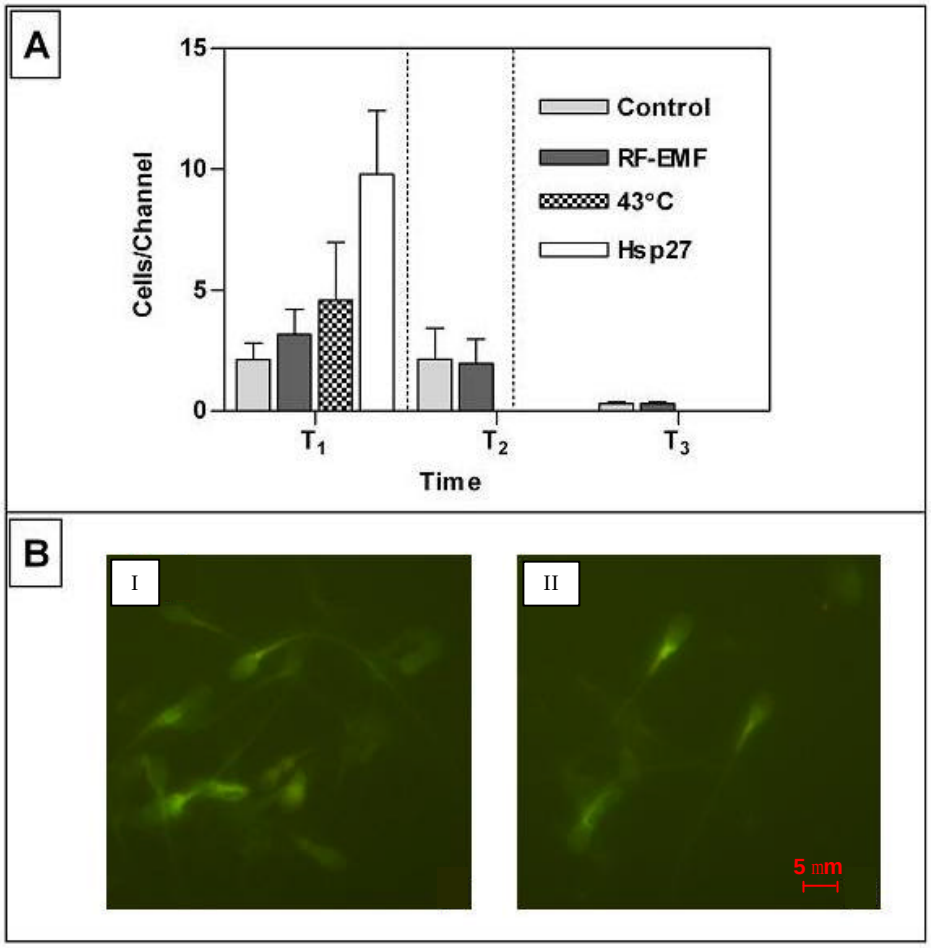

Figure 5.2 **(A)** Flow cytometric analysis of Hsp27 phosphorylation (dark grey) detected by anti-Hsp27P directly (T_1), 2 (T_2) and 24 hours (T_3) after an hour RF-EMF exposure at SAR 2.0 W/kg (n = 12). Baseline Hsp27 expression (white) as well as Hsp27 phosphorylation after a 1 hour heat shock at 43°C (black and white) are given at time 1. Control (light grey) samples were maintained at 37°C during the exposures. **(B)** Detection of Hsp27P expression by immunofluorescence staining directly after exposure (T_1), in (I) control and (II) RF-exposed sperm, Hsp27P fluorescence was mainly located in the neck area of the sperm.

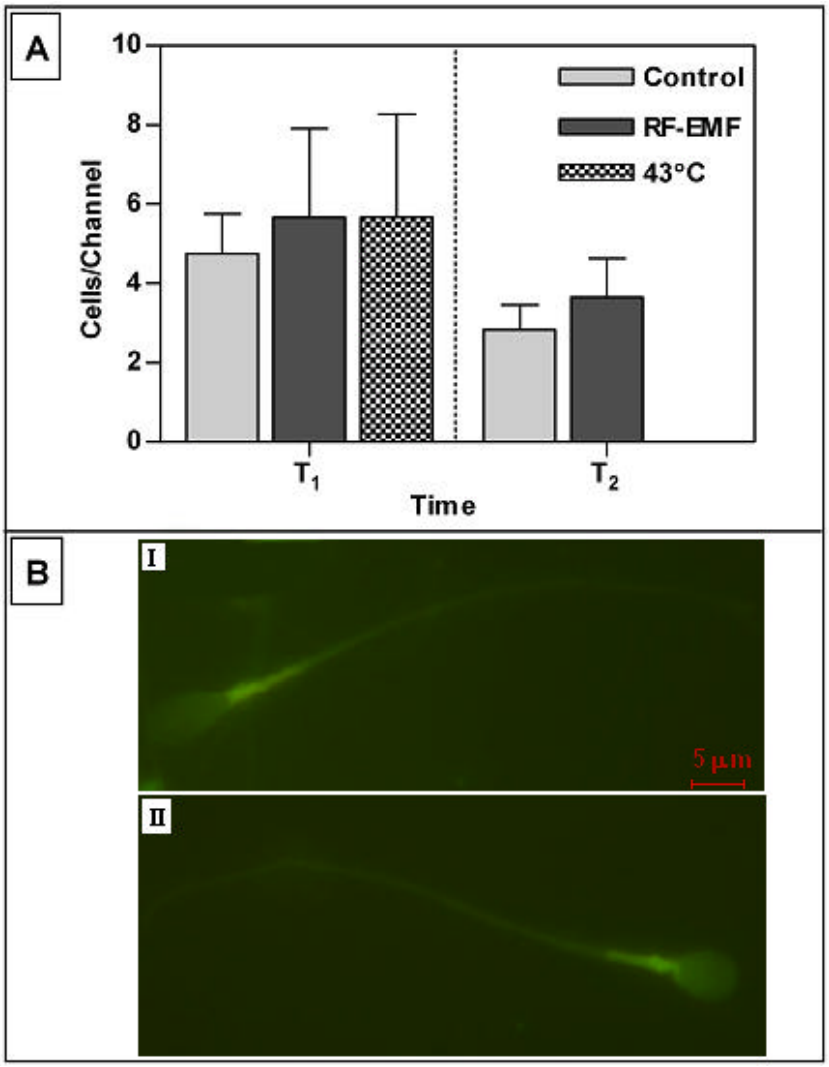

Figure 5.3 **(A)** Flow cytometric analysis of Hsp70 expression detected directly (T_1) and 2 (T_2) after an 1 hour RF-EMF exposure at SAR 2.0 W/kg or heat shock at 43°C (n = 12). Control samples were maintained at 37°C during the exposures. **(B)** Detection of Hsp70 immunofluorescence staining directly after exposure (T_1), in (I) control and (II) RF-exposed sperm, Hsp70 fluorescence was mainly located in the neck area of the sperm.

5.6.2 Western Blot analysis of Hsps 110, 90, 70, 75, 60, 40, and 27 expression

5.6.2.1 Western Blot analysis of Hsp27

A typical autoradiogram of Hsp27 expression in donor 2 (D_2)-I and donor 12 (D_{12})-II as well as in the epithelial cell line (AE.hy926)-III is illustrated in Figure 5.4 A. The 27 kD band corresponding to Hsp27 was confirmed by anti-Hsp27 antibody staining. Densitometric analysis of the Western Blots represents the results of six experiments (Figure 5.4 B). Statistical analysis (Wilcoxon matched pairs signed ranks test) between control, RF-EMF exposed or heat shocked sperm revealed no significant difference in Hsp27 expression determined for either of the two donors. The EA.hy926 cells expressing Hsp27 significantly differed ($p < 0.05$) from that of sperm cells.

5.6.2.2 Western Blot analysis of Hsp70

A strong 70 kD signal was observed in Western blots of SDS-PAGE resolved sperm proteins probed with an anti-Hsp70 polyclonal antibody (Figure 5.5 A). The densitometric analysis of the Western Blots (Figure 5.5 B), represent the results of six experiments. Hsp70 expression in sperm cells were significantly greater ($p < 0.05$) compared to EA.hy926 cells. For donor 2 (D_2) there was no difference in Hsp70 expression for any of the conditions (control, RF-EMF or 43°C). However, there was a marginally significant difference ($p = 0.067$) in Hsp70 expression in RF-EMF exposed sperm compared to control sperm for donor 12 (D_{12}). The expression of Hsp70 in heat shocked (43°C) sperm and RF-EMF exposed sperm for D_{12} did not differ significantly ($p > 0.05$) and this was also the case between control and heat shocked (43°C) sperm.

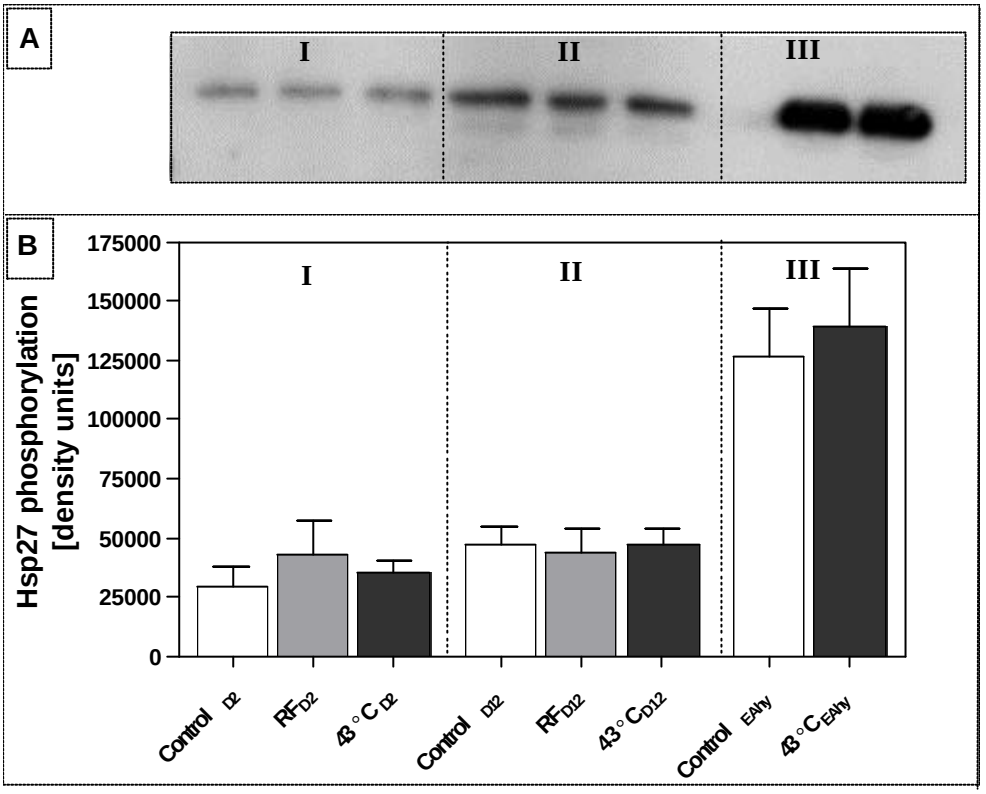

Figure 5.4 Western Blot analysis of Hsp27: (A) Autoradiogram of SDS-PAGE resolved proteins for donor 2 (I), donor 12 (II) and EA.hy926 cells (III). The position of the bands correspond to heat shock proteins of M_r 27 kD, specific for Hsp27. **(B)** Densitometric analysis of Hsp27 phosphorylation status in spermatozoa directly after an hour exposure to RF-EMF at SAR 2.0 W/kg or 43°C. Control samples were maintained at 37°C for the duration of the exposure. As a control Hsp27 expression in EA.hy926 cells (III) after heat shock at 43°C is also noted.

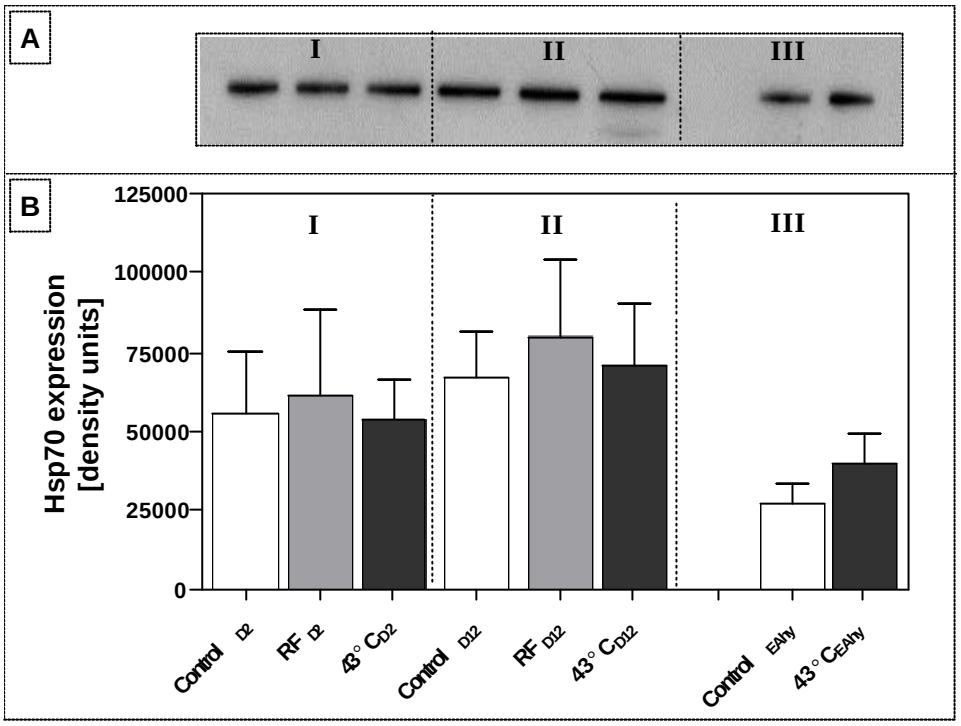

Figure 5.5 Western blot analysis of Hsp70: (A) Autoradiogram of SDS-PAGE resolved proteins for donor 2 (D_2- I), donor 12 (D_{12} - II) and EA.hy926 cells (III). The position of the bands correspond to heat shock proteins of M_r 70 kD, specific for Hsp70. **(B)** Densitometric analysis of Hsp70 expression in spermatozoa directly after an hour exposure to RF-EMF at SAR 2.0 W/kg or 43°C. Control samples were maintained at 37°C for the duration of the exposure. As a control Hsp70 expression in EA.hy926 cells (III) after heat shock at 43°C is also noted.

5.6.2.3 Western Blot analysis of Hsps 110, 90, 75, 60, and 40

It is not known if other spermatozoal heat shock proteins would respond to RF-EMF, therefore additional heat shock proteins were probed in cellular extracts from donor 2 and 12. The SDS-PAGE results and corresponding densitometric analysis of Hsps 110, 90, 75, 60, and 40 expression are presented in Figures 5.6 and 5.7 and are the result of single experiments conducted in each of the two donors. Densitometric values are the results of single Western blot analysis per donor. Hsps 60, 75, and 110 expression in donor 2 after RF-EMF was lower than that found in control samples (Figure 5.6 B-I), only Hsp75 expression showed a possible increase after heat shock. Interestingly, Hsp60 and 75 expression decreased after RF-EMF compared to control and 43°C exposed samples. However this effect was not observed in donor 12, on the contrary Hsp60 and 75 expression after RF-EMF compared well to control samples (Figure 5.6 B-II). The only possible effect noted in Hsp expression measured in donor 12 is the down regulation of Hsp60 after 43°C exposure – this was measured twice in donor 12 to confirm the low Hsp60 expression.

A very strong 40 kD signal was observed for both donors in WB analysis of SDS-PAGE resolved Hsp40 (Figure 5.7 A). Densitometric analysis demonstrated a marginally greater expression in Hsp40 for 43°C exposed samples in both donors. However, no difference in expression was noted between control and RF-EMF exposed samples (Figure 5.7 B-I and II). Hsp90 expression was unaffected by either RF-EMF and heat shock, with expression in control samples for both donors similar to that of the stressed (RF-EMF and 43°C) samples (Figure 5.7 B I and II).

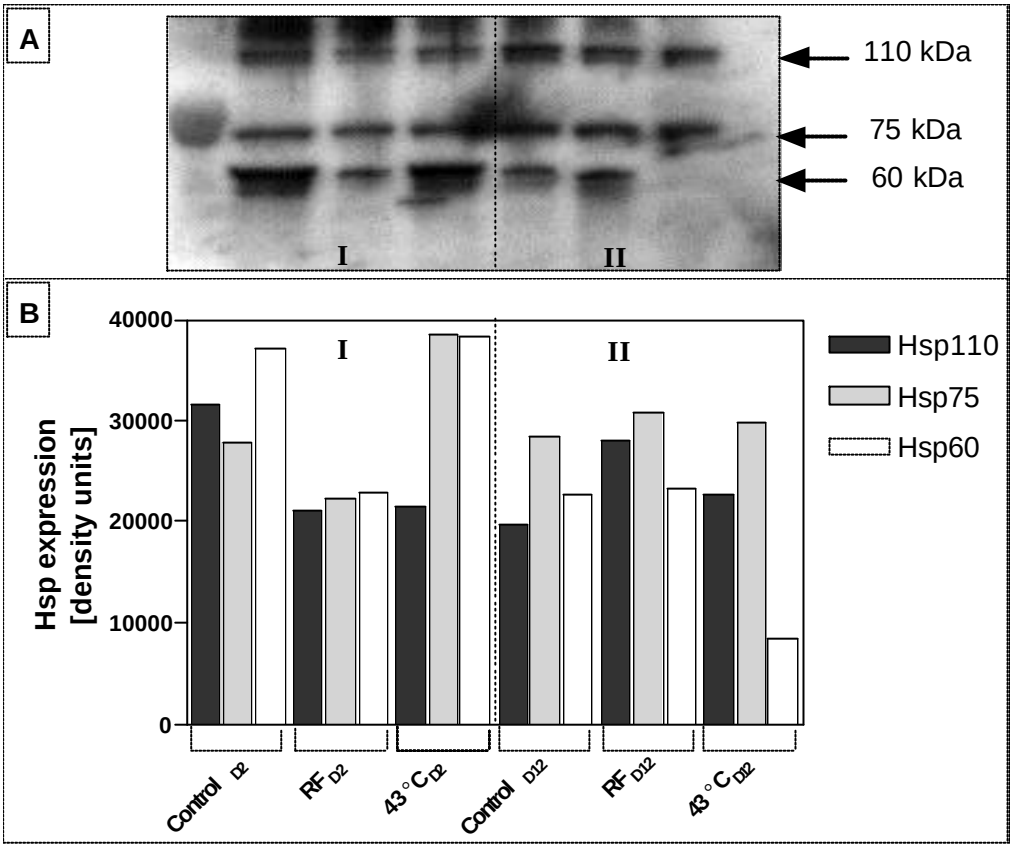

Figure 5.6 Western blot analysis of Hsps 110, 75 and 60: **(A)** Autoradiogram of SDS-PAGE resolved proteins for donor 2 (D2- I), and donor 12 (D12 - II). The position of the bands corresponds to heat shock proteins of M_r 110 kD, 75 kD and 60 kD specific for Hsp110, Hsp75 and Hsp60 respectively. **(B)** Densitometric analysis of Hsp110, Hsp75 and Hsp60 expression in spermatozoa directly after an hour exposure to RF-EMF at SAR 2.0 W/kg or 43°C. Control samples were maintained at 37°C for the duration of the exposure.

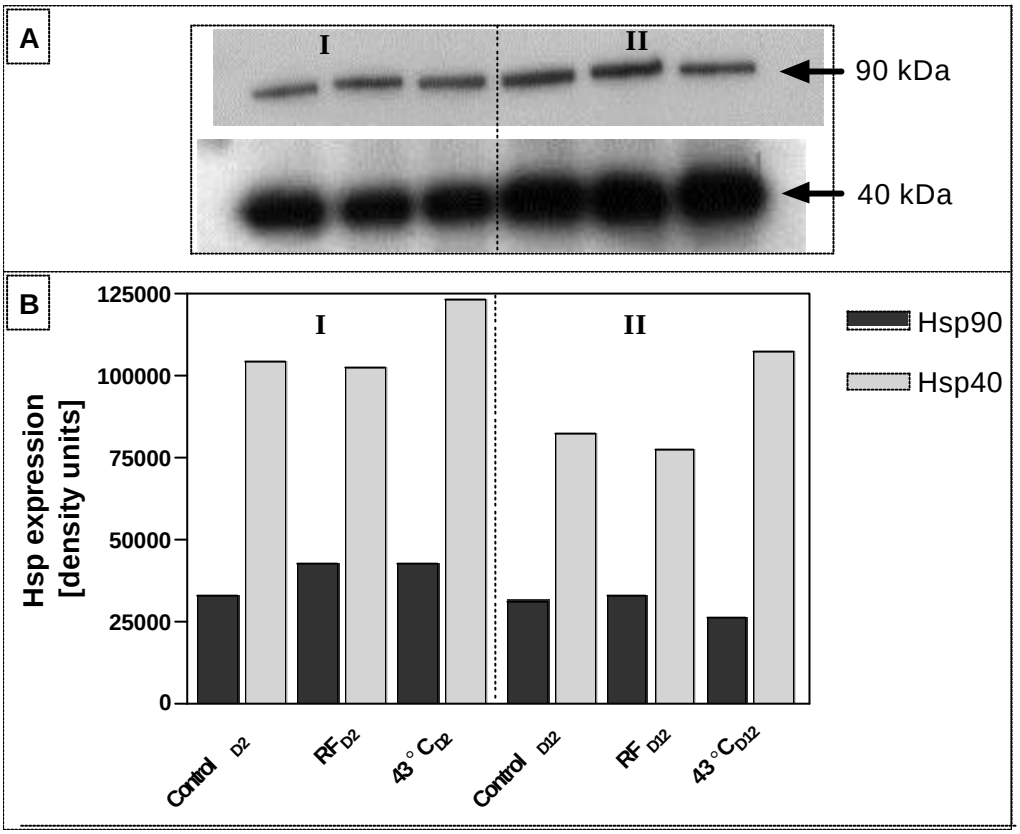

Figure 5.7 Western Blot analysis of Hsps 90 and 40: (A) Autoradiogram of SDS-PAGE resolved proteins for donor 2 (D_2- I), and donor 12 (D_{12} - II). The position of the bands corresponds to heat shock proteins of M_r 90 kD, and 40 kD specific for Hsps 90 and 40. **(B)** Densitometric analysis of Hsps 90 and 40 expression in spermatozoa directly after an hour exposure to RF-EMF at SAR 2.0 W/kg or 43°C. Control samples were maintained at 37°C for the duration of the exposure.

5.6.3 Detection of stress fibres

In order to establish if heat shock protein phosphorylation has a physiological affect on F-actin polymerisation, RF-EMF exposed cells were labelled with phalloidin, an inhibitor of F-actin depolimerisation. The distribution of F-actin in spermatozoa and MCF-7 cells are depicted in Figures 5.8 and 5.9 respectively.

5.6.3.1 F-actin polymerisation in RF-EMF exposed human spermatozoa

To determine the effect of heat shock on F-actin polymerisation, spermatozoa were exposed for a period of one hour to 37°C in a CO_2 incubator, 39°C in a warm oven and 43°C in a water bath. The temperatures were specifically chosen as it was previously reported that sperm cells subjected to a temperature increase from 35°C to 39°C did express Hsps whereas this effect was negated by a further temperature increase to 43°C (Nononguchi *et al.*, 2001). Hsp27 regulates F-actin polymerisation, therefore heat shock was applied at different temperatures to optimise the possible effect that Hsp27 expression/phosphorylation could have on F-actin polymerisation. Special care was taken in keeping the temperature of ejaculated spermatozoa constant at 35°C when processing the sperm. Directly after processing, sperm were subjected to the different temperature exposure regimes (Figure 5.8 A and C). No notable difference in F-actin concentration was seen in spermatozoa exposed to 37°C, 39°C and 43°C.

Slides made of fixed and permeabilised spermatozoa were frozen away at -20°C, until phalloidin staining on the day of analysis. Slides were prepared for all twelve donors, at each time point after exposure (T_1, T_2, T_3), for both control and RF-EMF exposed cells. Typical staining is represented in Figure 5.8 B. No difference in staining was noted between control and RF-EMF exposed spermatozoa. There were also no changes in phalloidin staining as a function of time.

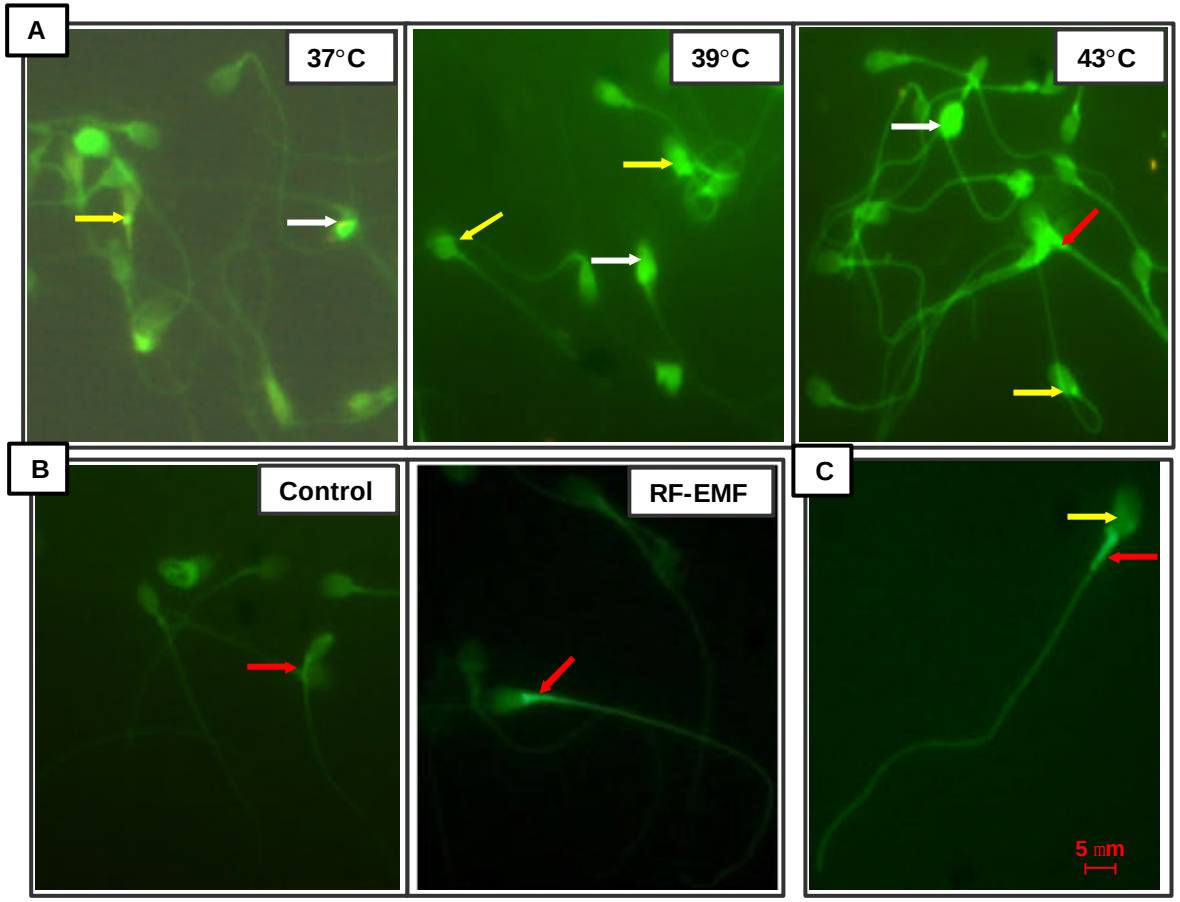

Figure 5.8 Immunolocalization of F-actin. (A) AlexaFluor-labelled phalloidin stained spermatozoa predominantly in the acrosome (white arrow), post-acrosomal area (yellow arrow), as well as neck and principal tail-piece areas (red arrow). **(B)** Cellular response of spermatozoa exposed to RF-EMF, control cells were maintained at 37°C for the duration of the exposure. **(C)** Typical staining of AlexaFluor-labelled phalloidin.

5.6.3.2 F-actin polymerisation in RF-EMF exposed MCF-7 cells

In control and RF-EMF exposed MCF-7 cells (Figure 5.9), the highest F-actin content was localised at the perimeters of the cell (yellow arrows), with a network of stress fibres staining over the whole cytoplasm of the cell (orange arrows). However, no marked difference in stress fibre stabilisation determined by increased phalloidin-AlexaFluor staining was seen between control cells and RF-EMF exposed cells. Interestingly, MCF-7 cells heat shocked at 43°C for one-hour show an increase in F-actin concentration localised in the nuclear mass of the cell. Rounding up of the cells was also clearly visible, while edge ruffling was noticed in some cells (white arrows). F-actin aggregation resulting in distinct pockets of high phalloidin concentration was distributed throughout entire cells (red arrows).

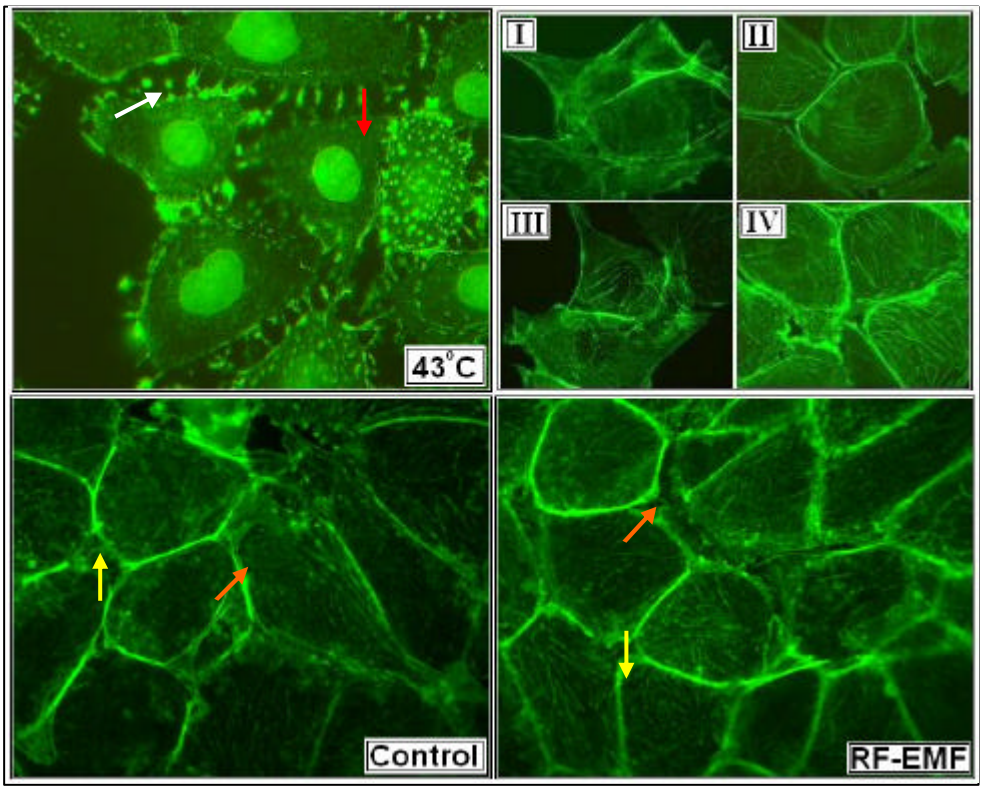

Figure 5.9 Cellular response of MCF-7 cells to RF-EMF and heat shock, control cells were maintained at 37°C for the duration of the exposures. Stress fibres are detected by AlexaFluor-labelled phalloidin. Inserts I and II show the distribution of F-actin in control cells compared to cells exposed to RF-EMF for 1 hour (inserts III and IV).

5.7 DISCUSSION

In the present study, we have identified the presence of Hsp27, a member of the small heat shock protein family (sHsp), in ejaculated density purified human spermatozoa by WB analysis and specific antibody staining. Hsp27 is a classically heat inducible Hsp, but also occurs in the absence of stress in various cells in the body (Pittenger *et al*., 1992; Sugiyama *et al*., 2000). As no *de novo* synthesis of proteins in fully differentiated spermatozoa is possible, the effect of RF-EMF on the phosphorylation status of Hsp27 was investigated.

Hsp27 phosphorylation was determined by flow cytometry using a FITC conjugated anti-Hsp27P antibody. No increased phosphorylation of Hsp27 in human spermatozoa was noted after RF-EMF exposure. This is in agreement with several other studies that have reported no increased Hsp27 phosphorylation after RF exposure in human lymphocytes (Lim *et al*., 2005), glioblastoma cells (Miyakoshi *et al*., 2005; Qutob *et al*., 2006), and HeLa and EA.hy926 cells (Vanderwaal *et al*., 2006). Heat shock, on the other hand, resulted in a mild (though not significantly different from controls) increase of Hsp27P fluorescence in spermatozoa. In contrast a high expression of Hsp27 was noted in heat shocked EA.hy926 cells. Immunomicroscopy probing using antibodies against phosphorylated Hsp27 revealed that Hsp27P was mainly confined to the neck area of spermatozoa. However, no difference in fluorescence in RF-exposed samples were noted compared to controls maintained at 37°C.

The possibility that Hsp70 could be up-regulated after RF-exposure via transverse scriptase was also investigated. Western blot probing with an Hsp70 polyclonal antibody resulted in a strong 70 kD signal compared to Hsp70 expression in EA.hy926 cells. Multiple isoforms of Hsp70 have been identified in male germ cells and spermatozoa including the sperm specific variant HspA2 (Miller *et al*., 1992; Huzar *et al*., 2000; Bohring and Krause, 2003). In addition, Hsp70 was reported to be an abundant surface protein, explaining the strong 70 kD signal observed. However, no up-regulation of cytoplasmic Hsp70 in response to RF exposure was observed. Using an antibody directed against the stress inducible form of Hsp70, we also noted no significant increase in Hsp70 fluorescence after RF exposure determined by flow

cytometric analysis. Several other studies have reported a lack in up-regulating Hsp70 expression after RF exposure in human lymphocytes (Capri *et al*., 2004; Lim *et al*., 2005), human glioblastoma cells (Miyakoshi *et al*., 2005), and mammalian cells (Laszlo *et al*., 2005) supporting these results.

In addition, Hsp70 in human sperm was not up-regulated by hyperthermia in contrast to EA.hy926 cells. This result was not unexpected, as it has previously been demonstrated that the murine Hsp70 gene is not heat inducible (Zakeri *et al*., 1988; Rosario *et al*., 1992; Son, 1999). Immunomicroscopy evaluation of Hsp70 staining was in accordance with Miller *et al*. (1992) who also noted Hsp70 staining located in the neck, mid-piece, and equatorial segment of fixed spermatozoa. In addition, RF exposure did not increase stress inducible Hsp70 fluorescence intensity.

One possible limitation of the data presented is that an anti-Hsp70 antibody was used for Western blotting and an antibody directed against the stress inducible form of Hsp70 was used for flow cytometric analysis, whereas HspA2, the male germ cell specific homologue for Hsp70, is the most abundant member of the heat shock protein 70 family in human germ cells. HspA2 has < 90% amino acid homology to other members of the human Hsp70 gene family and 83.3% to the stress inducible Hsp70 gene (Bonnycastle *et al*., 1994). Therefore, it is uncertain whether HspA2 or other members of the Hsp70 family of proteins was detected in the present study. However, Bohring and Krause (2003) concluded that it is unlikely that Hsp70 and HspA2 are involved in a stress response but rather have chaperone functions during capacitation, acrosome reaction, and oocyte binding.

Besides Hsp27 and 70, the expression of Hsps 40, 60, 90, and 110 were also investigated by Western blotting after RF exposure. In addition, the expression of another member of the Hsp70 family of proteins - Hsp75, a moderately stress inducible glucose regulated stress protein, present within the mitochondrial matrix (Creagh *et al*., 2000), was also probed. Bearing in mind that WB analysis of heat shock proteins 110, 90, 75, 60, and 40 were the result of single experiments in each of two donors, it cannot be concluded that these proteins are unaffected by RF-EMF. However, taking the bulk of evidence presented here, it seems unlikely that RF-EMF has an effect on the sperms ability to launch a stress response via the heat shock

protein pathway. None of the Hsps found in spermatozoa and probed using Western Blots or flow cytometric analysis showed a significant increase in expression or phosphorylation after RF-EMF. Furthermore, Hsp expression after heat shock (43°C) analysed with flow cytometry and Western Blots did not unequivocally show that heat stress can up-regulate Hsp expression in human spermatozoa.

The actin network plays an important role in regulating exocytosis in endocrine and secretory cells (Burgoyne *et al*., 1991; Dudani and Ganz, 1996). In spermatozoa, the AR is regarded as equivalent to exocytosis and is therefore regulated by similar processes (Liu *et al*., 2002). In the sperm head, actin occurs mainly in its monomeric form but polymerises to form filamentous F-actin during sperm capacitation (Rogers *et al*., 1989; Castellani-Ceresa *et al*., 1993; Spungin *et al*., 1995; Liu *et al*., 1999, 2005). In particular, F-actin increases during capacitation leading to the establishment of an F-actin network between the plasma and outer acrosomal membrane (Spungin *et al*., 1995; Breitbart and Spungin, 1997; Liu *et al*., 2005; Breitbart *et al*., 2005) and its depolymerisation is essential for the AR (Liu *et al*., 1999; Breitbart *et al*., 2005).

Liu *et al*. (1999) noted the preferential staining of actin, using an anti-actin antibody in the acrosomal region of acrosome intact spermatozoa, as well as the post acrosomal, mid-piece and tail sections of both acrosome reacted and intact spermatozoa. A similar staining pattern for F-actin was observed in the current study. We did not observe an increase in actin polymerisation in sperm exposed to different temperatures or in RF exposed spermatozoa. In contrast, heat stress in MCF-7 cells induced accumulation of F-actin, demonstrated by the aggregation of F-actin and their concentration around the nucleus of the cell. RF exposure, however, did not induce an increase in stress fibre stabilisation in MCF-7 cells. Zeng *et al*. (2006) recently reported that RF exposure of MCF-7 cells did not lead to any change in protein expression. Considering that actin polymerisation is modulated by Hsp27 phosphorylation, and that we noted no increased Hsp27P expression in RF exposed spermatozoa, it is thus plausible that no increase in F-actin was noted after RF exposure in either spermatozoa or MCF-7 cells.

Actin polymerisation in human spermatozoa also depends on tyrosine phosphorylation associated with capacitation (Brener, 2003). Hsp90 has the potential to mediate serine/threonine and/or tyrosine kinase signalling in the pathway to a global increase in protein tyrosine phosphorylation during capacitation (Ecroyd, 2003). If RF-EMF could have affected Hsp90 activity it would have indirectly affected actin polymerisation. Since neither increase in Western Blot expression of Hsp90 nor changes in actin polymerization was seen, it could be concluded that RF-EMF had no effect on protein tyrosine phosphorylation.

These results, taken together, seem to indicate that fully mature spermatozoa are unable to launch a stress response when exposed to high temperatures or RF-EMF exposure. Noting the specific roles of some Hsps in fertilisation (Eddy, 1999; Neuer *et al*., 2000), it would seem likely that the complement of heat shock proteins that spermatozoa are equipped with are functional mainly as chaperonens during fertilisation. This finding suggests that mobile phone radiation is not a stressor of human spermatozoa.

5.8 REFERENCES

Bachelet, M., Mariéthoz, E., Banzet, N., Souil, E., Pinot, F., Polla, C,Z., Durand, P., Bouchaert, I., Polla, B.S. 1998. Flowcytometry is a rapid and reliable method for evaluating heat shock protein 70 expression in human monocytes. *Cell Stress Chap*., 3, 168-75.

Baldi, E., Luconi, M., Bonaccorsi, L., Forti, G. 2002. Signal transduction pathways in human spermatozoa. *J Reprod Immunol*., 53, 121-31.

Bloom, S.E., Muscarella, D.E., Lee, M.Y., Rachlinski, M. 1998. Cell death in the avian blastoderm: resistance to stress induced apoptosis and expression of anti-apoptotic genes. *Cell Death Diff*., 5, 529-38.

Bohring, C., Krause, W. 2003. Characterisation of spermatozoa surface antigens by antisperm antibodies and its influence on acrosomal exocytosis. *Am J Reprod Immunol*., 50, 411-9.

Bonnycastle, L.L.C., Yu, C.E., Hunt, C.R. 1994. Cloning, sequencing and mapping of the human chromosome 14 heat shock protein gene (HspA2). *Genomics*., 23, 85-93.

Bradford, M.M. 1976. A rapid and sensitive method for the quantification of microgram quantities of protein utilizing the principle of protein dye binding. *Anal Biochem*., 72, 248-54.

Breitbart, H., Spungin, B. 1997. The biochemistry of the acrosome reaction. *Mol Hum Reprod*., 3, 195-202.

Breitbart, H., Cohen, G., Rubinstein, S. 2005. Role of actin cytoskeleton in mammalian sperm capacitation and the acrosome reaction. *Reprod*., 129, 263-8.

Brener, E., Rubinstein, S., Cohen, G., Shternall, K., Rivlin, J., Breitbart, H. 2003. Remodeling of the actin cytoskeleton during mammalian sperm capacitation and acrosome reaction. *Biol Reprod*., 68, 837-45.

Brouet, A., Sonveaux, P., Dessy, C., Moniotte, S., Balligand, J.L., Feron, O. 2001. Hsp90 and caveolin are key targets for proangiogenic nitric oxide-mediated effects of statins. *Circ Res*., 89, 866-73.

Burgoyne, R.D., Handel, S.E., Morgan, A. 1991. Calcium, the cytoskeleton and calpactin (annexin II) in exocytotic secretion from adrenal chromaffin and mammary epithelial cells. *Biochem Soc Trans*., 19, 1085-90.

Capri, M., Scarcella, E., Bianchi, E., Fumelli, C., Mesirca, P., Agostini, C., Remondini, D., Schuderer, J., Kuster, N., Bersani, F. 2004. 1800 MHz radio frequency (mobile phones, different Global System for Mobile communication modulations) does not affect apoptosis and heat shock protein 70 level in peripheral blood mononuclear cells from young and old donors. *Int J Radiat Biol*., 80, 389-97.

Castellani-Ceresa, L., Mattioli, M., Radaelli, G., Barboni, B., Brivio, M.F. 1993. Actin polymerization in boar spermatozoa: fertilization is reduced with use of cytochalasin D. *Mol Reprod Dev*., 36, 203-11.

Creagh, E.M., Sheehan, D., Cotter, T.G. 2000. Heat shock proteins – modulators of apoptosis in tumour cells. *Leukemia*., 14, 1161-73.

Czyz, J., Guan, K., Zeng, Q., Nikolova, T., Meister, A., Schonborn, F., Schuderer, J., Kuster, N., Wobus, A.M. 2004. High frequency electromagnetic fields (GSM signals) affect gene expression levels in tumor suppressor p53-deficient embryonic stem cells. *Bioelectromagnetics*., 25, 296-307.

Dadoune, J.P., Pawalak, A., Alfonsi, M.F., Siffroi, J.P. 2005. Identification of transcripts by microarrays, RT-PCR and *in situ* hybridisation in human ejaculate spermatozoa. *Mol Hum Reprod*., 11, 133-40.

Daniells, C., Duce, I., Thomas, D., Sewell, P., Tattersall, J., de Pomerai, D. 1998. Transgenic nematodes as biomonitors of microwave-induced stress. *Mutant Res*., 339, 55-64.

Díez-Sánchez, C., Ruiz-Pesini, E., Montoya, J., Pérez-Martos, A., Enríquez, J.A., López-Pérez, M.J. 2003. Mitochondria from ejaculated human spermatozoa do not synthesize proteins. *FEBS Letters*., 553, 205-8.

Dudani, A.K., Ganz, P.R. 1996. Endothelial cell surface actin serves as a binding site for plasminogen, tissue plasminogen activator and lipoprotein (a). *Br J Haematol*., 95, 168-78.

Ecroyd, H., Jones, R.C., Aitken, R.J. 2003. Tyrosine Phosphorylation of HSP-90 during mammalian sperm capacitation. *Biol Reprod*., 69, 1801-7.

Eddy, E.M. 1999. Role of heat shock protein Hsp70-2 in spermatogenesis. *Rev Reprod*., 4, 23-30.

Ficarro, S., Chertihin, O., Westerbrook, V.A., White, F., Jayes, F., Kalab, P., Marto, J.A., Shabanowitz, J., Herr, J.C., Hunt, D.F., Visconti, P.E. 2003. Phospho-proteome analysis of capacitated human sperm. Evidence of tyrosine phosphorylation of a kinase-anchoring protein 3 and valosin-containing protein /p97 during capacitation. *J Biol Chem*., 278, 11579-89.

Fouquet, J.P., Kann, M.L. 1992. Species-specific localisation of actin in mammalian spermatozoa: fact or artifact? *Microsc Res Tech*., 20, 251-8.

Giordano, R., Magnano, A.R., Zaccagnini, G., Pitoogi, C., Moscufo, N., Lorentini, R., Spadafora, C. 2000. Reverse transcriptase activity in mature spermatozoa of mouse. *J Cell Biol*., 148, 1107-13.

Grunewald, S., Paasch, U., Glander, H.J., Anderegg, U. 2005. Mature human spermatozoa do not transcribe novel RNA. *Andrologia*., 37, 69-71.

Hahn, G.M., Li, G.C. 1990. Thermotolerance, thermoresistance and thermosensitization. In: R.I. Morimoto, A. Tissieres, C. Georgeopoulus, eds., *Stress Proteins in biology and medicine*. Cold Spring Harbour, NY: Cold Spring Harbour Press, 79.

Harris, M.B., Ju, H., Venema, V.J., Blackstone, M., Venema, R.C. 2000. Role of heat shock protein 90 in bradykinin-stimulated endothelial nitric oxide release. *Gen Pharmacol*., 35, 165-70.

Huot, J., Houle, F., Spitz, D.R., Landry, J. 1996. HSP27 phosphorylation-mediated resistance against actin fragmentation and cell death induced by oxidative stress. *Cancer Res*., 56, 273-9.

Huot, J., Lambert, H., Lavoie, J.N., Guimond, A., Houle, F., Landry, J. 1995. Characterisation of 45/54 kD Hsp27 kinase, a stress kinase which may activate the phosphorylation-dependant protective function of mammalian heat-shock protein 27. *Eur J Biochem*., 227, 416-27.

Huzar, G., Stone, K., Dix, D., Vigue, L. 2000. Putative creatine kinase m-isoform in human sperm is identified as the 70-kilodalton heat shock protein HspA2. *Biol Reprod*., 63, 925-32.

Kramer, J.A., Krawetz, S.A. 1997. RNA in spermatozoa: implications for the alternative haploid genome. *Mol Hum Reprod*., 3, 473-8.

Kreps, S., Banzet, N., Christiani, D.C., Polla, B.S. 1997. Molecular biomarkers of early response to environmental stressors: implication for risk assessment and public health. *Rev Environ Health*., 12, 261-80.

Lalancette, C., Faure, R.L., Leclerc, P. 2006. Identification of the proteins present in the bull sperm cytosolic fraction enriched in tyrosine kinase activity: A proteomic approach. *Proteomics*., 6, 1-18.

Landry, J., Lambert, H., Zhou, M., Lavoi, J.N., Hickey, E., Weber, L.A., Anderson, C.W. 1992. Human Hsp27 is phosphorylated at serines 78 and 82 by heat shock and mitogen-activated kinases that recognise the same amino acid motif as S6 kinase II. *J Biol Chem*., 267, 794-803.

Laszlo, A., Moros, E.G., Davidson, T., Bradbury, M., Straube, W., Roti Roti, J. 2005. The heat-shock factor is not activated in mammalian cells exposed to cellular phone frequency microwaves. *Rad Res*., 164, 163–72.

Lee, S., Johnson, D., Dunbar, K., Dong, H., Ge, X., Kim, Y.C., Wing, C., Jayathilaka, N., Emmanuel N., Wang, S.M. 2005. 2.45 GHz radio frequency fields alter gene expression in cultured human cells. *FEBS Lett*., 579, 4829-36.

Lees-Miller, S.P., Anderson, C.W. 1989a. The human double-stranded DNA-activated protein kinase the 90 kD heat shock protein, hsp90 alpha at two NH2-terminal threonine residues. *J Biol Chem*., 164, 17275-80.

Lees-Miller, S.P., Anderson, C.W. 1989b. Two human 90 kD heat shock proteins are phosphorylated in vivo at conserved serines that are phosphorylated in vitro by casein kinase II. *J Biol Chem*., 264, 2431-7.

Leszczynski, D., Joenväärä, S., Reivinen, J., Kuokka, R. 2002. Non-thermal activation of the Hsp27/p38MAPK stress pathway by mobile phone radiation in human endothelial cells: Molecular mechanism for cancer-and blood brain barrier-related effects. *Differentiation*., 70, 120-9.

Leszczynski, D., Kuokka, R., Joenväärä, S., Reivinen, J. 2004. Applicability of discovery science approach to determine biological effects of mobile phone radiation. *Proteomics*., 4, 426-31.

Lim, H.B., Cook, G.G., Barker, A.T., Coulton, L.A. 2005. Effect of 900 MHz electromagnetic fields on nonthermal induction of heat shock proteins in human leukocytes. *Rad Res.*, 163, 45-52.

Liu, D.Y., Martic, M., Clarke, G.N., Dunlop, M.E., Baker, H.W.G. 1999. An important role of actin polymerization in the human zona pellucida induced acrosome reaction. *Mol Hum Reprod.*, 5, 941-9.

Liu, D.Y., Martic, M., Clarke, G.N., Grkovic, I., Garrett, C., Dunlop, M.E., Baker, H.W.G. 2002. An anti-actin monoclonal antibody inhibits the zona pellucida-induced acrosome reaction and hyperactivated motility of human sperm. *Mol Hum Reprod.*, 8, 37-47.

Liu, D.Y., Clarke, G.N., Baker, H.W.G. 2005. Exposure of actin on the surface of the human sperm head during in vitro culture relates to sperm morphology, capacitation and zona binding. *Hum Reprod.*, 20, 999-1005.

Luconi, M., Barni, T., Vanelli, G.B., Krausz, C., Marra, F., Benedetti, P.A., Evangelista, V., Fancavilla, S., Properzi, G., Forti, G., Baldi, E. 1998. Extracellular signal-regulated kinases modulate capacitation of human spermatozoa. *Biol Reprod.*, 58, 1476-89.

Martínez-Heredia, J., Estanyol, J.M., Ballescà, J.L., Oliva1, R. 2006. Proteomic identification of human sperm proteins. *Proteomics.*, 6, 4356-69.

Matwee, C., Kamaruddin, M., Betts, D.H., Basrur, P.K., King, W.A. 2001. The effects of antibodies to heat shock protein 70 in fertilisation and embryo development. *Mol Hum Reprod.*, 7, 829-37.

Miller, D. 2000. Analysis and significance of messenger RNA in human ejaculated spermatozoa. *Mol Reprod Dev.*, 56, 259-64.

Miller, D., Brough, S., Al-Harib, O. 1992. Characterization and cellular distribution of human spermatozoal heat shock proteins. *Hum Reprod.*, 7, 645-637.

Miyakoshi, J., Takemasa, K., Takashima, Y., Ding, G.R., Hirose, H., Koyama, S. 2005. Effects of exposure to a 1950 MHz radio frequency field on expression of Hsp70 and Hsp27 in human glioma cells. *Bioelectromagnetics.*, 26, 251-7.

Moustafa, M.H., Sharma, R.K., Thornton, J., Mascha, E., Abdel-Hafez, M.A., Thomas, A.J., Agarwal, A. 2004. Relationship between ROS production,

apoptosis and DNA denaturation in spermatozoa from patients examined for infertility. *Hum Reprod*., 19, 129-38.

Muscarella, D.E., Rachlinski, M.K., Bloom, S.E. 1998. Expression of cell death regulatory genes and limited apoptosis induction in avian blastodermal cells. *Mol Reprod Dev*., 51, 130-42.

Naz, R.H. 1999. Involvement of protein serine and threonine phosphorylation in human sperm capacitation. *Biol Reprod*., 60, 1402-9.

Neuer, A., Spandorfer, S.D., Giraldo, P., Dieterle, S., Rosenwaks, Z., Witkin, S.S. 2000. The role of heat shock proteins in reproduction. *Hum Reprod Update.*, 6, 149-59.

Neuer, A., Mele, C., Liu, H.C., Rosenwaks, Z., Witkin, S.S. 1998. Monoclonal antibodies to mammalian heat shock proteins impair mouse embryo development *in vitro*. *Hum Reprod*., 13, 987-90.

Nonoguchi, K., Tokuchi, H., Okuna, H., Watanabe, H., Egawa, H., Saito, K., Ogawa, O., Fujita, J. 2001. Expression of Apg-l a member of the Hsp110 family, in the human testis and sperm. *Int J Urol*., 8, 308-14.

Nylund, R., Leszczynski, D. 2006. Mobile phone radiation causes changes in gene and protein expression in human endothelial cell lines and the response seems to be genome- and proteome-dependent. *Proteomics*., 6, 4769-80.

Ostermeier, G.C., Dix, D.J., Miller, D., Khatri, P., Krawetz, S.A. 2002. Spermatozoal RNA profiles of normal fertile men. *Lancet*., 360, 772-7.

Ostermeier, G.C., Miller, D., Huntriss, J.D., Diamond, M.P., Krawetzm, S.A. 2004. Reproductive biology: delivering spermatozoan RNA to the oocyte. *Nature*., 429, 154.

Pittenger, G.L., Gilmont, R.R., Welsh, M.J. 1992. The low molecular weight heat shock protein (Hsp27) in rat Sertoli cells: evidence for identity of Hsp27 with a germ cell-responsive phosphoprotein. *Endocrinology*., 130, 3207-15.

Qutob, S.S., Chauhan, V., Bellier, P.V., Yauk, C.L., Douglas, G.R., Berndt, L., Williams, A., Gajda, G.B., Lemay, E., Thansandote, A., McNameea, J.P. 2006. Microarray gene expression profiling of a human glioblastoma cell line exposed in vitro to a 1.9 GHz pulse-modulated radio frequency field. *Rad Res*., 165, 636-44.

Rogalla, T., Ehrnsperger, M., Preville, X., Kotlyarov, A., Lutsch, G., Ducasse, C., Paul, C., Wieske, M., Arrigo, A.P., Buchner, J., Gaestel, M. 1999. Regulation of Hsp27 oligomerisation, chaperone function and protective activity against oxidative stress/tumour necrosis factor α by phosphorylation. *J Biol Chem*., 27, 1847-56.

Rogers, B.J., Bastias, C., Coulson, R.L., Russell, L.D. 1989. Cytochalasin D inhibits penetration of hamster eggs by guinea pig and human spermatozoa. *J Androl.*, 10, 275-82.

Rosario, M.O., Perkins, S.L., O'Brien, D.A., Allen, A.L., Eddy, E.M. 1992. Identification of the gene for the developmentally expressed 70 kD heat shock protein (p70) of mouse spematogenic cells. *Dev Biol*., 150, 1-11.

Rosseau, S., Houle, F., Landry, J., Huot, J. 1997. MAP kinase activation by vascular endothelial growth factor mediates actin reorganisation and cell migration in human endothelial cells. *Oncogene*., 15, 2169-77.

Rouse, J., Cohen, P., Trignon, S., Morange, M., Alonzo-Llamazares, A., Zamanillo, D., Hunt, T., Nebreda, A.R. 1994. A novel kinase cascade triggered by stress and heat shock that stimulates MAPKAP kinase-2 and phosphorylation of the small heat shock protein. *Cell*., 78, 1027-37.

Senisterra, G.A., Huntley, S.A., Escaravage, M., Sekhar, K.R., Freeman, M.L., Borrelli, M., Lepock, J.R. 1997. Destabilization of the Ca^{2+}-ATPase of sarcoplasmic reticulum by thiol-specific, heat shock inducers results in thermal denaturation at 37 °C. *Biochem*., 36, 11002-11.

Son, W-Y., Hwang, S-H., Han, C-T, Lee, J.H. 1999. Specific expression of heat shock protein HspA2 in human male germ cells. *Mol Hum Reprod*., 5, 1122-6.

Spungin, B., Margalit, I., Breitbart, H. 1995. Sperm exocytosis reconstructed in a cell-free system: evidence for the involvement of phospholipase C and actin filaments in membrane fusion. *J Cell Sci*., 108, 2525-35.

Sugiyama, Y., Suzuki, A., Kishikawa, M., Akutsu., R., Hirose, T., Waye, M.M., Tsui, S.K., Yoshida, S., Ohno, S. 2000. Muscle develops a specific form of small heat shock protein complex composed of MKBP/HspB2 and HspB3 during myogenic differentiation. *J Biol Chem*., 275, 1095-104.

Vanderwaal, R.P., Cha, B., Moros, E.G., Roti Roti, J.L. 2006. HSP27 phosphorylation increases after 45ºC or 41ºC heat shocks but not after non-thermal TDMA or GSM exposures. *Int J Hyperthermia*., 22, 507-19.

Visconti, P.E., Westbrook, V.A., Chertihin, O., Demarco, I., Sleight, S., Diekman, A.B. 2002. Novel signalling pathways involved in sperm acquisition of fertilising capacity. *J Reprod Immunol*., 53, 133-50.

Zakeri, Z.F., Wolgemuth, D.J., Hunt, C.R. 1988. Identification and sequence analysis of a new member of the mouse HSP70 gene family and characterisation of its unique cellular and developmental pattern of expression in the male germ line. *Mol Cell Biol*., 8, 2925-32.

Zeng, O., Chen, G., Weng, Y., Wang, L., Chiang, H., Lu, D., Xu, Z. 2006. Effects of Global System for Mobile Communications 1800 MHz radiofrequency electromagnetic fields on gene and protein expression in MCF-7 cells. *Proteomics*., 6, 4732-8.